The synthesis and reactivity of nickel complexes supported by mixed, *o*-Tolyl and cyclohexyl diphosphine benzophenone pincer-type ligands

Masterthesis

Sam Huizing

19-11-2018

Supervisors:

A.F. Orsino, MSc
Dr. M.-E. Moret
Prof. Dr. R.J.M. Klein Gebbink

Organic Chemistry and Catalysis
Debye Institute for Nanomaterial Science
Utrecht University

Abstract

Most homogeneous catalytic processes based on transition metal complexes make use of late row transition metals such as Pd and Pt, which are scarce, expensive and toxic. To facilitate the transition to base metals such as Fe, Co and Ni, which are cheaper, more abundant and less toxic, smart ligand design plays an important role. Late row metals favour $2e^-$ processes, which is necessary for elementary chemical steps such as bond breaking and making. Base metals favour $1e^-$ processes, associated with radical formation. Bifunctional or hemilabile ligands can help base metals overcome this problem.

In this project the synthesis of two new phosphine ketone ligands, (2-(di-o-tolylphosphaneyl)phenyl)(2-(diphenylphosphaneyl)phenyl)methanone ($^{o\text{-}Tol}$PCO^{Ph}P) and (2-(dicyclohexylphosphaneyl)phenyl)(2-(diphenylphosphaneyl)phenyl)methanone (^{Cy}PCO^{Ph}P), is demonstrated. These ligands are derivatives of the previously researched bis(2-(diphenylphosphaneyl)phenyl)methanone (^{Ph}dpbp) ligand, which was shown to have a hemilabile and bifunctional character when bound to Ni(0), ariding from the ketone moiety in the backbone of the ligand. Complexes of ^{Ph}dpbp and Ni(0) required a co-ligand however, to prevent the formation of a dinuclear species. This hampered its usefulness in catalysis.

In order to make a complex where the nickel centre is exclusively stabilized by the ligand ($^{o\text{-}Tol}$PCO^{Ph}P or ^{Cy}PCO^{Ph}P), the substituents on the phosphine arms are changed. Going from PPh$_2$ to P(o-Tol)$_2$ greatly increases the steric bulk around the nickel centre, which may weaken the bond between the nickel centre and a co-ligand. The same applies to PCy$_2$, which also increases the steric bulk around the nickel centre, and is much more electron-donating, binding stronger to the metal centre.

In this research the coordination behaviour of both ligands is investigated. Coordination $^{o\text{-}Tol}$PCO^{Ph}P failed to give complexes, except when phenylacetylene was used as co-ligand. The complex formed is not known but assumed to be a nickel-alkyne species where the ketone moiety of the ligand is not bound.

Coordination of ^{Cy}PCO^{Ph}P without co-ligand, or with phenylacetylene or acetophenone, resulted in a species which is most likely the nickel centre supported only by ^{Cy}PCO^{Ph}P, but isolation proved unsuccessful. Stable complexes with PPh$_3$ and BPI as co-ligands were obtained.

A catalytic comparison for the [2+2+2] cyclotrimerization of alkynes was done. Changing the system from ^{Ph}dpbp and Ni(COD)$_2$ to $^{o\text{-}Tol}$PCO^{Ph}P or ^{Cy}PCO^{Ph}P showed no significant change in the catalytic outcome, so the increase in bulk and/or change in electronic properties does not influence this reaction.

The reactivity of (^{Cy}PCO^{Ph}P)Ni(BPI) towards small molecules was investigated as well. (^{Cy}PCO^{Ph}P)Ni(BPI) proved inactive towards H$_2$ activation in the tried conditions, but proved reactive towards diphenyl silane. As a proof of concept, the hydrosilylation of alkenes and alkynes was investigated. (^{Cy}PCO^{Ph}P)Ni(BPI) proved slightly active in the hydrosilylation of 1-octene, and more active in the hydrosilylation of diphenylacetylene.

Contents

List of abbreviations

General

Å	-	Ångström
δ	-	Chemical shift, in PPM
DCD	-	Dewar-Chatt-Duncanson
O.N.	-	Overnight
IS	-	Internal Standard
RT	-	Room Temperature

Analysis methods

APT	-	Attached Proton Test
ATR-IR	-	Attenuated Total Reflectance Infrared
EA	-	Elemental Analysis
EI-MS	-	Electron Ionization-Mass Spectrometry
ESI-MS	-	Electron Spray Ionization-Mass Spectrometry
NMR	-	Nuclear Magnetic Resonance

Chemicals

BPI	-	Benzophenone imine
^{n}BuLi	-	N-butyllithium
^{t}BuLi	-	*Tert*-butyllithium
C_6D_6	-	Deuterated Benzene
COD	-	cyclooctadiene
Cy	-	cyclohexyl
DiPPF	-	1,1'-Bis(di-isopropylphosphino)ferrocene
DMCC	-	N,N-dimethylcarbamyl chloride
dme	-	dimethoxyethane
Et_3N	-	triethylamine
Et_2O	-	diethylether
EtOAC	-	EthylAcetate
MeOH	-	Methanol
$Pd(OAc)_2$	-	Palladium(II)acetate
$Pd(PPh_3)_4$	-	Tetrakis(triphenylphosphine)Palladium(0)
PE	-	Petroleum Ether
^{i}PrOH	-	isopropanol
THF	-	tetrahydrofuran
o-Tol	-	*o*-tolyl

1. Introduction

Catalysis plays a very important role in our current chemical industry. Roughly 90% of all chemicals are produced in processes using a catalyst[1]. Catalysts have play roles such as reduction of energy costs, increasing selectivity or allowing a reaction to occur in the first place. The global demand for catalysts amounted to 33.5 billion $ in 2014, and is still growing[2]. While most processes in industry are catalysed by heterogeneous catalysts, the field of homogeneous catalysis, in which the catalyst is in the same phase as the substrates, contrary to heterogeneous catalysis, also plays an important part[3]. Homogeneous catalysis is usually based on transition metal complexes, built around 2nd or 3rd row transition metals. Here the reaction steps necessary for the formation of the desired product usually revolve around a transition metal centre supported by ligands, together forming a metal complex. Many well understood and well behaving homogeneous catalysts are based on noble metals like platinum, palladium and rhodium [4–7]. Complexes of noble metals like these usually favor $2e^-$ processes, which are favourable for elementary chemical steps like the breaking and formation of bonds. These metals are, however, expensive, quite rare and rather toxic. Looking at their 1st row counterparts, we find base metals like Iron, Cobalt and Nickel. These metals are more abundant, cheaper (Table 1) and less toxic, making them good alternatives in term of green chemistry and costs. However, base metal complexes react differently than noble metal complexes, and tend to facilitate $1e^-$ processes, resulting in radical reaction pathways. While catalysis involving radical pathways is possible, and sometimes beneficial, the generated radical species are often hard to predict, control and study. Also comparing the reactivity with mechanisms for noble metal complexes is not possible, as the reactivity is completely different. In literature, strategies exist to tune the reactivity of base metal complexes from $1e^-$ to $2e^-$ processes, called cooperative strategies[8].

Element	Price (USD/mol)[9,10]	Estimated abundancy in earth's crust (ppm)[11]
Fe	3.9e-3	56300
Co	3.5	25
Ni	0.76	84
Cu	0.38	60
Ru	8.5e2	0.001
Rh	8.4e3	0.001
Pd	3.5e5	0.015
Ag	50	0.075

Table 1: Price in USD/mol (august 2017) and estimated abundance of some base metals and their heavy counterparts.

1.1. Cooperative Catalysis

The 1e⁻ processes that base metal complexes usually undergo can be helped by a ligand scaffold to behave more like 2e⁻ processes. This is widely seen in biological systems, where enzymes incorporate a base metal such as iron and nickel[12] into a very specifically tailored active site. In these sites the ligands are usually not traditional spectator, but so-called actor or cooperative ligands. Their role is not only to stabilize the metal centre, but they are designed in such a way that they can take part in catalytic steps. There are multiple ways for ligands to implement cooperative behaviour, as shown in Figure 1[8].
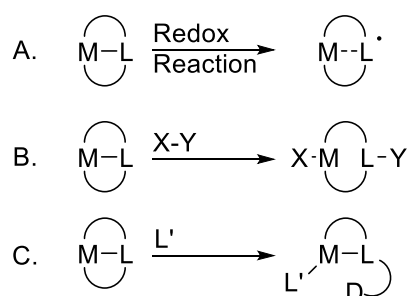

Figure 1: Three classes of cooperative ligands. A Redox-non-innocent ligand scaffold. B: Bifunctional ligand scaffold. C: Hemilabile ligand scaffold[8].

First, in the case of so-called redox non-innocent ligands (Figure 1A), the ligand scaffold can cooperate in catalysis by changing its oxidation state, allowing for storage or releasing of electrons. Combining a 1e⁻ change in the ligand with a 1e⁻ change in the oxidation state of the metal centre can result in an overall 2e⁻ process. The ligand then functions as an electron sink, allowing the complex to accept or release electrons depending on the requirements of the catalytic cycle. A representative example of a redox-active ligand, used in the production of H_2, is found in the work of Crabtree[13] (Scheme 1). Troughout the catalytic cycle, the complex overall gets reduced and oxidized, but the nickel centre retains its formal 2+ oxidation state, as the electrons are stored in radical form on the ligand backbone.
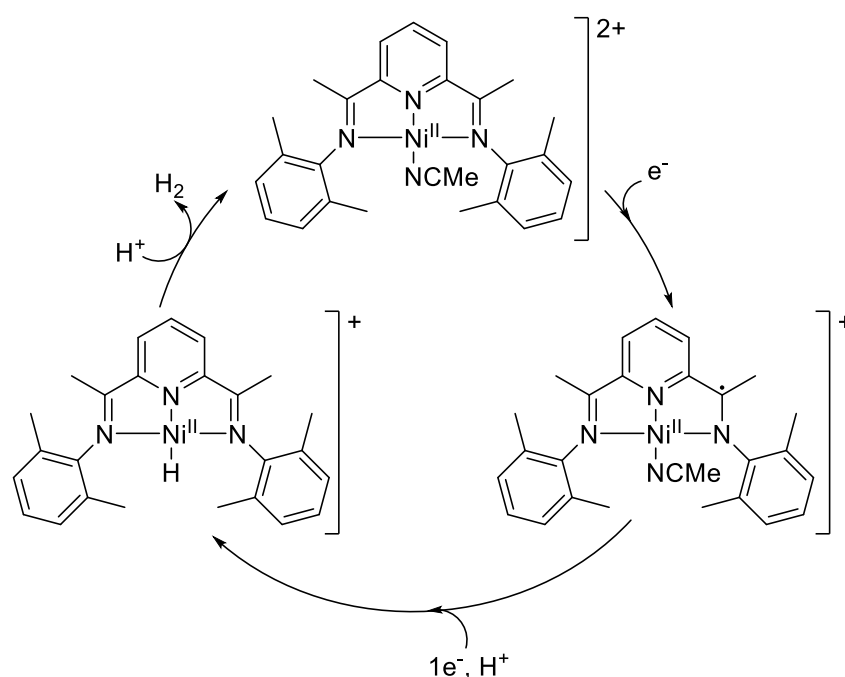

Scheme 1: Reduction of protons using a nickel centre and bisaryliminopyridine catalyst. The nickel centre retains its formal +2 oxidation state through the cycle.
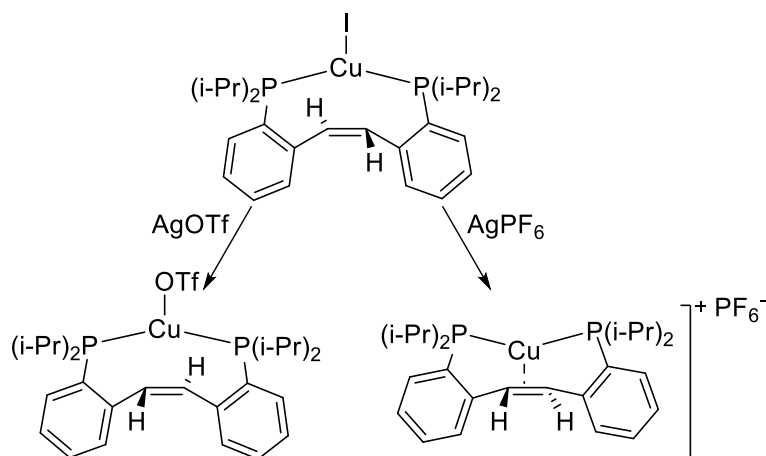
Scheme 3: A PC=CP ligand with a copper centre. The alkene moiety in the backbone can be free or coordinated, depending on the electronic demands of the copper centre.

A second kind of cooperative behaviour is called hemilability (Figure 1B), which was first introduced by Jeffrey and Rauchfuss 1979[14]. The concept of hemilability is based on the possibility for multidentate ligands to vary their coordination to a metal depending on the electronic and steric properties of the ligand. During the catalytic cycle, the chelate arms can (de)coordinate to the metal centre, creating and/or filling vacant sites, which can be useful to stabilize multiple different catalytic intermediates. The hemilability of a ligand can be quite easily tuned by varying the strength of the donor groups or the length and rigidity of the linker arms. Labile ligands usually consist of a weak donor group, such as an ether[15] (OR_2) or amine[16] (NR_3). A σ-acceptor, such as boranes[17] (BR_3) or π-accepting moiety such as alkenes ($R_2C=CR_2$) or ketones[18] ($R_2C=O$) can also function as hemilabile groups. A representative example of a hemilabile π-ligand is found in the work of Iluc *et al.*[19], in which an alkene moiety was introduced in the backbone of a ligand with two chelating phosphorus groups, as shown in Scheme 3. It was demonstrated that the alkene moiety can be coordinated or not, depending on the electronic requirements of the copper centre.
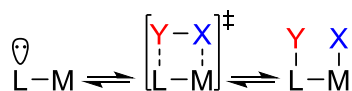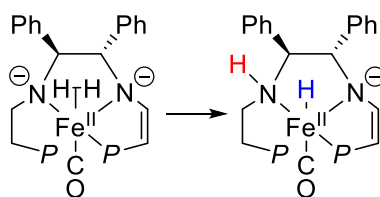

Scheme 2: General scheme of bifunctional activation.

Finally, the last class of cooperative system is based on a bifunctional ligand. In cases like this the substrate is usually heterolytically split into an electrophile and a nucleophile, respectively X and Y in Scheme 2. The nucleophile usually binds to the electrophilic metal centre and the ligand scaffold takes up the electrophile. In the example of dihydrogen activation this would result in a metal hydride and
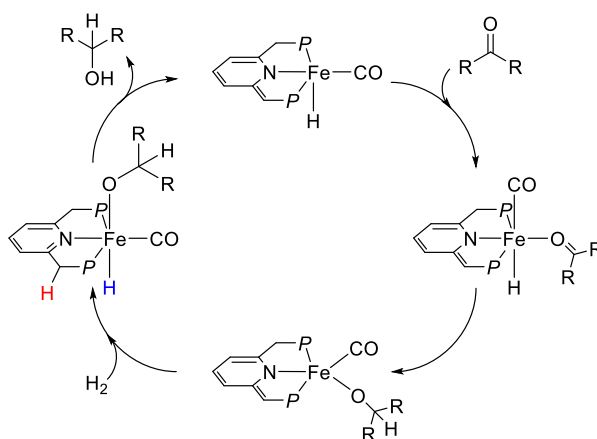

Scheme 4: Example of bifunctional activation by the group of Milstein [20]. The dihydrogen is heterolytically split, with the hydride (in blue) binding to the metal and the proton on the ligand scaffold (in red).

a protonated ligand. This activation of dihydrogen is researched extensively, because it would add a very atom-efficient method for reducing molecules to a chemist's synthetic toolbox. The group of Milstein investigated the activation of hydrogen via an iron PNP complex, which was active in the catalytic hydrogenation of ketones[20] (Scheme 4). The dihydrogen was heterolytically split over the complex, ending as a hydride on the iron centre and a protonated ligand arm. The ligand arm is then again deprotonated in the product formation, giving back the original complex. Other work in this field is done by the group of Chirik[21]. For this system, shown in Scheme 6, iron and a PNNP ligand, the same principle applies. Here the proton ends up on a nitrogen atom, which changes its coordination to iron from X-type to L-type. The L-type dihydrogen goes to an X-type hydride, so the total coordination around iron does not change during this catalytic step.

Scheme 6: Example of bifunctional activation by the group of Chirik [21]. The complex heterolytically splits the dihydrogen, protonating a backbone imine and forming a metal hydride.

E= H, SiH$_2$Ph, SiHPh$_2$
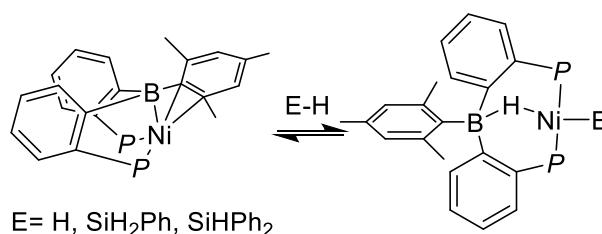
Scheme 5: Catalyst used by the group of Peters, which was able to activate dihydrogen and silanes[22,23]. P = PPh$_2$

The group of Peters also designed a catalyst that showed bifunctional behaviour, both in the activation of hydrogen[22] and silanes (Si-H)[23]. As shown in Scheme 5, the catalyst consists of two phosphine arms and a borane moiety in the backbone. This borane binds the hydrogen upon activation of the substrate, thus giving the ligand its bifunctional character. This is one of the very few examples of bifunctional silane activation.

Our group recently reported the hemilabile beavhiour of a diphosphine ketone ligand ligand ([Ph]dpbp) when complexated to nickel[18] and other base metals[24], as described in section 1.2.3. Additionally, the [Ph]dpbp ligand is also hypothesized to show bifunctional behaviour from its ketone moiety.

1.2. The diphosphine benzophenone ligand

1.2.1. Background

The **Phdpbp** (bis(2-(diphenylphosphaneyl)phenyl)methanone) **(1)** ligand is, as previously mentioned, based on research by Moret *et al.* and master students in the group[18,25,26]. It consists of two chelating phosphorus atoms, with a carbonyl function built in the linker, as shown in Figure 2.
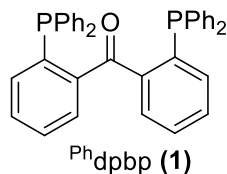

*Figure 2: **Phdpbp** ligand used by Moret et al.*

As shown in Scheme 7 the ketone moiety in the ligand backbone can coordinate in multiple ways with to the metal centre. The carbonyl moiety can bind in two ways to the metal centre: An η^1 binding mode, where the oxygen atom donates a lone pair and an η^2 binding mode, which is described by the Dewar-Chatt-Duncanson model. The η^1 binding mode is preferred by more electrophilic metals, as this increases the electron density on the metal centre, and the η^2 binding mode is preferred by more
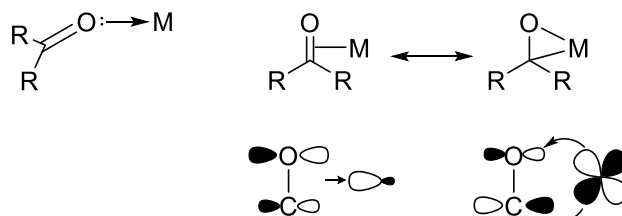
Scheme 7: Different binding modes of a ketone moiety to a metal centre.

electron rich metals, such as Ni(0). The η^2 binding mode is described by two extremes. In the Dewar-Chatt extreme[3], the filled π orbital of the C=O double bond donates to an empty d-orbital on the metal, like an L-type ligand. In the metallocycle extreme a filled metal d-orbital donates to the π* orbital of the double bond. This, in the most extreme case, results in breaking of the π-bond and formation of a metallo-cycle, similar to an X_2-type ligand. For both extremes the charge on the metal can be reasoned out, going from 0 to +2, but as the actual binding of the ketone is somewhere in between these extremes, the exact charge on the metal centre is ambiguous.

1.2.2. Reactivity of **Phdpbp** with noble metals

The groups of Baratta[27] and Ding[28] used this ligand in combination with a diamine ligand and Osmium or Rhodium, respectively (Figure 3). Both groups were investigating the asymmetric hydrogenation of ketones, and for both the **1** ligand was chosen because of its propeller-like structure, which, upon complexation, results in chirality (Scheme 8). For both they obtained catalytically very active complexes, using catalytic loadings as low as 0.01% and ee's up to 90% (Baratta) and 97% (Ding). However, they did not look into the possible bifunctional character. The non-innocent character was investigated by the Young group, in a ruthenium complex[29]. They showed that when adding a
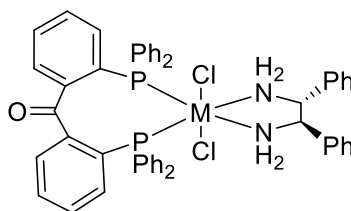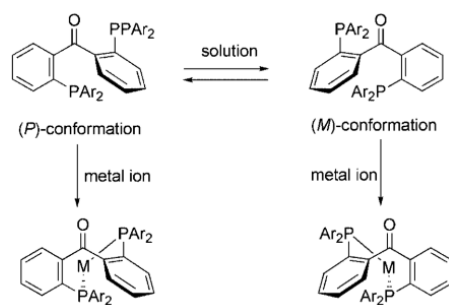

Figure 3: Complex used by Baratta and Ding, where M= Os or Rh, respectively[27,28].

Scheme 8: The propeller-like structure of dpbp ligands in solution and the resulting chirality upon complexation. Figure taken from [20][28].

ruthenium hydride, the carbonyl picked up the hydrogen, resulting in an alcohol and metal-alkyl bond. The same complex could be obtained by adding the ruthenium hydride to the alcohol derivative of [Ph]dpbp, where dihydrogen is formed as well.
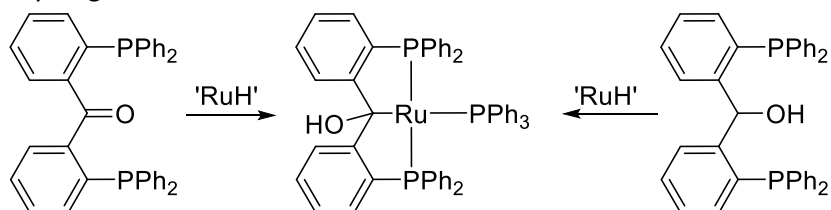

*Scheme 9: Formation of a Ruthenium complex using a Ruthenium-Hydride source, from the [Ph]**dpbp** ligand as well as its alcohol derivative.*

1.2.3.   Reactivity of [Ph]dpbp with base metals

The hemilabile properties of the **1** ligand have been demonstrated in our group[18], by complexating the ligand to nickel in different oxidation states, as shown in Scheme 10. When the ligand was used in combination with $Ni(COD)_2$ (COD = 1,5 cyclooctadiene), a Ni(0) source, and PPh_3 as co-ligand, compound **4** was obtained. The crystal structure of the **4** showed the ketone was bound to the metal. Using a Ni(II) source, $(dme)NiCl_2$, instead of $Ni(COD)_2$ gave compound **3**. For **3** the crystal structure showed the ketone was not bound to the nickel centre. A complex with Ni(I) was also obtained, compound **2**, by comproportionation of $(dme)NiCl_2$ (dme = dimethoxyethane) and $Ni(COD)_2$ in presence of the [Ph]dpbp ligand. This resulted in a complex where the carbonyl was again bound to the nickel centre. Ketone binding is observed only for the complexes where nickel has a higher electron density, and **1** can be classified as a hemilabile ligand.

Complex **4** proved not very effective in catalysis. It is hypothesized that the PPh_3 co-ligand is bound too strongly to the nickel centre and does not dissociate or exchange for a substrate to come in and bind to the nickel centre. Complexation of **1** to $Ni(COD)_2$ without co-ligand led to compound **5**, a dinuclear complex bearing three ligands.

Complexing **1** to other base metals showed similar trends[24]. When complexing **1** to an M^I -Metal, the ketone moiety showed an η^2 coordination mode. Complexes with an M^{II} metal (M = Fe, Co, Ni) showed no binding between the ketone moiety and the metal centre. The C=O bond did lengthen slightly, however, when using more electron-rich metals. The exact origin of this trend is thought to be a through-bond inductive effect, not an effect of geometry changes or overlap with the metal orbitals.
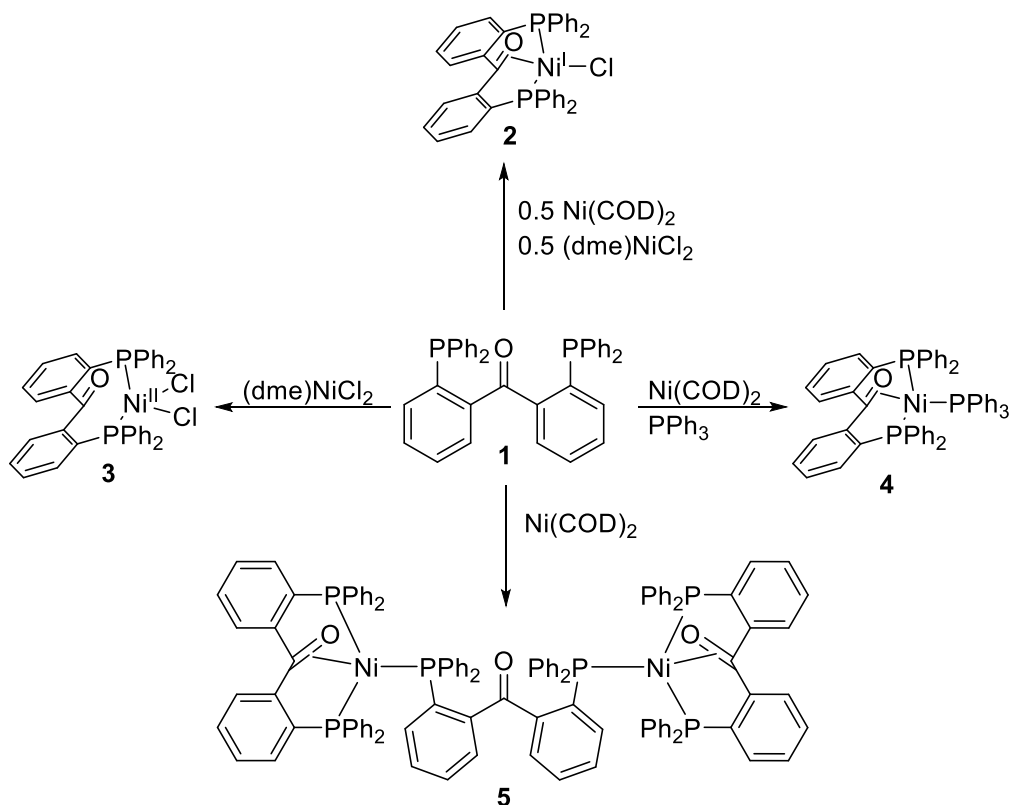
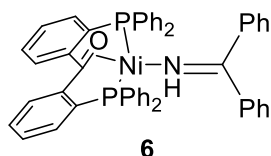*Scheme 10: Reactive behaviour of **1** with nickel in different oxidation states, or with a co-ligand[18].*

*Figure 4: Result of the complexation of **1** Ni(COD)₂ and BPI*

A complex with benzophenone imine (BPI) as co-ligand was also formed, as shown in Figure 4. The BPI co-ligand could be easily exchanged with a number of other co-ligands, such as phosphines, nitriles or olefins[30]. This already demonstrates that it is a weaker co-ligand than PPh₃, which proved too strongly bound for catalysis. Complex **6** proved active in the [2+2+2] cyclotrimerization of alkynes and showed
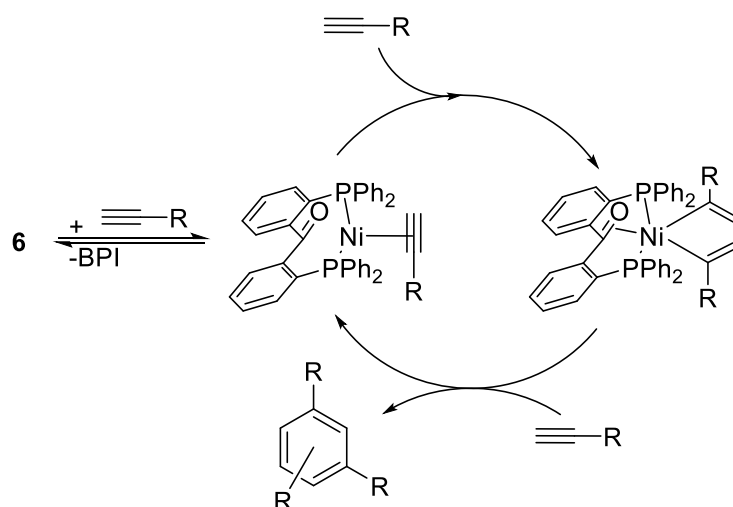
*Scheme 11: [2+2+2] cyclotrimerization of alkynes using **6** as precatalyst[31].*

hemilabile behaviour during catalysis, as shown in Scheme 11[31]. Upon binding the first alkyne, the ketone decoordinates from the nickel centre, and binds again upon binding of the second alkyne.
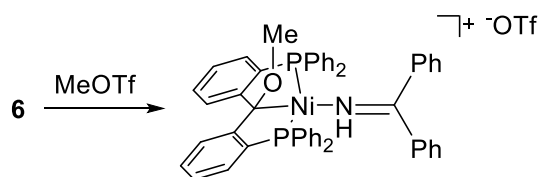
*Scheme 12: Activation of MeOTf by **6**.*

The bifunctional character was probed using the methylating agent methyl triflate (MeOTf)[30]. When reacting **6** with MeOTf, the methyl group ended on the oxygen of the backbone, and the triflate stayed in solution as counterion (Scheme 12). The oxygen picking up the methyl group demonstrates that this catalyst system can be used to activate substrates in a bifunctional fashion.

1.2.4. Ligand modification

To increase the reactivity of complexes like **5** and **6**, the bond between the metal and co-ligand should be weakened, allowing for an easier exchange with the substrate. Obtaining a complex without co-ligand or a solvent molecule as co-ligand, as shown in Figure 5, would be optimal, as this makes it facile for a substrate to bind to the complex. To weaken bond between the metal and the co-ligand, more steric bulk can be introduced around the metal centre, or the electronic properties of the metal can be tuned. To achieve either in the case of this ligand, the substituents on the phosphorus atoms can be altered.
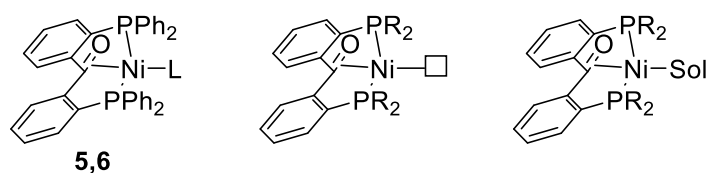

*Figure 5: Left: Complex **5** (PPH₃) and **6** (BPI). Middle: Desired complex without co-ligand. Right: Desired complex with a solvent molecule (Sol) as co-ligand.*

The effect of changing the substituents of the phosphines has both an impact on the steric and electronic properties of the phosphine group, which were extensively studied by Tolman[32]. Looking at the so-called Tolman plot in Figure 6A, where the cone angle and v_{CO} are plotted, one can easily see what properties change for a PR_3 functioning as ligand when the R-groups are exchanged. The cone angle is a parameter which describes the size of the PR_3 group. It is defined as the size of the cone in which all the R-groups still fit (Figure 6B). The Tolman electronic parameter v_{CO} is a parameter which describes how electron-donating the PR_3 group is. It is found by measuring the IR-frequency of the C=O stretch of a $(PR_3)M(CO)_n$ complex. When CO binds to a metal the C=O bond is weakened due to backdonation into the π^* orbital. This results in a decrease in v_{CO}. When the PR_3 group is very donating, the electron density on the metal increases, and with it the amount of backdonation. So, a very donating PR_3 group lowers the v_{CO} more than a less donating group, allowing you to compare different PR_3 groups.
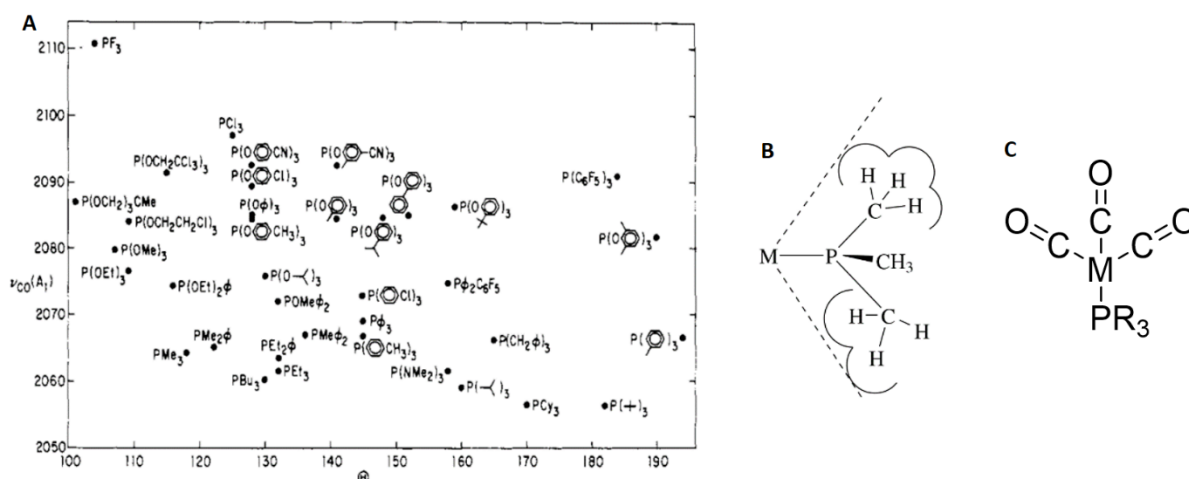
Figure 6: A: Tolman plot of phosphines. The Tolman electronic parameter v(CO) is plotted against the Tolman cone angle. B: visualization of how the Tolman cone angle is measured, using PMe$_3$ as phosphine. C: the Tolman electronic parameter v(CO) is measured using a MPR$_3$(CO)$_3$ complex and measuring the frequency of the CO stretch vibration with IR-spectroscopy.

The strength of the bond between the metal and its co-ligand can be changed by changing both the bulk or electronic properties. An increase in bulk simply leaves less space around the metal centre, preventing the co-ligand from coming too close to the centre and thus binding too strongly. Exchanging the R-groups around phosphorus to make it more donating makes it bind more strongly to the metal and increases its electron density, which can also weaken the bond between the metal and co-ligand.
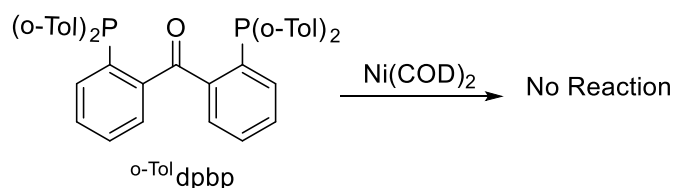
Scheme 13: Attempted complexation with the $^{o\text{-}Tol}$dpbp ligand

An increase in bulk around the nickel centre can be achieved by exchanging the PPh$_2$-groups with P(o-Tol)$_2$ groups. This increases only the steric properties, as the electronic properties of these groups are almost the same. The $^{o\text{-}Tol}$**dpbp** ligand (bis(2-(di-o-tolylphosphaneyl)phenyl)methanone) was synthesized in our group[30], but the yield was quite low, 10% at most. Also, when trying to complexate the ligand to nickel (Scheme 13) no reactivity towards nickel was observed. Both the low yield and the unsuccessful complexation most likely come from the increase in bulk, which was too large, making complexation too sterically demanding.
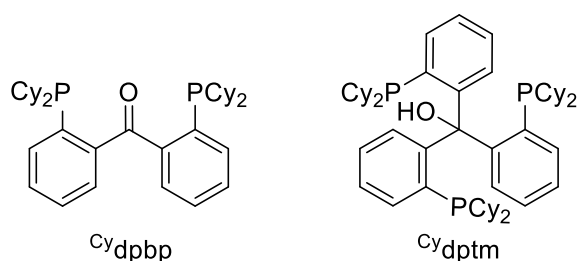

*Figure 7: The ^{Cy}**dpbp** and ^{Cy}**dptm** ligands.*

Exchanging the phenyl substituents for cyclohexyl substituents increases the steric bulk around nickel as well, but less than for *o*-tolyl substituents. More importantly, PCy$_2$ is a much more donating phosphine than PPh$_2$, so it will bind more strongly to the metal centre. An attempt to synthesize the ^{Cy}**dpbp** (bis(2-(dicyclohexylphosphaneyl)phenyl)methanone) ligand has been done in our group, but the synthesis proved difficult, as only the oversubstituted compound, ^{Cyd}**dptm** (tris(2-

15

(dicyclohexylphosphaneyl)phenyl)methanol) was observed[25] (Figure 7). No method to prevent this side-reaction has been found.
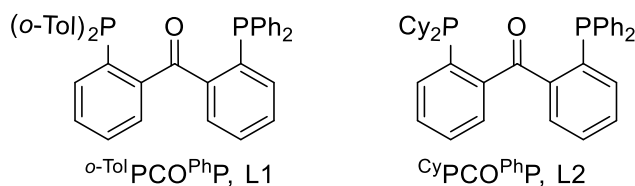

Figure 8: $^{o\text{-}Tol}PCO^{Ph}P$ and $^{Cy}PCO^{Ph}P$ ligands

As substituting both phosphines proved unsuccessful, in this work only one of the phosphine arms will be substituted, yielding a mixed ligand (Figure 8). With these mixed ligands we hope to avoid the drawbacks of $^{o\text{-}Tol}$dpbp and ^{Cy}dpbp, but still impose the desired properties on the new ligands.

1.3. Envisioned Cooperative behaviour

If the ligand behaves as desired and complexes are formed, its' activity towards small molecules can be investigated. The activation of small molecules should ideally go in a bifunctional fashion (Scheme 14). The nickel complex should ideally not have to carry an extra co-ligand, allowing substrates to access the nickel centre more easily.
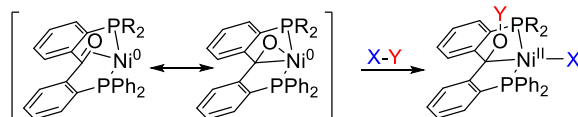
Scheme 14: Envisioned cooperative activation of small molecules.

Other methods of activation, using the backbone, can be thought of. While unlikely, the electrophile (Y) can end up on the carbon of the ketone moiety, or the whole substrate could be split over the backbone (Figure 9).
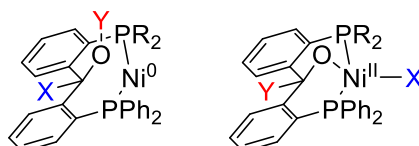

Figure 9: Other possible ways of activating small molecules no the backbone of the ligand.

2. Research aims

To further improve the reactivity of nickel complexes bearing a benzophenone diphosphine ligand (**^{Ph}dpbp**) towards the activation of small molecules, nickel complexes bearing the modified ligands **L1** and **L2** are aimed to be synthesized. The project can be divided into 4 major parts.

The first goal is to find an effective synthesis route for the mixed ligands **L1** ($^{o\text{-}Tol}$PCO^{Ph}P) and **L2** (^{Cy}PCO^{Ph}P) (Figure 10). The synthesis route relies on a modified version of the previously reported **^{Ph}dpbp**. Based on the problems encountered for $^{o\text{-}Tol}$**dpbp** (low yields) and **^{Cy}dpbp** (oversubstitution) we would like to find out if this approach is useful for the mixed ligands proposed here.
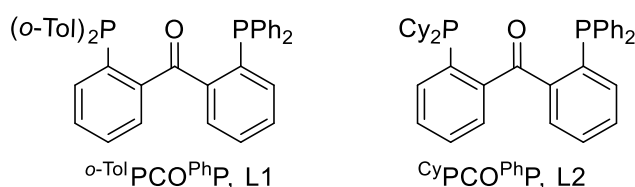

Figure 10: Proposed ligands **L1** and **L2**.

Secondly the coordination chemistry of **L1** and **L2** to Ni(0) will be investigated. The modifications presented are envisioned to change the steric bulk and/or electronic properties around the nickel centre in such a way the bond between nickel and co-ligand is weakened. In the ideal case complexes without co-ligand, or a solvent molecule filling the vacancy, can be accessed (Scheme 15). If these are obtained, the binding of the carbonyl moiety will be studied. Also, we would like to investigate how the change in steric and electronic properties influences the coordination to nickel.
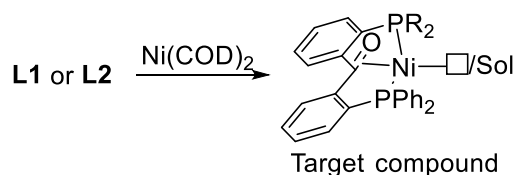

Scheme 15: Target complex of the reaction between **L1** or **L2** with Ni(COD)$_2$

Thirdly, complexes of **L1** or **L2** and nickel will be tested as catalysts in the [2+2+2] cyclotrimerization of alkynes to assess if the change in properties of the phosphines influences the catalytic outcome.
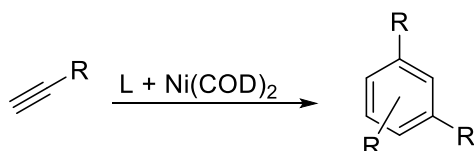
Scheme 16: Envisioned [2+2+2] cyclotrimerization of alkynes

Finally, the activation of small molecules (H$_2$ and H$_2$SiPH$_2$) will also be investigated (Scheme 17). During these reactions the behaviour of the carbonyl moiety should be investigated to see if the envisioned bifunctional or hemilabile character indeed plays a role in the activation. As a proof of concept the activated complexes (when accessible) will be tested for catalytic activity *e.g.* hydrogenation or hydrosilylation reactions.
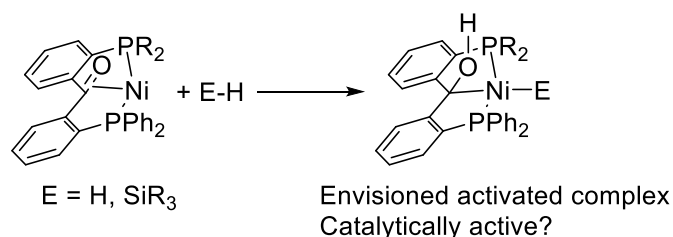
Scheme 17: Envisioned activation of small molecules with the desired complex

3. Results & Discussion

3.1. Ligand Synthesis

Both ligands, **L1** and **L2**, shown in Figure 11 were synthesized using a similar route. The first step starts with a palladium catalysed carbon-phosphorus cross-coupling, as shown in Scheme 18. **7** ((2-
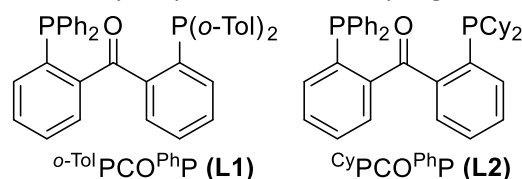

$^{o\text{-Tol}}$PCO^{Ph}P **(L1)** ^{Cy}PCO^{Ph}P **(L2)**

Figure 11: Both desired ligands, targets of these syntheses

bromophenyl)diphenylphosphane) and **8** ((2-bromophenyl)di-*o*-Tolylphosphane) were obtained in a yield of 89% and 94%, respectively, by the coupling of *o*-iodobromobenzene with diphenylphosphine or di(*o*-tolyl)phosphine, respectively, with Pd(PPh$_3$) as catalyst and Et$_3$N as base[18]. **9** ((2-bromophenyl)dicyclohexylphosphane) was obtained according to a procedure by the group of Buchwald[33] and was isolated in a yield of 49%. Here Pd(OAc)$_2$ and DiPPF formed the catalyst, and Cs$_2$CO$_3$ functioned as base.
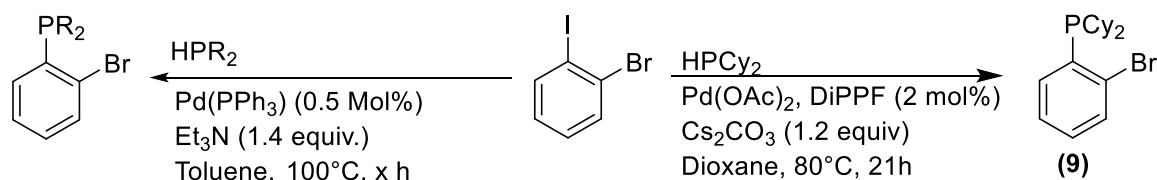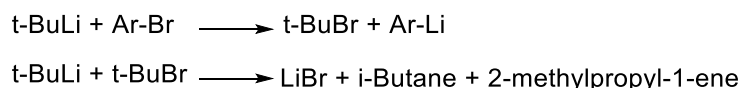

(7): R = Ph, x = 18
(8): R = *o*-Tol, x = 36

*Scheme 18: Conditions of the cross-coupling reaction of disubstituted phosphines with o-iodobomobenzene, yielding the desired phosphine-bromine species **(7-9)**.*

The next step in synthesis is a lithium-halogen exchange followed by nucleophilic substitution with one equivalent of the carbonyl source, N,N-dimethyl carbamoylchloride (DMCC). The **DMCC** has two leaving groups with very different properties: The chloride is a better leaving group than the dimethylamine and will thus be substituted more easily. The first equivalent of the lithiated phosphine will therefore only substitute the chlorine, and the second equivalent the dimethylamine. Via this stepwise approach, mixed diphosphines with different substituents on the phosphine arms could be
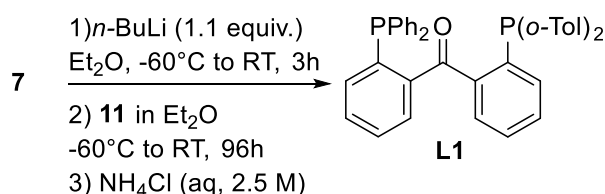

(7): R = Ph
(8): R = *o*-Tol

(10): R = Ph
(11): R = *o*-Tol

(9)

(12)
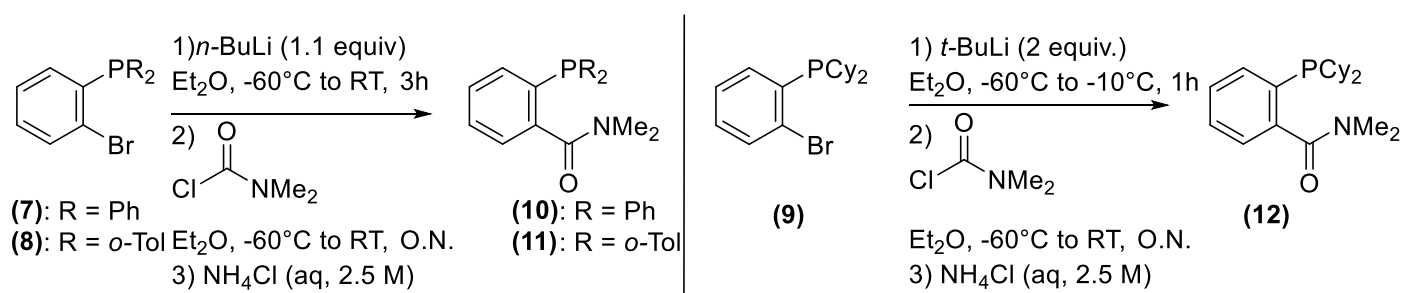
Scheme 19: Lithiation and nucleophilic substitution conditions of the arylphosphines 3 and 4 (left), yielding compounds 6 and 7, and of 5 (right), yielding compound 8.

obtained. As Scheme 19 shows, to introduce the **DMCC**, the phosphorus species was first lithiated at -60°C in Et$_2$O, after which it was allowed to warm to RT over 3 hours to promote lithiation. Both arylphosphines (**7** (R=Ph) and **8** (R = *o*-Tol)) were first lithiated using *n*-BuLi. However, for **9** (R = Cy) *t*-BuLi was needed to prevent alkylation as side reaction. As Scheme 20 shows, 2 equivalents of *t*-BuLi were needed, due to the formation of *t*-butylbromide, which is also very reactive towards *t*-BuLi, forming LiBr, butene and butane. After lithiation, the DMCC was introduced at -60°C and then stirred

$$t\text{-BuLi} + Ar\text{-Br} \longrightarrow t\text{-BuBr} + Ar\text{-Li}$$

$$t\text{-BuLi} + t\text{-BuBr} \longrightarrow LiBr + i\text{-Butane} + 2\text{-methylpropyl-1-ene}$$

Scheme 20: Self quenching reaction of [t]BuLi.

O.N. at RT. The obtained mixtures were quenched with a solution of NH_4Cl and the phosphine amide species were obtained. The isolated yield of **10** (2-(diphenylphosphaneyl)-N,N-dimethylbenzamide) and **11** (2-(di-*o*-Tolylphosphaneyl)-N,N-dimethylbenzamide) was 61% and 59%, respectively. Due to the high sensitivity of **12** towards air and moisture, the isolation of **12** was not successful. Most of the purification methods attempted either failed to isolate a (side)product or resulted in the formation of more oxidated product. For this reason, the crude mixture of **12** was used in the further synthesis of **L2**, with a purity of 74% according to ^{31}P-NMR. Additionally, it has to be mentioned that during the synthesis of **10** (R = Ph), the ^{Ph}dpbp ligand was observed as a side product, ranging from 1 to 22 % based on ^{31}P-NMR. This is the result of a double substitution reaction, instead of the desired monosubstitution. Adding the DMCC solution to the lithiated **10** at once instead of slowly dripping decreased the amount of oversubstituted product, but it still was always present as an impurity at the end of reaction.

Scheme 21: Lithiation and nucleophilic substitution conditions of 7 , leading to the formation of L1.

Finally, the second phosphine arm was introduced in a similar way, as shown in Scheme 21, starting with lithiation of **7** (R = Ph) again at -60°C in Et_2O. The reaction is allowed to warm to RT for three hours to promote the lithiation. After lithiation a solution of **11** (R = *o*-Tol) in Et_2O was added at -60°C and left stirring for 96 hours at RT. **L1** was isolated in 33% yield using column chromatography, with neutral alumina and a solvent system of PE and EtOAc. This brings the overall yield of **L1** to 16%.
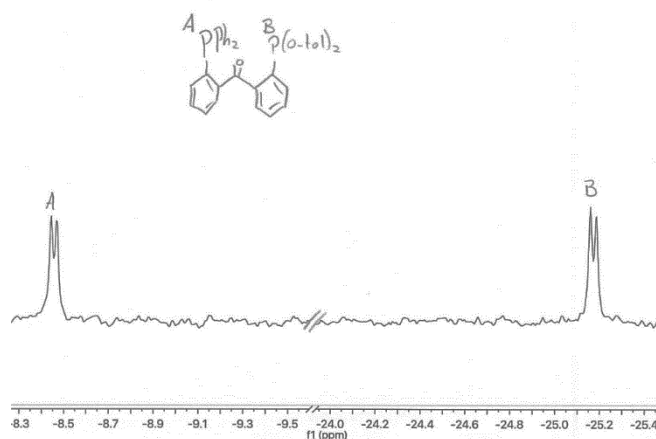
Figure 12: Zoom of the ^{31}P-NMR spectrum of L1

L1 ($^{o\text{-Tol}}PCO^{Ph}P$) was isolated as a bright yellow solid. As Figure 12 shows, the ^{31}P-NMR spectrum shows two doublets, at -8.5 and -25.2 ppm. The coupling between the phosphorus atoms goes through 6 bonds and hence is quite small, $^{6}J_{P,P}$ = 4.3 Hz. The carbonyl peak is found in the ^{13}C-NMR spectrum (Figure 13), at 197 ppm, as a triplet coupling to both phosphorus atoms ($^{3}J_{C,P}$ = 3.4 Hz). It is also observed in IR, at 1658 cm^{-1}. All spectroscopic data point to a successful synthesis of **L1**, with no

oversubstitution. This is further confirmed by ESI-MS, where the found weight for [M + Ag]⁺ is 687.0983, which agrees with the calculated weight of 687.0979.
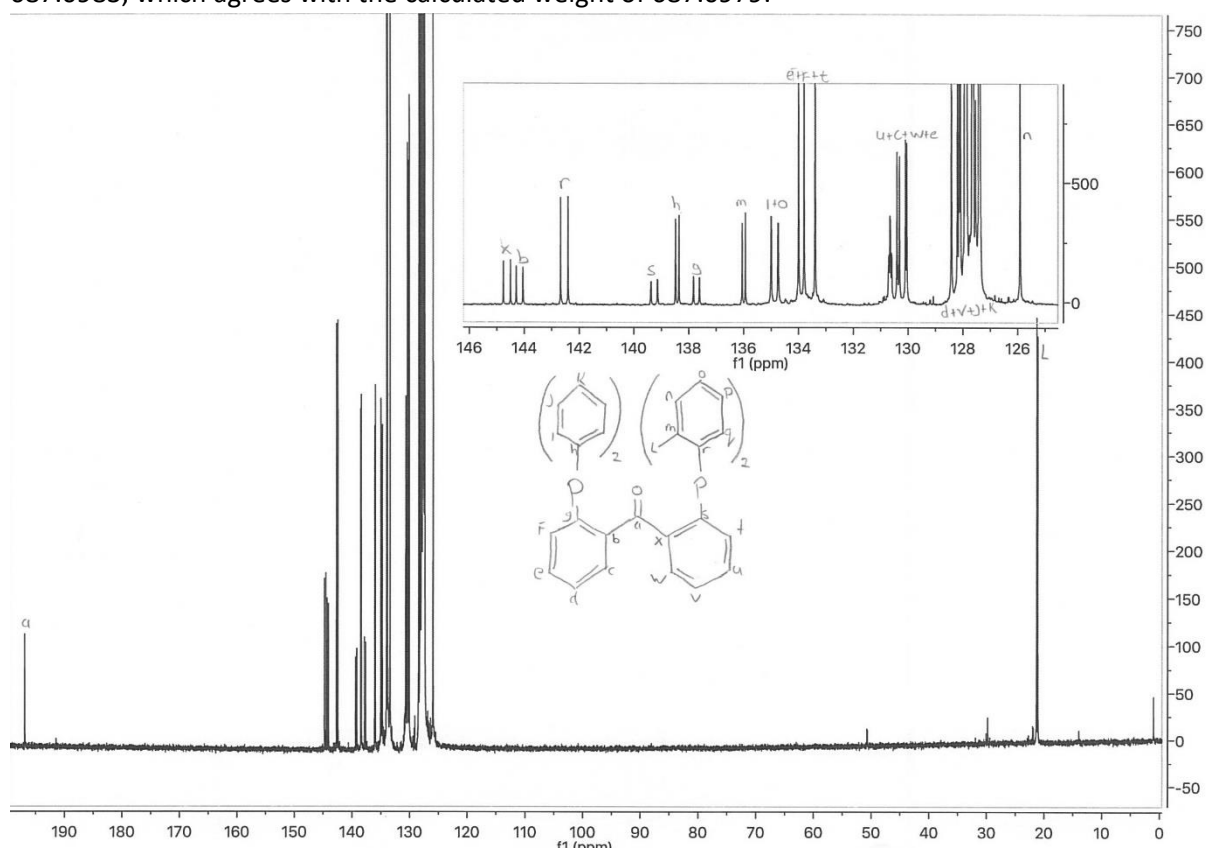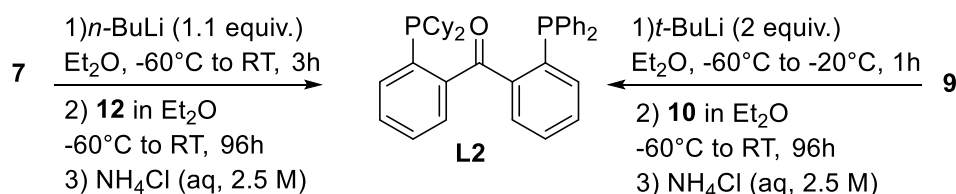

*Figure 13: ¹³C-NMR spectrum of **L1**.*

*Scheme 22: Lithiation and nucleophilic substitution conditions of **9** and **7**, leading to the formation of **L2**.*

Again, as the final step, the second phosphine arm was introduced, as shown in Scheme 21 (left reaction), starting with lithiation of **7** (R = Ph) again at -60°C in Et$_2$O. The reaction is allowed to warm to RT for 3 hours to promote the lithiation. After lithiation a solution of impure **12** (R =Cy) in Et$_2$O was added at -60°C and left stirring for 96 hours at RT. In the ³¹P-NMR of the crude mixture peaks that can be ascribed to the ligand can be seen, but the purity is only 50% based on integrals. Starting with the impure **12** made the work-up more difficult, so the approach to **L2** was changed. Now a solution of **9** was lithiated using *t*-BuLi at -60°C, after which it was allowed to warm to -20°C for one hour. Then a solution of **10** in Et$_2$O was introduced to the mixture at -60°C and stirred for 96 hours at RT. **L2** was isolated in a yield of 14% using column chromatography, with neutral alumina and a solvent system of PE and EtOAc. The overall yield of **L2** now comes to 4%. The low yield of **(L2)** can be partly ascribed to its sensitivity towards air and water, and most likely oxidized partly while running the column. No other way to isolate **(L2)** has been found.
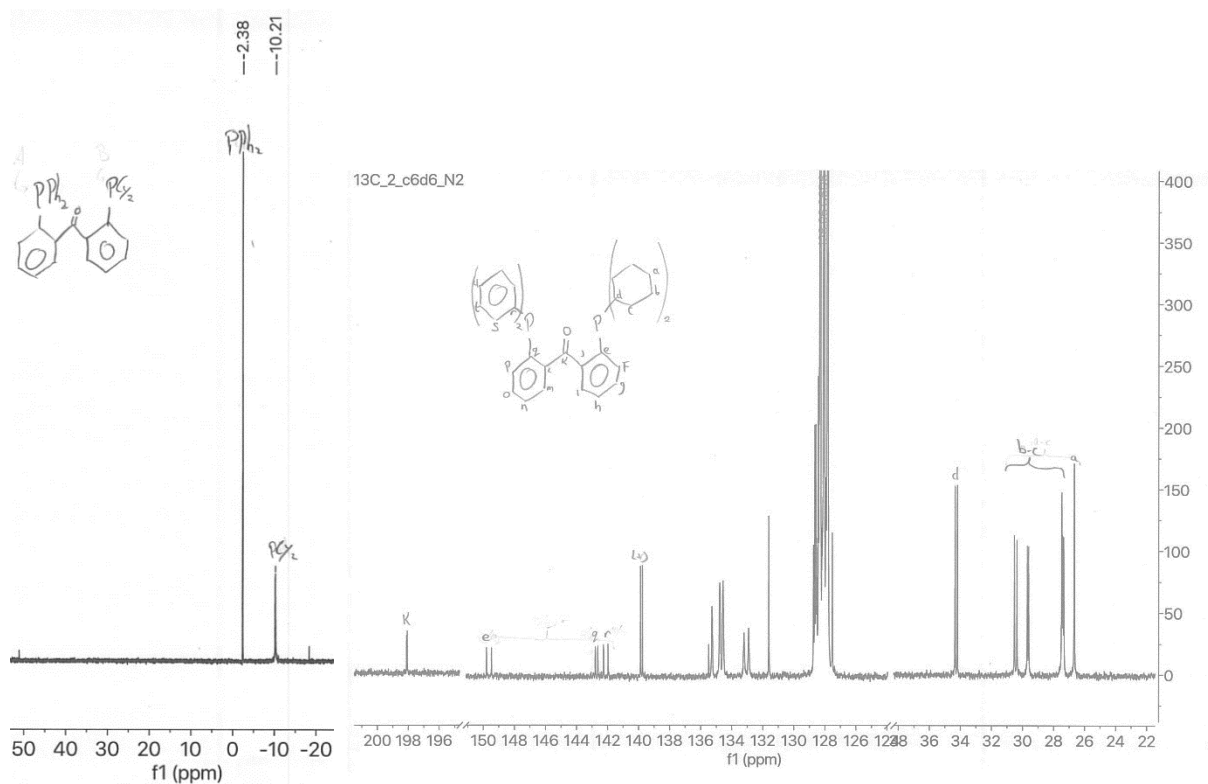
*Figure 14: Left: Zoom of the ^{31}P-NMR spectrum of **L2**. Right: ^{13}C-NMR spectrum of **L2**.*

L2 (^{Cy}PCO^{Ph}P), was isolated as a bright yellow solid. This ligand is quite moisture and air sensitive and started oxidizing immediately when using non-dried and degassed solvents. In the ^{31}P-NMR spectrum the ligand appears as two peaks, a doublet at -3.5 with a coupling constant of $^6J_{P,P}$ = 5.3 Hz, and a broad singlet at -10.2 (Figure 14, Left). ^{13}C-NMR shows the carbonyl at 189 ppm, this time as a doublet with $^3J_{C,P}$ =6.1 Hz (Figure 14, Right).   All the spectroscopic data point to the successful formation of **L2**, without any oversubstitution product.The weight found with ESI-MS, 671.1608 m/z, nicely matches with the calculated value of 671.1605.

3.2. Coordination chemistry of mixed phosphine ligands to Nickel (0)

As the synthesis of the desired ligands **L1** ($^{o\text{-Tol}}$PCO^{Ph}P) and **L2** (^{Cy}PCO^{Ph}P) proved successful, their complexation behaviour with Ni^0 was investigated. Ni^0 is a d^{10} metal, which makes it quite electron-rich. Coordination of the carbonyl moiety is expected, as previously observed with the ^{Ph}**dpbp** ligand[18].

Complexations of **L1** and **L2** without co-ligands were first attempted, as the aim is to form a stable complex without neeing a co-ligand. Ideally the co-ligand, if necessary, would be just a solvent molecule like THF, but other co-ligands such as BPI were investigated as well. In the previous work[18] done with the ^{Ph}**dpbp** ligand dinuclear species was observed when no co-ligand was present (Figure 15). We aim to avoid the formation of this dinuclear species by the extra steric bulk introduced in **L1** and **L2** compared to ^{Ph}**dpbp.**

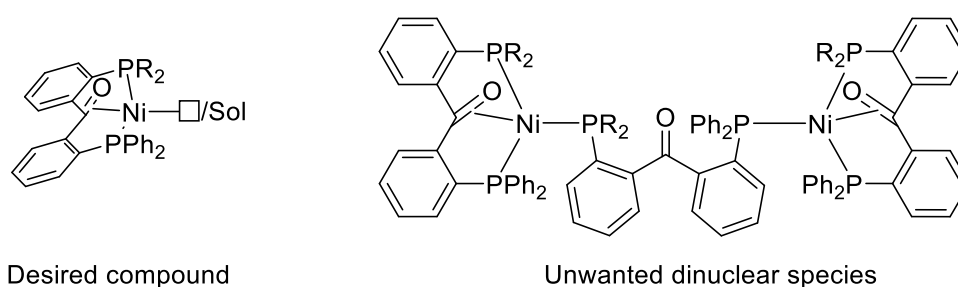|	
Desired compound	Unwanted dinuclear species

Figure 15: Right: The desired complex with a vacancy or loosely coordinating solvent molecule. Left: Dinuclear species, avoided by the increase in bulk.

Secondly, also complexations of **L1** and **L2** to Ni(0) in the presence of co-ligands were attempted. The increase in bulk or the more electron-rich properties provided by **L1** and **L2** are expected to weaken the coordination of the co-ligand to the nickel centre (Figure 16). Ideally a solvent molecule (*e.g.* THF) would act as a stabilizing co-ligand, but other co-ligands such as BPI and PPh$_3$ were also investigated.
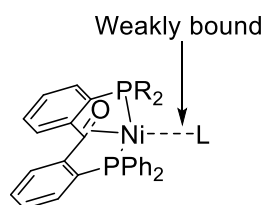

*Figure 16: Target complex of **L1** and **L2** and nickel, with a weakly bound co-ligand.*

Most of the information presented in the coming sections comes from the ^{31}P-NMR spectra, as they give an indication about whether and how the phosphorus arms are bound to the metal. In addition, ^{31}P-NMR can also be used to see if the ligand has reacted. ^{1}H-NMR can be used to observe if COD is released from the nickel source, Ni(COD)$_2$, during the reaction. With ^{13}C-NMR the binding of the carbonyl can be observed. In the free ^{Ph}dpbp ligand the carbonyl appears around 197 ppm, but when it is bound to a nickel centre, which is supported by the crystal structure, this peak shifts to 120 ppm[26]. For **1** and **2** the free carbonyl is observed at 197 and 189 ppm respectively and are expected to show a similar shift in the ^{13}C-NMR when binding to the nickel centre.

In the next two sections the coordination behaviour to Ni(0) of **L1** (Section 3.2.1) and **L2** (section 3.2.2) are investigated and compared to the coordination chemistry of ^{Ph}**dpbp.**

3.2.1. Coordination chemistry of $^{o\text{-Tol}}$PCO^{Ph}P

The coordination chemistry of **L1** to Ni(COD)$_2$ was studied, as summarized in Scheme 24. For all complexation attempts, except for phenylacetylene as co-ligand, ^{31}P-NMR analysis of the reaction mixtures shows the presence of complicated mixtures, characterized by very broad resonances in

NMR. A colour change from yellow to brown-black does indicate a reaction is occurring, however, none of the isolation attempts proved successful.
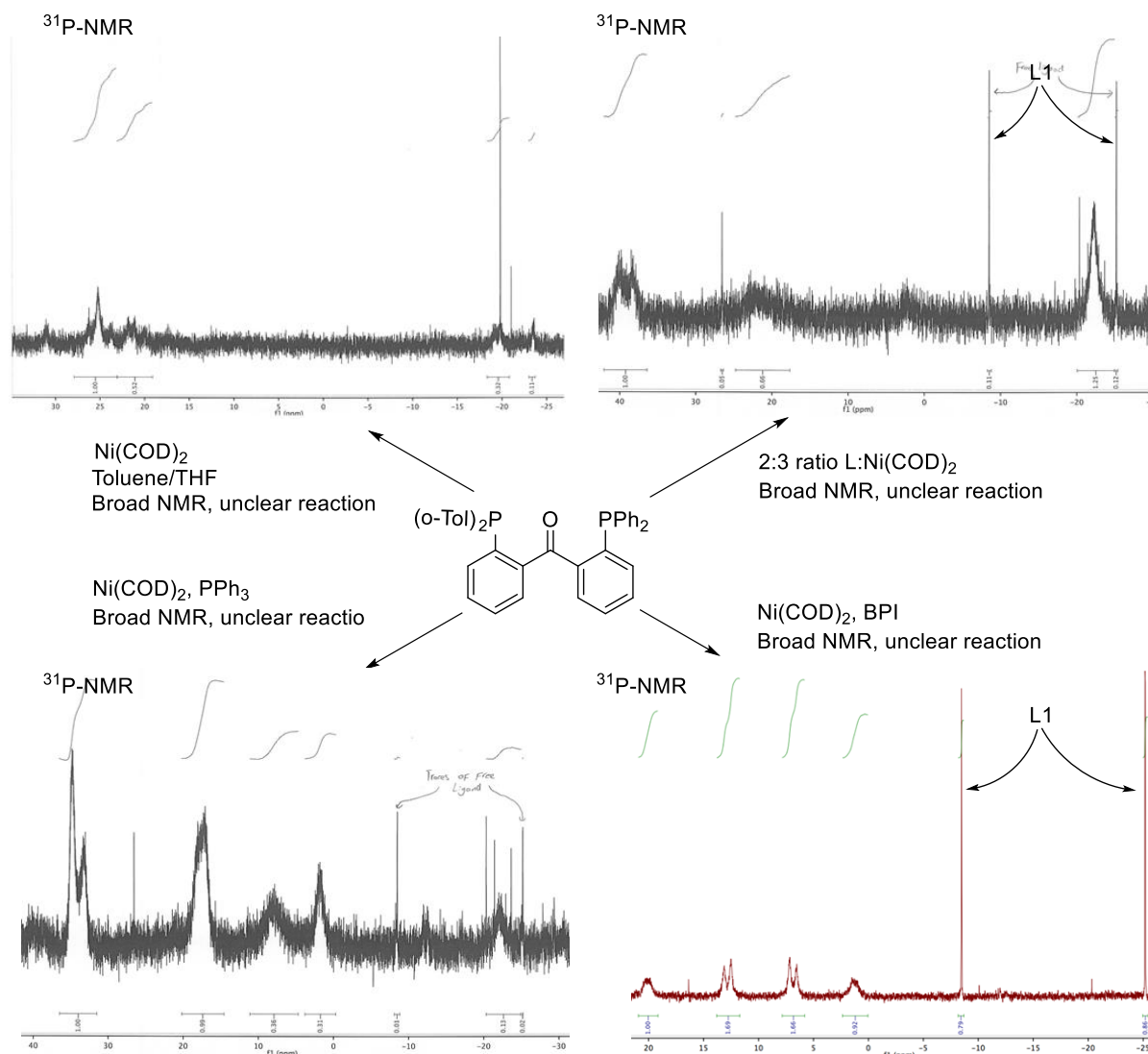

Scheme 24: Coordination behaviour of **L1** without co-ligand, or in the presence of BPI and PPh$_3$, analysed using ^{31}P-NMR.
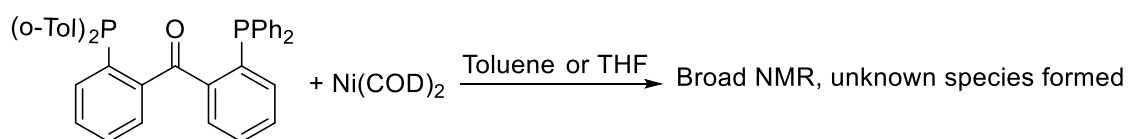
Scheme 23: Complexation attempt of **L1** to Ni(0) in THF and Toluene

First, complexations of **L1** and Ni(COD)$_2$ without a co-ligand were attempted (Scheme 23). The reaction was performed in both THF and toluene, which gave the same result according to ^{31}P-NMR (Scheme 24, Top left). Both complexations resulted in a black-brown solution, indicating a reaction occurred. In ^{31}P-NMR spectrum traces of free **L1** are observed, in addition to two very broad peaks around 25 and 22 ppm. ^{1}H-NMR indicates the COD was released, confirming that a reaction occurred. What the species formed is, is unknown, as isolation proved unsuccessful. To see if the dinuclear species, which was observed with the ^{Ph}**dpbp** ligand (Scheme 10, Bottom) is formed, an complexation with a 3:2 ratio of **L2**:Ni(COD)$_2$ was attempted.
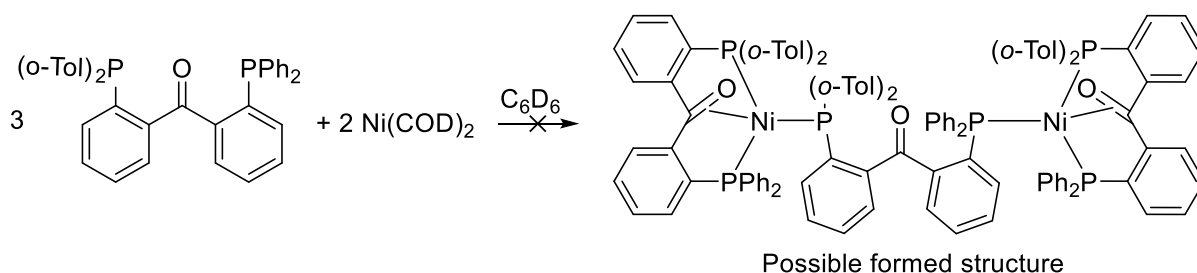
*Scheme 25: Attempted complexation with a ratio of 3:2 **L1**:Ni(COD)₂. The dinuclear species was not observed.*

From the attempted complexation of **L1** and Ni(COD)$_2$ in a 3:2 ratio again a black-brown solution was obtained. The ^{31}P-NMR, shown in Scheme 24 (Top right) again shows some free **L1**, in addition to broad resonances, at 40, 22 and -18 ppm, with an integral ratio of 1.5:1:2 respectively. These do not agree with the dinuclear complex, as that would give a peak pattern of 4 peaks, with an integral ratio of 2:2:1:1. No further evidence for the species formed was obtained, and isolation proved unsuccessful.

As complexations without co-ligand did not behave well, complexations with different co-ligands were attempted. PPh$_3$ and BPI were tried, as they were shown to form a well-defined complex with the **^{Ph}dpbp** ligand[18,30].
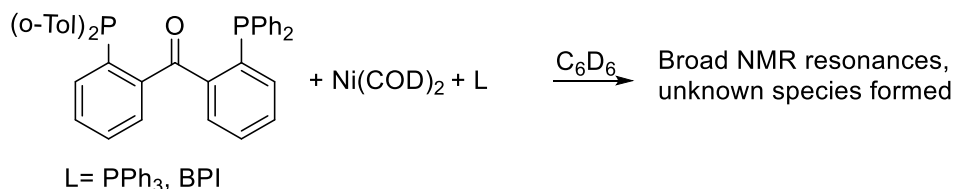
*Scheme 26: Attempted complexation of **L1**, Ni(COD)₂ and PPh₃ or BPI.*

Both the complexation with **L1** and Ni(COD)$_2$ with PPh$_3$ and BPI did not behave as expected. Again an unclear brown-black mixture was formed, with broad resonances in ^{31}P-NMR (Scheme 24: Bottom left: PPh$_3$, Bottom right: BPI). Since isolation of these complexes was again unsuccessful, and due to their unclear behaviour in solution characterizing these compounds was not straightforward, and no further evidence for a formed species was obtained.

All the reactions shown in Scheme 24 resulted in unclear, broad NMR spectra. Most likely the increase in bulk from PPh$_2$ to P(o-Tol)$_2$ is too large, so no stable complexes can be formed. The formed species might be in an equilibrium within the NMR time scale, which explains the broadness of the peaks.
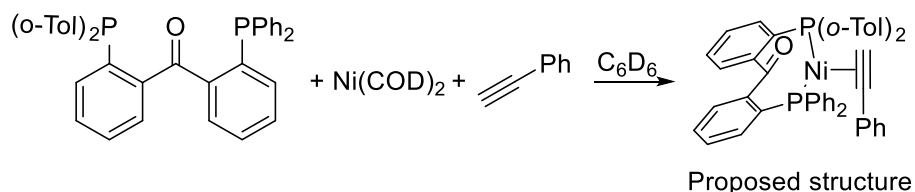
*Scheme 27: Attempted complexation of **L1** and Ni(COD)₂ with phenylacetylene.*

Oppositely, *in-situ* complexation of **L1** and Ni(COD)$_2$ with phenylacetylene as co-ligand (Scheme 27) gave a clear ^{31}P-NMR spectrum, with 2 sharp doublets at 35 and 25 ppm, coupling with each other with 27.6 Hz. **L1** has fully reacted, but quite some minor impurites between -5 and -30 ppm are still present. ^{1}H-NMR shows all the COD is released. Isolation of the major species was unsuccessful, and decomposition happened quickly. Isolation was unsuccessful, so no further evidence towards the proposed complex could be given. However, from previous work with the **^{Ph}dpbp** ligand it is known that upon complexation of an alkyne, the ketone is unbound. This makes the ligand backbone slightly more flexible, possibly allowing for a geometry where the P(o-Tol)$_2$ group can bind, whereas

for the previous complexation attempts the ketone was bound, putting too much strain on the system.

In summary, looking at all the attempted complexations with **L1**, all resulted in unclear species, with the exception of the complexation with phenylacetylene, and all isolation attempts proved unsuccessful. Using only one phosphine arm substituted with *o*-tolyl groups still seems to result in a ligand that is too bulky to complexate in the desired fashion. An exception can be made when the ketone moiety is not coordinating, as proposed for the reaction with phenylacetylene.

3.2.2. Coordination chemistry of ^{Cy}PCO^{Ph}P

As complexation of the **L1** ligand proved difficult, the focus was changed to **L2** (^{Cy}PCO^{Ph}P). The PCy$_2$ group is not only less bulky than its *o*-Tolyl analogue, but also binds stronger to transition metals because it is more electron-donating. Both these properties should lead to more stable complexes.
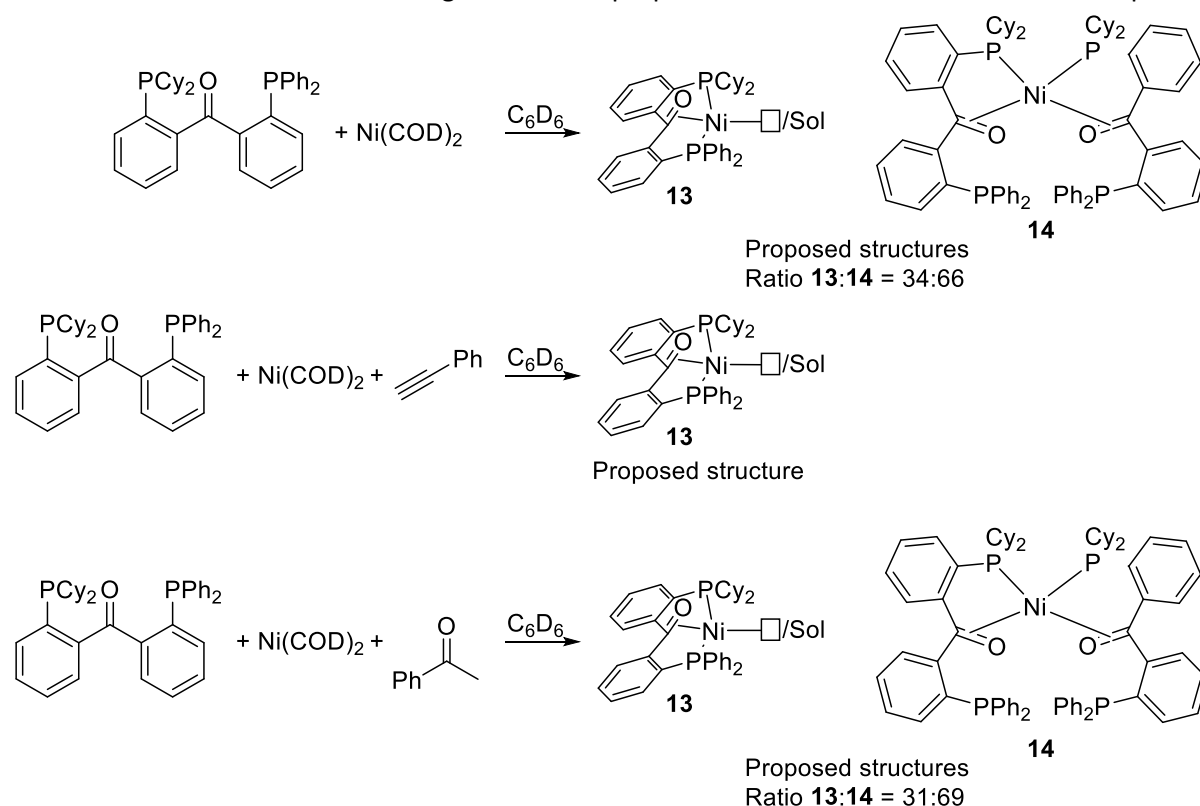
Scheme 28: Coordination attempts of L2 with Ni(COD)$_2$ and different co-ligands: Top: No co-ligand. Middle: Acetophenone. Bottom: Phenylacetylene. The products are proposed structures, the ratios of which differed per reaction.

Again first coordination of **L2** to Ni(COD)$_2$ without co-ligand was attempted (Scheme 28). Complexation attempts with acetophenone and phenylacetylene gave similar results, as the ^{31}P-NMR spectra shown in Figure 17. All free **L2** was consumed, and no bound COD was observed in 1H-NMR. Because the species observed in ^{31}P-NMR (Figure 17, 1-3) appeared to form with different co-ligands, the co-ligand does not influence the structure. Therefore complex **13** ((**L2**)Ni), without co-ligand or a solvent molecule, is proposed to be the species observed at 17.5 and 28.2 ppm (Coupling with $^2J_{P,P}$ = 82 Hz). A second species is observed in the complexation without co-ligand or with acetophenone. Both peaks appear as singlets, at 44.0 and 3.5 ppm. As the value of 3.5 is close to the value of free **L2**, a structure is proposed with one of the arms bound, and one free. As no bound COD is observed in the ^{1}H-NMR spectrum, a structure like **14** is proposed, with a nickel centre stabilized by two **L2**, with
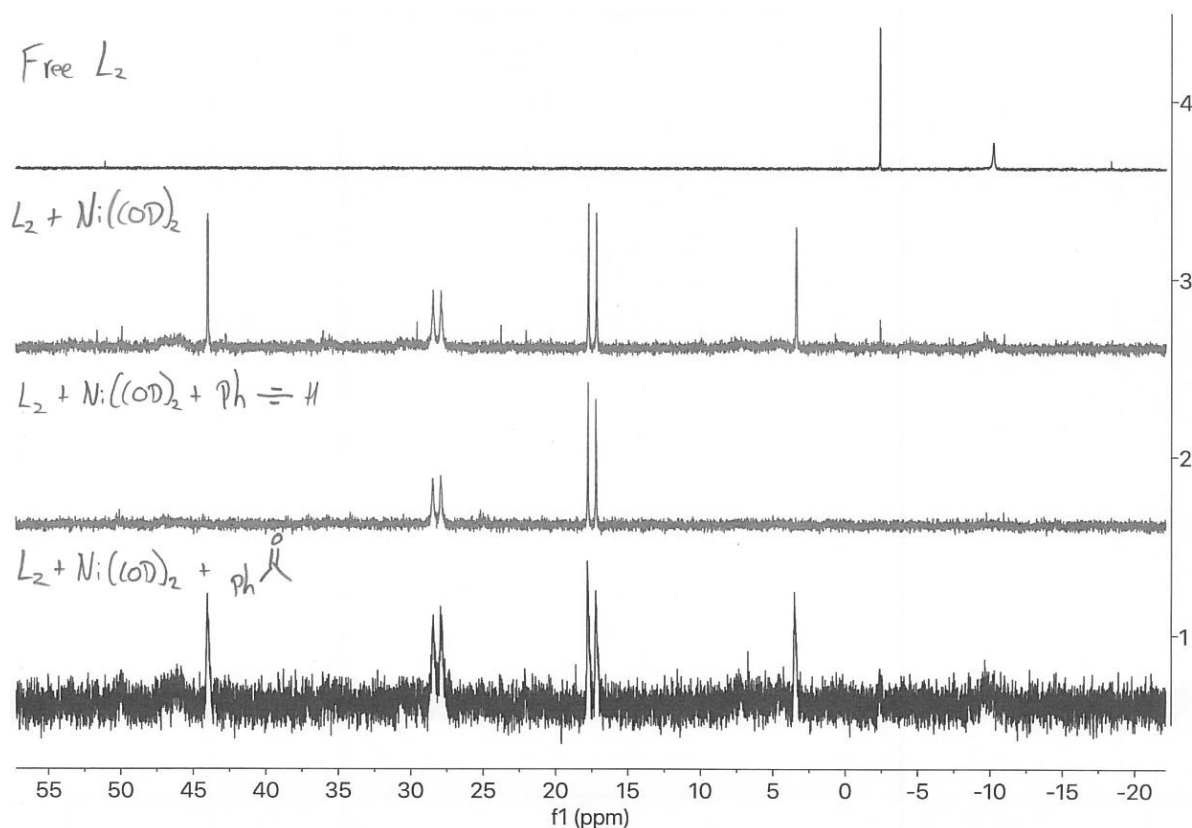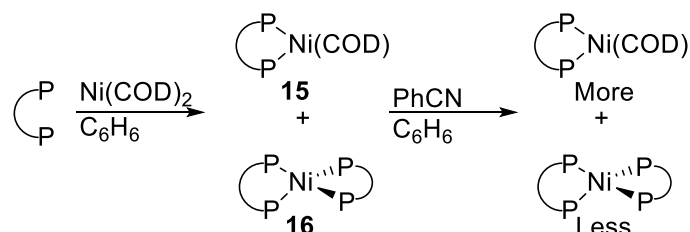
*Figure 17: ^{31}P-NMR spectra of: (4): Free **L2**. (3): Coordination of **L2** and Ni(COD)$_2$. (2): Coordination of **L2** to Ni(COD)$_2$ with phenylacetylene. (1): Coordination of **L2** to Ni(COD)$_2$ with acetophenone.*

one phosphine arm of both ligands bound, and one free. The binding phosphines of **14** should be the equivalent, as no coupling is observed.


Scheme 29: Coordination of a chelating phosphine to Ni(cod)$_2$, and the influence of a non-coordinating benzonitrile

A similar observation was made by Louie *et al.*[34]*,* where a range of chelating phosphines were coordinated to Ni(COD)$_2$ (Scheme 29). A mixture of compounds **15** and **16** was observed. Adding PhCN (benzonitrile) did not exchange any of the ligands, but did change the ratio **15:16**, favouring compound **15**. It is hypothesized that the addition of PhCN creates an equilibrium between **15** and **16**. A similar equilibrium could exist between our proposed compounds **13** and **14**, promoted by phenylacetylene in our case, as no **14** was observed when coordinating **L2** to Ni(COD)$_2$ in the presence of phenylacetylene. The presence of acetophenone does not seem to influence the coordination products, as the ratio **13:14** found (31:69) is similar to that found when coordinating **L2** to Ni(COD)$_2$ without co-ligand (33:69).

As isolation of either species proved unsuccessful, no further evidence toward the proposed structure was obtained. However, matching the spectroscopic data of the experiments shown in Scheme 28, it is proposed that compound **13** was formed.

.

Because isolation of proposed compound **13** proved unsuccessful, coordination of **L2** to Ni(COD)$_2$ in the presence of PPh$_3$ or BPI was done as well. These co-ligands gave stable complexes for the ^{Ph}dpbp analogue of the ligand[26,35].
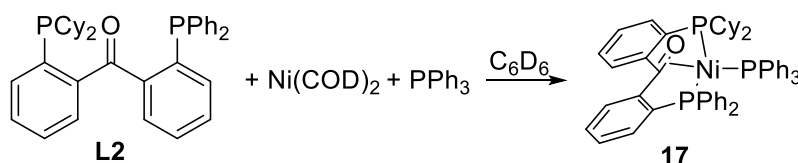
*Scheme 30: Complexation of **L2**, Ni(COD)$_2$ and PPh$_3$, resulting in complex **15** (**L2**)Ni(PPh$_3$)*

When coordinating **L2** to Ni(COD)$_2$ with PPh$_3$ as co-ligand, as shown in Scheme 30, the ^{31}P-NMR (Figure 18) shows three signals, all doublets of doublets, at 39.0 ppm ($^2J_{P,P}$ = 17.1 Hz, $^2J_{P,P}$ =34.7 Hz), 29.4 ppm ($^2J_{P,P}$ = 17.1 Hz, $^2J_{P,P}$ = 65.3 Hz) and 10.8 ppm($^2J_{P,P}$ = 34.7 Hz, $^2J_{P,P}$ = 65.3 Hz). These signals come from the two phosphorus groups from the ligand and one from PPh$_3$, all coupling with each other. ^{1}H and ^{31}P-NMR are in agreement with the proposed structure and are comparable with the related (^{Ph}**dpbp**)NiPPh$_3$ analogue reported by Moret *et al.*[18]
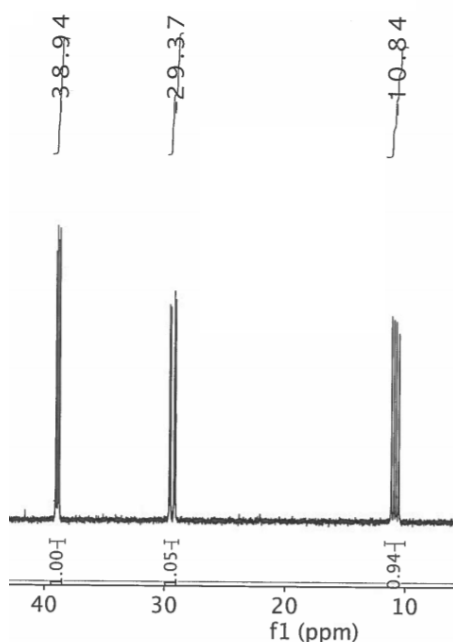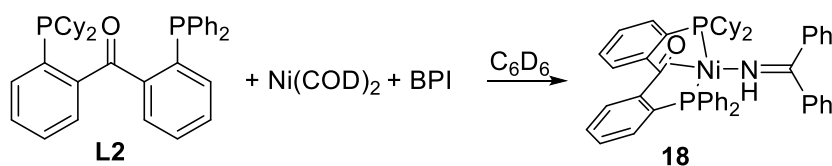

Figure 18: Zoom of the ^{31}P-NMR spectrum of the (^{Cy}PCO^{Ph}P)Ni(PPh$_3$)

*Scheme 31: Complexation of **L2**, Ni(COD)$_2$ and BPI, resulting in complex **16**, (**L2**)Ni(BPI)*

Coordination of **L2** to Ni(COD)$_2$ with BPI as co-ligand (Scheme 31) also resulted in a clean ^{31}P-NMR spectrum, shown in Figure 20. Two doublets are observed, at 35.1 and 7.7 ppm, coupling with $^2J_{P,P}$ = 82Hz. The ^{1}H-NMR shows a peak of bound BPI at 9.90 ppm, and traces of free, but no bound, COD left. In the ^{13}C-NMR shown in Figure 19 both the C=O and C=N were observed as double doublets, appearing at 117.70 ($^2J_{P,C}$ = 4.1 Hz, $^2J_{P,C}$ = 6.2 Hz) and 167.88 ($^3J_{P,C}$ = 4.7 Hz, $^3J_{P,C}$ = 6.2 Hz), respectively. This indicates the ketone moiety is bound, as well as the BPI. Single crystals suitable for XRD diffraction
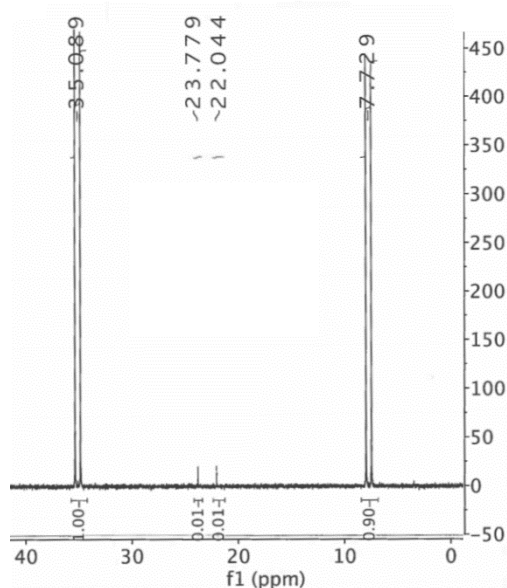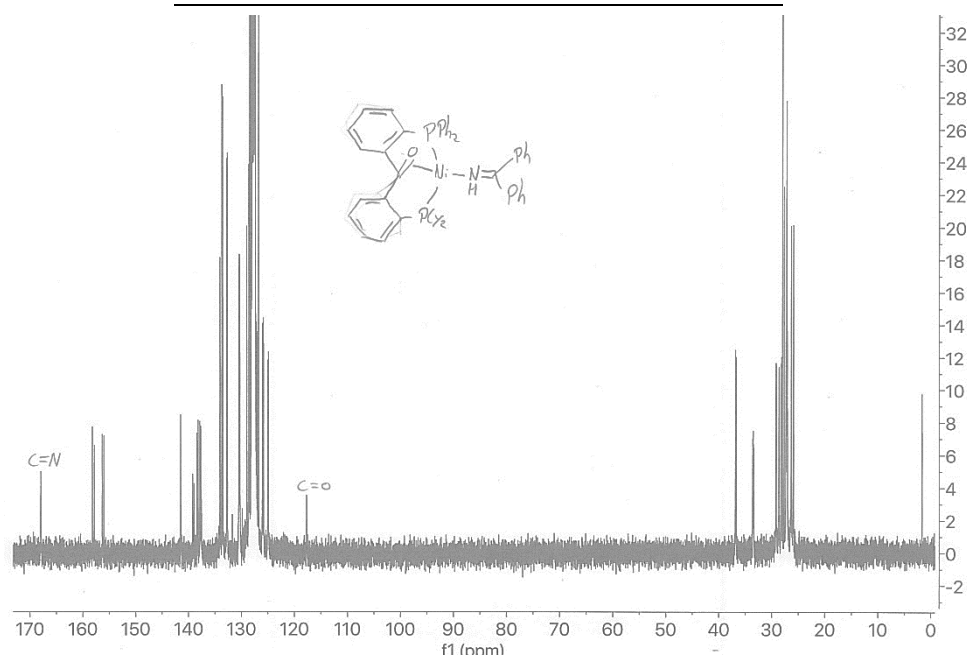
Figure 20: Zoom of the ³¹P-NMR spectrum of (ᶜʸPCOᴾʰP)Ni(BPI)

*Figure 19: ¹³C-NMR spectrum of (**L2**)Ni(BPI).*

were obtained by vapour diffusion with a toluene/hexane system, in which the crystal structure of this complex was obtained (Figure 21). The most important bond lengths and angles, and their comparison with the (ᴾʰdpbp)Ni(BPI) complex are shown in Table 2. In accordance with the ¹³C-NMR, the structure of **18** contains a side-on bound ketone moiety, with Ni1-C7 and Ni1-O1 bond lengths of 1.968 and 2.018 Å, respectively. The C7-O1 binding length (1.318 Å) is between that of the unbound ᴾʰdpbp (1.213 Å)[28] and that of a single C-O bond (1.43 Å in ethanol)[36]. This binding length is similar to that of **6** (ᴾʰdpbp)Ni(BPI), indicating a similar extent of activation of the ketone in both species. The sum of bond angles around C7 (Å) lies between the expected values for sp² and sp³ hybridization (328.5° and 360°, respectively), as expected from the Dewar-Chatt-Duncanson model. The N1-C38 bond length of 1.284 Å lies close to the value of the free ligand (1.28 Å)[36] and is comparable to the binding length of η¹ bound BPI, 1.294 Å, as found by Zhao *et al.*[37], using an NHC-based Ni(0) complex ((IPr)Ni(η²-BPI)(η¹-BPI), IPr = 1,3-bis(diisopropylphenyl)-imidazolium)), indicating the π-backdonation to the imine is small. The P1-Ni1-P2 bite angle of 126.08° is slightly larger than that of **6** and indicates that the
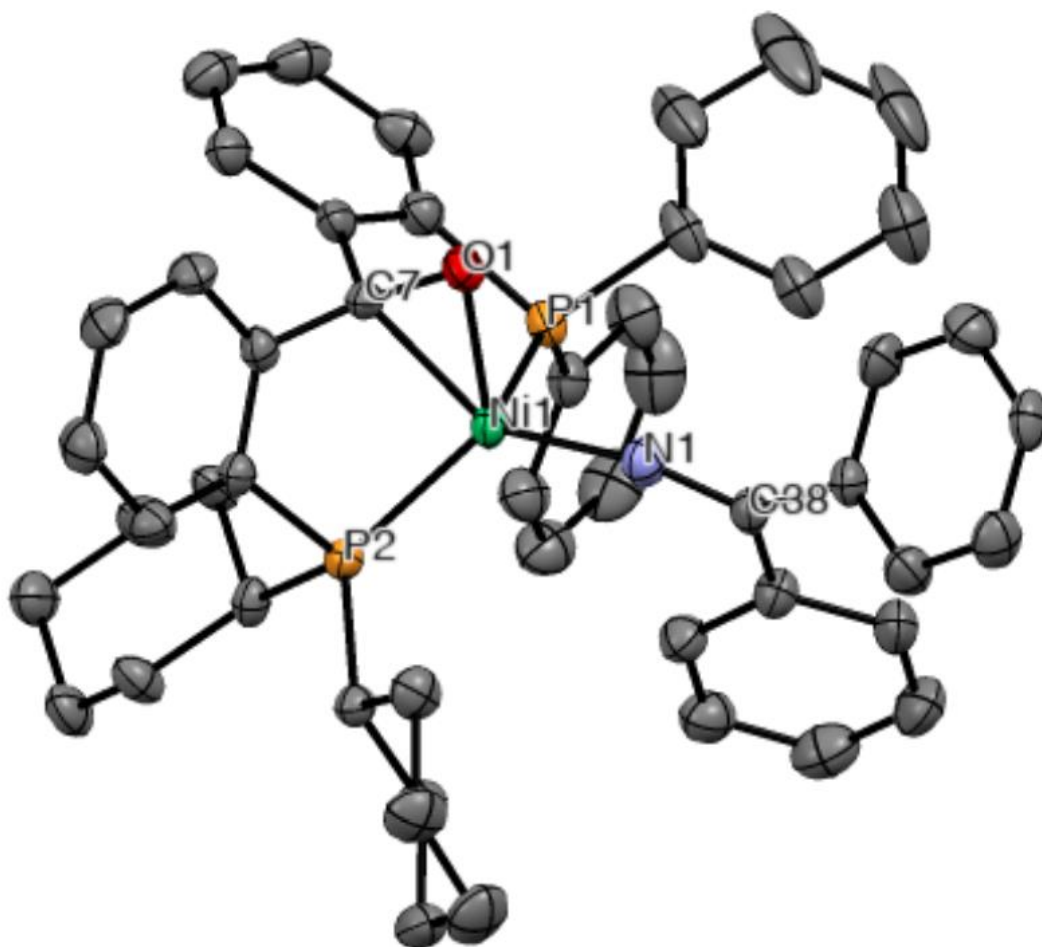
*Figure 21: X-ray structure of (**L2**)Ni(BPI). Co-crystallized toluene and hydrogen atoms were omitted for clarity. Ellipsioids are shown at 50% probability level.*

geometry around the nickel is a distorted tetrahedral. All in all the crystal structure of **18** is very similar to that of **6**, indicating that the change in bulk and electronic properties of the PCy$_2$-group does not influence the crystal structure.

	^{Cy}PCO^{Ph}P	^{Ph}dpbp
Ni1-C7	1.968	1.976
Ni1-O1	2.018	2.022
C7-O1	1.318	1.320
P1-Ni1-P2	126.08	123.08
N1-C38	1.284	1.289

*Table 2: Selected bond distances (Å) and bond angles (°) for **17** and **6***

All in all, **L2** behaves better in complexation reactions than **L1**. Coordination without co-ligand, with acetophenone or phenylacetylene resulted in a similar species in the ^{31}P-NMR, proposed to be compound **13**. Obtaining a complex like **13** was one of the goals of this project, but as isolation and further characterization proved unsuccessful, the project was continued with another complex.

Coordinating **L2** to Ni(COD)$_2$ with PPh$_3$ or BPI as co-ligand resulted in a clean reaction, respectively obtaining compounds **17** (**L2**)Ni(PPh$_3$) and **18** (**L2**)Ni(BPI). A crystal structure of **18** was obtained, and

comparison with the [Ph]dpbp analogue[18] showed coordination occurred in a similar fashion, so the change in bulk or electronic properties does not influence the coordination of **L2** to Ni(0).

3.3. Catalytic comparison in alkyne cyclotrimerization

Recently our group found that **1** (^{Ph}dpbp) in combination with Ni(COD)$_2$ efficiently catalyses the [2+2+2] cyclotrimerization reaction of terminal alkynes[31] (Scheme 32). The origin of the high catalytic activity was assigned to the hemilabile character of the ligand. In order to see the effect of substitution of the phosphine arms, nickel systems supported by **L1** and **L2** were tested as catalyst for the cyclotrimerization of methylpropiolate.
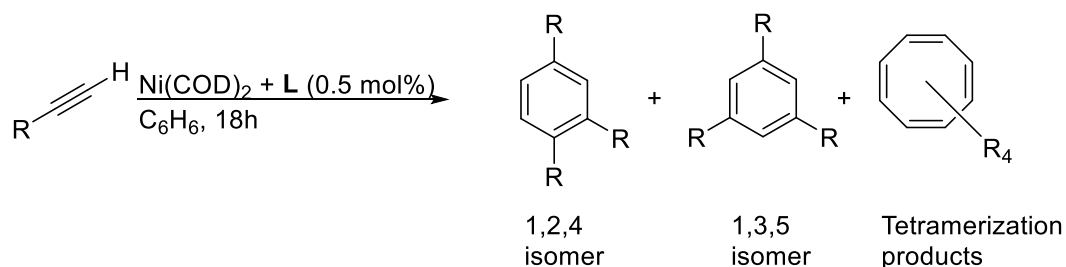
Scheme 32: General scheme of the [2+2+2] alkyne cyclotrimerization reaction. The ratios between the different products depended on the catalyst and alkyne used.
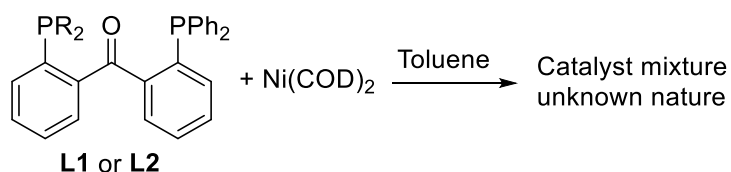
The [2+2+2] alkyne cyclotrimerization reaction catalysed by transition metals is an efficient reaction to get substituted benzene-derivatives. These reactions themselves are very atom-efficient, but multiple isomers can be formed, potentially leading to side-products. Not only are there 2 isomers formed in the trimerization, isomers with a 1,2,4 and 1,3,5 substitution pattern, but also tetramerization products can be observed[38,39]. A scheme showing the origins of the different isomers is shown in Scheme 33.
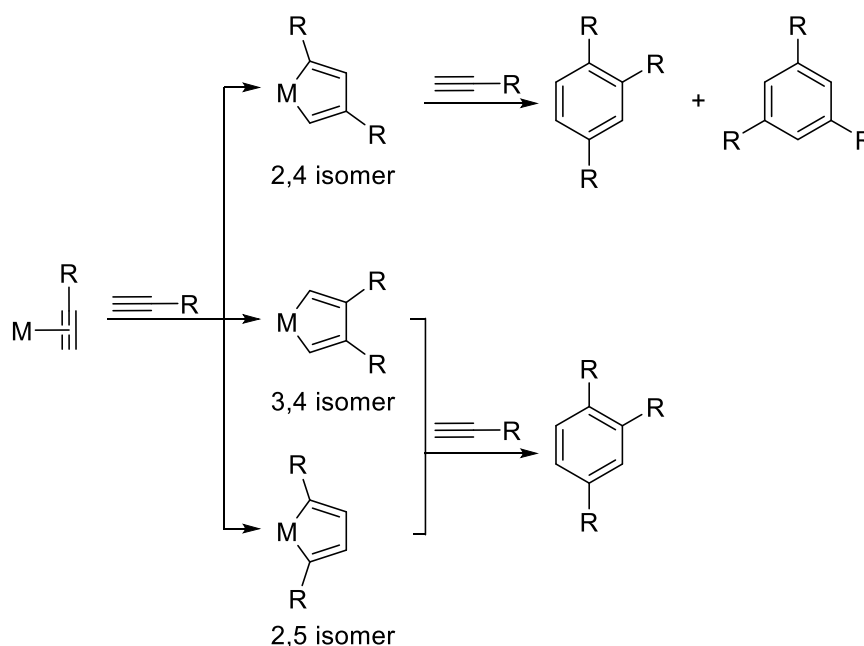
Scheme 33: Different pathways lead to different isomers in the [2+2+2] cyclotrimerization reaction. The 2,4 intermediate (Top) can lead to both isomers, where the 3,4 (middle) and 2,5 (bottom) intermediates always lead to the 1,3,5 isomer.

The ^{Ph}dpbp ligand, in combination with Ni(0), proved active in the cyclotrimerization of alkynes[31]. As the modified ligands used in this research have their bulk increased on only one side of the ligand, it is possible that one of the intermediates is favoured due to steric hindrance. Also, the more electron-donating properties of the PCy$_2$ group can influence the catalytic outcome.

As a model substrate methylpropiolate is chosen. This proved an easily activated substrate in previous research[31], most likely because of the very electron-withdrawing carboxylic ester group, leaving the alkyne relatively electron-poor.

Scheme 35: Preparation of the catalyst mixture used in cyclotrimerization reactions

Cyclotrimerization reactions were carried out by making a catalyst solution first, as shown in Scheme 35. **L1** or **L2** and Ni(COD)$_2$ were combined and dissolved in toluene, yielding the black catalyst solution. The exact nature of the active catalyst mixture is unknown. Then slowly a solution of the alkyne (200 equivalents) in toluene was added to the catalyst mixture and stirred for 18 hours (Scheme 34).
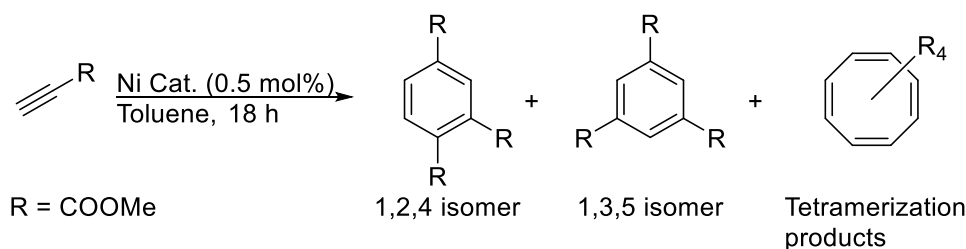
Scheme 34: [2+2+2] cyclotrimerization reaction of methylpropiolate, using 0.5 mol% of nickel catalyst. Multiple isomers can be formed in this reaction.

The reactions were analysed using ^{1}H-NMR. The integral of the peak of the 1,3,5 isomer could be compared with the integrals of the peaks of the 1,2,4-isomer, and from these integrals the ratio between the isomers could be calculated. The results of these reactions, and their comparison with the $^{p\text{-Tol}}$dpbp analogue[31] are shown in Table 3.

Ligand	Alkyne	1,2,4 (%)	1,3,5 (%)	Tetramerization products (%)
L1, $^{o\text{-Tol}}$PCO^{Ph}P	H≡COOMe	92	8	<1
L2, ^{Cy}PCO^{Ph}P	H≡COOMe	91	9	<1
1, ^{Ph}dpbp[31]	H≡COOMe	91	7	2

Table 3: Results of the [2+2+2] cyclotrimerization reaction using a different ligand and methylpropiolate. The ratio between the isomers is based on NMR integrals. The results for 1 are from the literature[31].

The calculated ratios do not differ significantly from each other. The system using **1** as ligand gives a selectivity for the 1,2,4 isomer of 91%, which is comparable for the selectivities found for the **L1** or **L2** systems (92 and 91%, respectively). Tetramerization products were not observed in ^{1}H-NMR with the **L1** and **L2** systems, but the formation of these products is also very minor in the system using **1** (2%). Overall, the modification of the phosphine on the ligand by bulkier and/or electron-rich substituents does not affect the performance of the catalyst in term of selectivity for the investigated conditions.
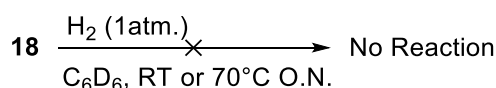
3.4. Reactivity of (^{Cy}PCO^{Ph}P)Ni(BPI) towards the activation of small molecules

Next the reactivity of (^{Cy}PCO^{Ph}P)Ni(BPI) towards the activation of small molecules was investigated. **L2** was chosen over **L1** because it behaved much better in coordination reactions. From the complexes formed with **L2** the (**L2**)Ni(BPI) complex (Compound **18**) was chosen. The bifunctional character of the ^{Ph}dpbp analogue, compound **6**, was already demonstrated using MeOTf, making **18** a potential candidaite for bifunctional activation as well.

First the reactivity towards dihydrogen (H$_2$) was investigated (Section 3.4.1). Secondly the activity towards diphenylsilane is investigated in section 3.4.2, and as a proof of concept the catalytic activity in the hydrosilylation of alkenes and alkynes is shown (Section 3.4.2.1). The focus will lie on the hydrosilylation of alkynes, as currently only few examples exist in the literature of the hydrosilylation of alkynes using a nickel catalyst[40–42].

3.4.1. Attempted hydrogenation

First the reactivity of **18** towards H$_2$ was investigated. Hydrogen gas (approx. 1 atm.) was introduced to a degassed solution of **18** in C$_6$D$_6$ and the reaction was followed *in situ* with NMR in a J. Young type NMR tube. Following the reaction shown in Scheme 36 over time, no changes in NMR were observed for the starting materials, neither at room temperature or at 70°C O.N. at the tested conditions. Complex **18** is inactive in the activation of hydrogen at the tested conditions

$$\textbf{18} \xrightarrow[\text{C}_6\text{D}_6,\text{ RT or 70°C O.N.}]{\text{H}_2\text{ (1atm.)}} \text{No Reaction}$$

*Scheme 36: Reaction conditions to test the reactivity of **17** towards H$_2$*

3.4.2. Reactivity of (^{Cy}PCO^{Ph}P)Ni(BPI) towards H$_2$SiPh$_2$

Secondly the activation of **18** towards H$_2$SiPh$_2$ was investigated, as shown in Scheme 37. Reactions were carried out on NMR scale in C$_6$D$_6$ at RT and monitored using ^{1}H- and ^{31}P-NMR.
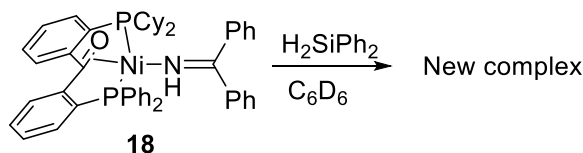
*Scheme 37: Reaction between complex **17** and H$_2$SiPh$_2$ in C$_6$D$_6$.*

In Figure 22 and Figure 23 the reaction between **18** and H$_2$SiPh$_2$ is monitored using ^{1}H and ^{31}P-NMR respectively. Adding one equivalent of silane to a solution of **18** changed the colour from black to dark green. In the ^{31}P-NMR (Figure 23,Spectrum 4) a new major species is observed with two doublets at 59.64 ppm and 46.29 ppm, with a quite large coupling constant of J = 192 Hz. This species disappears over the course of 6 hours, and a species at 22.84 ppm and 20.64 ppm, coupling with 51 Hz can be observed (Figure 23,Spectrum 3). ^{1}H-NMR shows that for the H$_2$SiPh$_2$ is not consumed after 1 hour (Figure 22, spectrum 4), but is fully consumed after 6 hours (Figure 22, spectrum 3). The peak of bound BPI seems to lose intensity and a new peak is observed at 10.46 ppm, indicating the release of BPI.

Adding a second equivalent of silane changed the colour of the solution from dark green to yellow/orange. Looking at the ^{31}P-NMR spectrum of the reaction after 1 hour (Figure 23, spectrum 2) shows the previously observed species are still present, and a new, third, species at 16.51 ppm and 28.33 ppm is formed, coupling with J = 21 Hz. Leaving the reaction overnight resulted in more of this new species (Figure 23, spectrum 1). In the ^{1}H-NMR, shown in (Figure 22, Spectrum 2), free H$_2$SiPh$_2$ is present after 1 hour, as well as some unknown silane species between 5 and 6.5 ppm. More of the
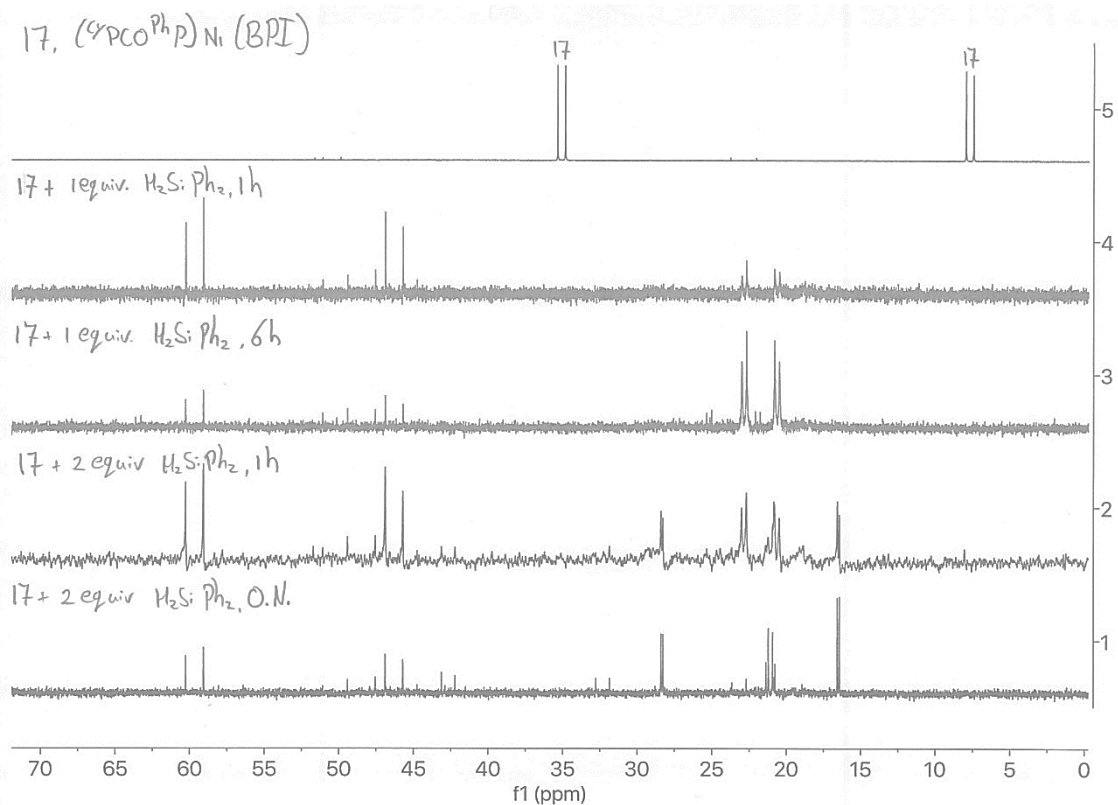
*Figure 23: ³¹P-NMR spectra of **18** with H₂SiPh₂. 5: No H₂SiPh₂. 4: 1 equiv. H₂SiPh₂, after 1 hour. 3: 1 equiv. H₂SiPh₂, after 6 hours. 2: 2 equiv. H₂SiPh₂, after 1 hour. 1: 2 equiv. H₂SiPh₂, after O.N. reaction.*

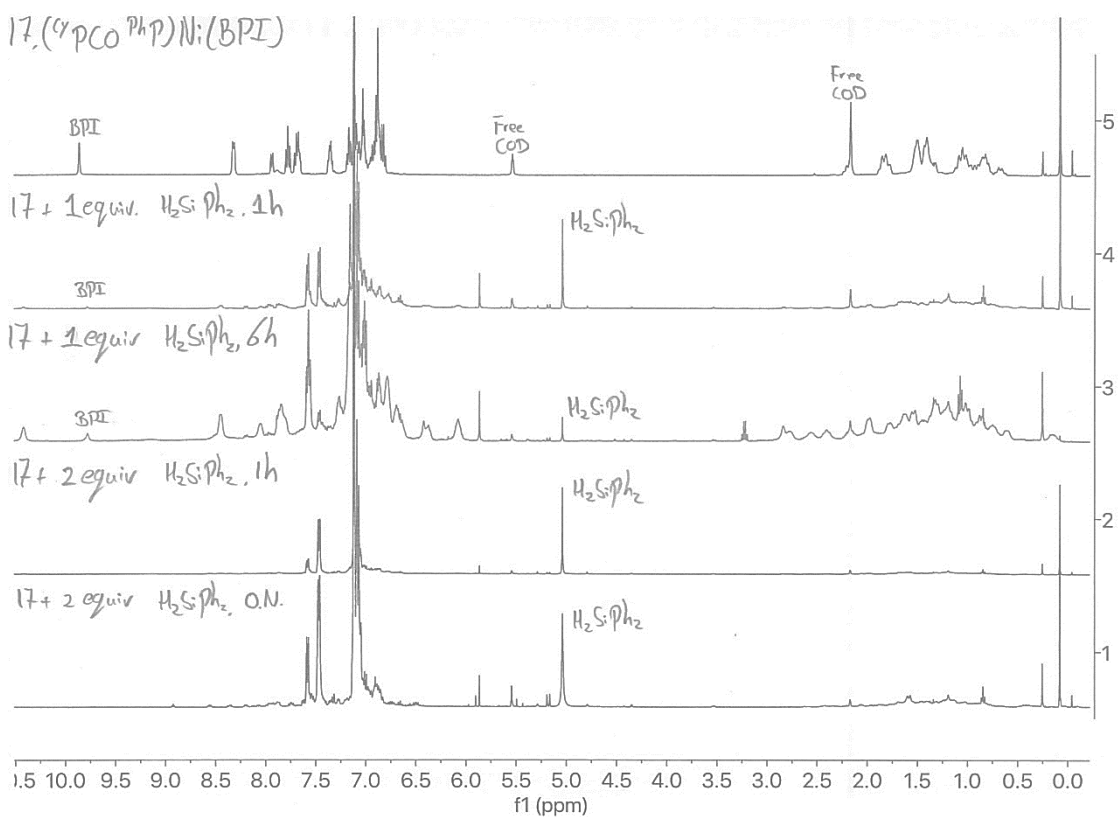*Figure 22: ¹H-NMR spectra of **18** with H₂SiPh₂. 5: No H₂SiPh₂. 4: 1 equiv. H₂SiPh₂, after 1 hour. 3: 1 equiv. H₂SiPh₂, after 6 hours. 2: 2 equiv. H₂SiPh₂, after 1 hour. 1: 2 equiv. H₂SiPh₂, after O.N. reaction.*

silane species appear after reaction overnight, and still not all the H₂SiPh₂ is consumed (Figure 22, spectrum 1). No species are observed in the region below 0 ppm, so it is unlikely a nickel-hydride

species is obtained.

The nature of the complexes formed when reacting (^{Cy}PCO^{Ph}P)Ni(BPI) with H_2SiPh_2 is still unknown, as isolation proved unsuccessful. No further evidence towards a formed species was obtained. However, the colour change upon adding 1 equivalent of silane to **18**, turning the solution dark green, indicates a reaction is occurring, and this reaction is completed, or a second reaction occurs, when a second equivalent of silane is added and reacted O.N, turning the solutions yellow/orange. According to the colour change, the consummation of H_2SiPh_2 and the release of BPI, **18** is reactive towards H_2SiPh_2. Subsequently, **18** will be tested for catalytic activity in hydrosilylation reaction.

3.4.3. Proof of concept in Hydrosilylation reactions with (^{Cy}PCO^{Ph}P)Ni(BPI)

As **18** proved reactive towards H_2SiPh_2, the reactivity of **18** in the hydrosilylation of alkenes was investigated. In previous work with the ^{Ph}dpbp ligand[43] complexed to Co(I) and Co(II), it proved active in the hydrosilylation of 1-octene (Scheme 38).
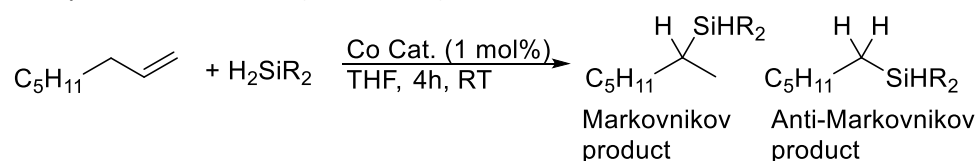
Scheme 38:Hydrosilylation of 1-octene with H_2SiPh_2 using a Cobalt catalyst bearing a ^{Ph}dpbp ligand

In ^{1}H-NMR the Markovnikov and anti-Markovnikov products will be observed as a doublet and triplet for the Si-H, respectively. If the ^{1}H-NMR is not sufficiently clear, an APT-NMR measurement can be used to establish which product is formed, as the Markovnikov has two CH_3 and a CH group, and the anti-Markovnikov only one CH_3 group.
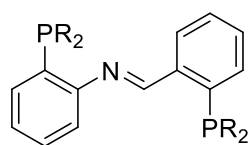

Figure 24: The imine derivative of the ^{R}dpbp ligand, ^{R}PCN^{R}P

Also, the imine derivative of this ligand, ^{R}PCN^{R}P (Figure 24), bearing an imine group in the backbone instead of a ketone, shows activity in hydrosilylation when complexated to a Ni^0 centre[44].

For **L2** the catalysis was done using complex **18** (^{Cy}PCO^{Ph}P)Ni(BPI). For **L1** a mixture of **L1** and Ni(COD)$_2$ in benzene was used. As Scheme 39 shows, in a normal hydrosilylation experiment, a solution of 1.1 equivalent H_2SiPh_2 and 1-octene in benzene was stirred overnight in the presence of 1 mol% nickel catalyst. The yields reported are the NMR yields, based on mesitylene as internal standard.
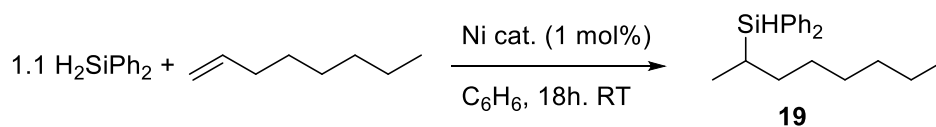
Catalyst	Conversion of H_2SiPh_2 (%)	Yield of **19**
L1 + Ni(COD)$_2$	<1	<1
17	38	15

Scheme 39: Hydrosilylation reaction of 1-octene with H_2SiPh_2, using 1 mol% of nickel catalyst, stirring O.N. at RT in benzene. The product is the anti-Markovnikov product. The results are shown in the table above. Yields are calculated from ^{1}H-NMR, with mesitylene as internal standard.

For the hydrosilylation of 1-octene the catalyst solution of **L1** and Ni(COD)$_2$ proved inactive (Scheme 39). **18** performed better as a catalyst for the hydrosilylation of 1-octene. According to the ^{1}H-NMR, octyldiphenylsilane was formed with a yield of 33 mg, or 15%. The product is observed as a triplet in

the NMR, which means it is the anti-Markovnikov product. The conversion of H_2SiPh_2 was calculated to be 38%. Still **18** proved to be not a very good catalyst for the hydrosilylation of 1-octene under the tried conditions.

Next, the hydrosilylation of alkynes was investigated using our catalyst system. The products of these reactions, vinylsilanes, are important building blocks in synthetic chemistry[45]. Very few examples of hydrosilylation of alkynes using a nickel catalyst are found in literature. The groups of Montgomery[46] and Bouwman[47] both investigated this reaction using a NHC-nickel complex, as shown in Figure 25
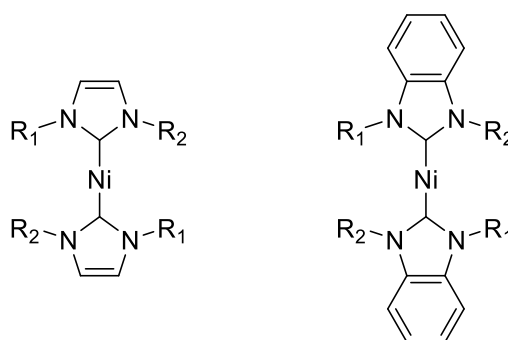
Figure 25: NHC-nickel complexes used in the hydrosilylation of alkynes. R_1 = Me, iPr, Bn. R2 = Me, iPr, Ph, Bn[42].
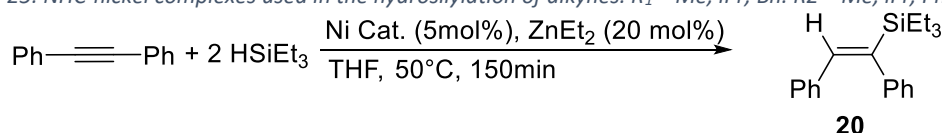
Scheme 40: Hydrosilylation of diphenylacetylene with triethylsilane. The catalyst used is shown in Figure 25. 99% conversion was reached in 150 min.

With catalyst systems shown in Figure 25, diphenylacetylene could efficiently be hydrosilylated to **20**, using 5 mol% of catalyst at 50°C, reaching 99% yield after 150 minutes (Scheme 40)[42]. The group of
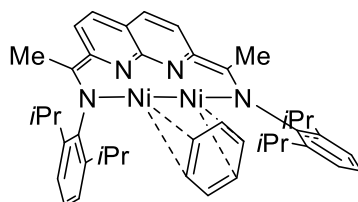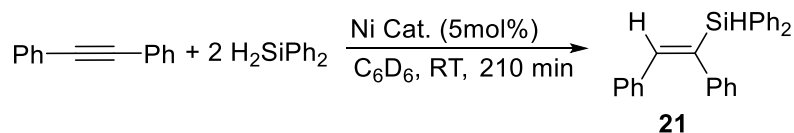

Figure 26: Dinuclear nickel catalyst used by Uyeda et al[40].

Scheme 41: Hydrosilylation of diphenylacetylene with H_2SiPh_2. The catalyst used is shown in Figure 26. 20 was obtained in 93% yield [48].

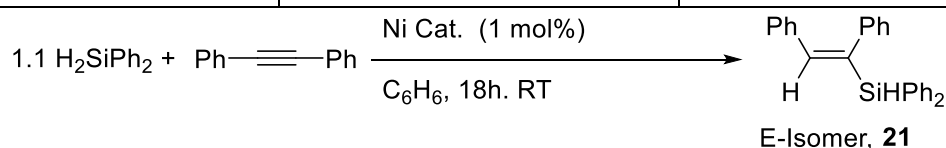Uyeda made use of a dinuclear nickel catalyst, shown in Figure 26.

Using the catalyst shown in Figure 26, the hydrosilylation of diphenylacetylene ws done in benzene, at RT, and reached 93% yield after 210 minutes (Scheme 41).

Diphenylacetylene was used as a model alkyne. For **L2** the catalysis was done using complex **18** (^{Cy}PCO^{Ph}P)Ni(BPI). For **L1** a mixture of **L1** and Ni(COD)$_2$ in benzene was used. As Scheme 42

Catalyst	Conversion of H$_2$SiPh$_2$ (%)	Yield of **21**
L1 + Ni(COD)$_2$	<1	<1
18	91	49

Scheme 42: Hydrosilylation of diphenylacetylene with H$_2$SiPh$_2$, using 1 mol% of catalyst. Both the E and Z-isomer can be formed, but the product is the E-isomer. The results are shown in the table above. Yields are calculated from ^{1}H-NMR, with mesitylene as internal standard.
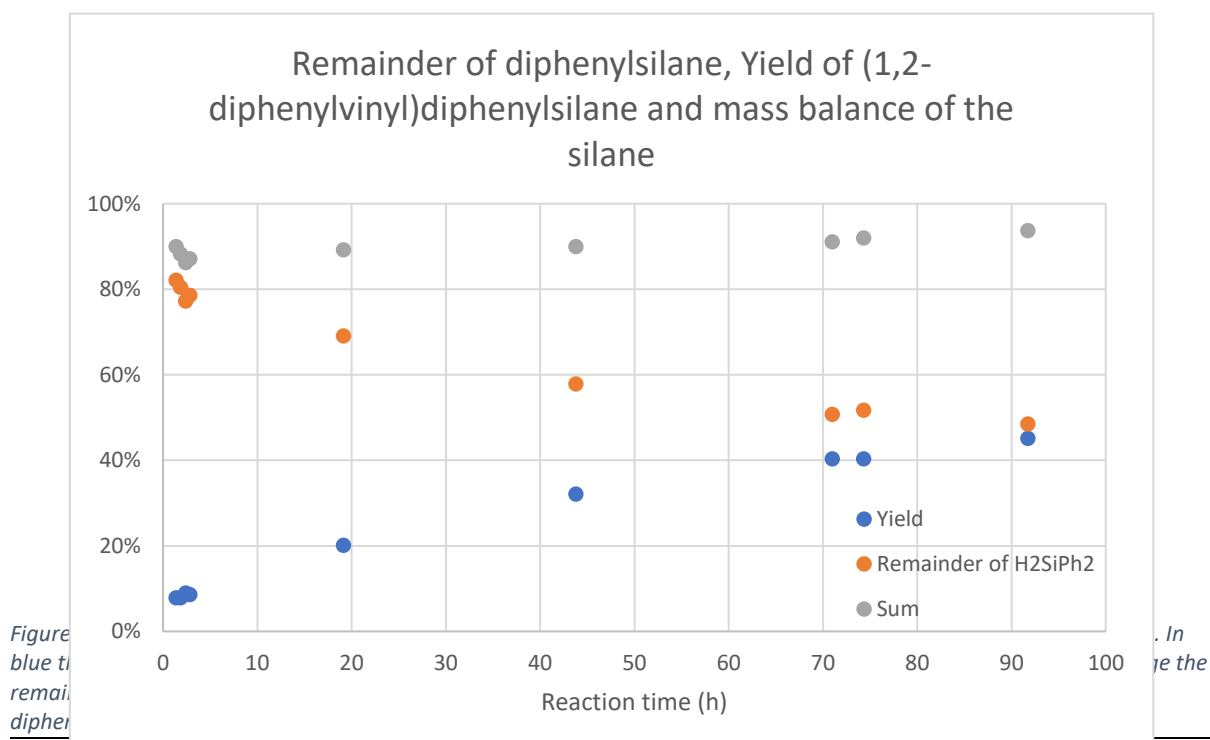
Catalyst	Conversion of H$_2$SiPh$_2$ (%)	Yield of **19**
L1 + Ni(COD)$_2$	<1	<1
17	38	15

$$1.1\ H_2SiPh_2 + Ph{=}\!\!=\!\!{=}Ph \xrightarrow[\text{C}_6\text{H}_6,\ 18\text{h. RT}]{\text{Ni Cat. (1 mol\%)}} \begin{array}{c} \text{Ph} \quad\ \text{Ph} \\ \diagdown\quad\diagup \\ \\ \text{H}\quad\ \ \text{SiHPh}_2 \end{array}$$

E-Isomer, **21**

shows, in a normal hydrosilylation experiment, a solution of 1.1 equivalent H$_2$SiPh$_2$ and diphenylacetylene in benzene was stirred overnight in the presence of 1 mol% nickel catalyst. The yields reported are the NMR yields, based on mesitylene as internal standard.

The isomer formed is the E-isomer, based on ^{1}H-NMR and comparison with the literature[48]. From ^{1}H-NMR the yield could be calculated, based on mesitylene as internal standard. The system of **L1** proved inactive in the hydrosilylation of phenylacetylene under the tried conditions. **18** showed a high conversion of H$_2$SiPh$_2$ (91%) and a moderate yield (49%).

The reaction was done again on NMR-scale, with mesitylene added as internal standard and monitoring over time. The reaction was carried out in a J. Young type NMR tube, without stirring. The results of this reaction are shown in Figure 27. The yield of **21** increases slowly over time, approaching 50% only after 92 hours. Even though the yield is quite low, the selectivity stays quite high, as the


Remainder of diphenylsilane, Yield of (1,2-diphenylvinyl)diphenylsilane and mass balance of the silane

● Yield
● Remainder of H2SiPh2
● Sum

Reaction time (h)

Figure ... In blue t... ... ...e the remai... dipher...

37

amount of H_2SiPh_2 remaining and desired product formed together account for about 90% of the starting amount of silane over the whole course of the reaction. Stirring of the reaction mixture greatly increases both the yield and conversion.
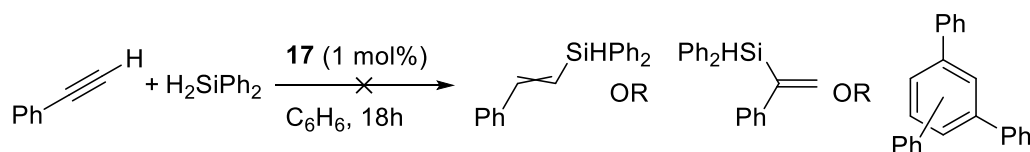
Scheme 43: Hydrosilylation of phenylacetylene with H_2SiPh_2, and the different possible products.`

The hydrosilylation of phenylacetylene, a terminal alkyne, was also attempted. Scheme 43 shows that this reaction can give different isomers of the hydrosilylated product, both of which have been seen in literature using a different cobalt catalyst[49,50]. Another possibility is that the hydrosilylation does not occur, but that the cyclotrimerization product is formed. When analysing the reaction with ^{1}H-NMR, none of the proposed products were observed, so **18** is inactive in the hydrosilylation of terminal alkynes under the tried conditions.
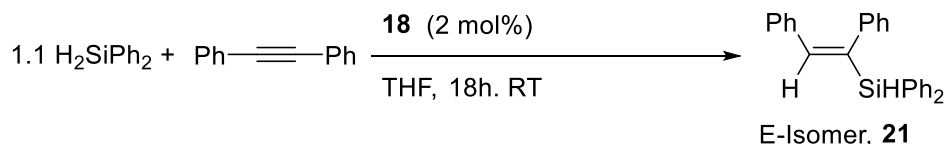
The hydrosilylation of diphenylacetylene using **18** as catalyst was carried out in different solvents. These reactions were carried out as described above, changing the solvent from benzene to THF, Et_2O or toluene. The results of these reactions, which were stirred O.N. at RT, are shown in Scheme 45.
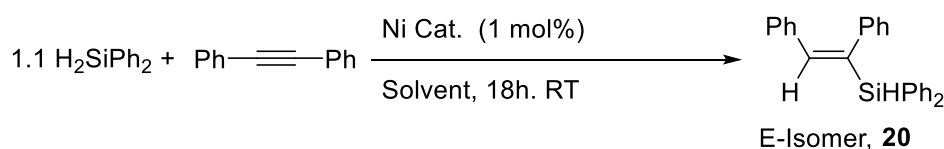
Solvent	Conversion of H_2SiPh_2 (%)	Yield of **21**(%)	Mass balance of H_2SiPh_2 and **21** (%)
Benzene	91	49	56
THF	28	25	97
Et_2O	81	55	75
Toluene	73	41	76

Scheme 45: Results of the hydrosilylation of diphenylacetylene with H_2SiPh_2 and (^{Cy}PCO^{Ph}P)Ni(BPI) as catalyst, in different solvents at RT. The values were calculated from ^{1}H-NMR integrals, based on mesitylene as IS. The yield of E-(1,2-diphenylvinyl)diphenylsilane is calculated with respect to the starting amount of H_2SiPh_2.

The reactions in benzene, Et_2O and toluene all behaved similarly. The conversion of H_2SiPh_2 is quite high in all case (91%, 81% and 73%, respectively), and the yields of **21** lie close to each other (49%, 55% and 41%). The results of the reaction done in THF are quite different. The conversion and yield are quite low, only 28% and 25% respectively. What stands out however, is the very high mass balance, indicating little side-reactions occur during this reaction.

*Scheme 44: Hydrosilylation of diphenylacetylene with H_2SiPh_2, using **17** as catalyst in THF. **20** was obtained in 91% yield, calculated from ^{1}H-NMR based on mesitylene as IS.*

As the mass balance of the hydrosilylation of diphenylacetylene with H_2SiPh_2 (**18** as catalyst) in THF was quite promising, a reaction with a higher catalyst loading was executed (Scheme 44). The yield of **21** was 91%, calculated from ^{1}H-NMR, using mesitylene as internal standard. H_2SiPh_2 was fully converted. The hydrosilylation of diphenylacetylene using H_2SiPh_2 in THF with a catalyst loading of 2

mol% looks like a promising reaction, although the reaction time of 18 hours is still longer than that for other nickel-based catalyst (99% and 93% yield in 150 min[42] or 210 min[48], respectively).

For the hydrosilylation reactions attempted, using the catalyst system with **L1** proved inactive towards either the hydrosilylation of alkenes or alkynes. **18** proved moderately active in the hydrosilylation of 1-octene, reaching a yield of 15% after 18 hours under the attempted conditions. **18** proved more active in the hydrosilylation of diphenylacetylene, achieving a yield of 91% after 18 hours, in THF at RT. Still, compared to the reaction times in the literature, the reaction time of 18 hours is quite long.

4. Conclusions

In conclusion, the synthesis of the new, mixed bulky diphosphine ketone ligands proved to be successful. **L1** and **L2** were synthesized with an overall yield of 16% and 4%, respectively.

Attempts were done to complexate **L1** to Ni(0) without success. Nonetheless, the complexation of **L1** to nickel in the presence of phenylacetylene results in the possible formation of a nickel-alkyne species, in which the ketone is not bound to the metal centre. This observation, that the ketone is unbound, might be an explanation to the difference in reactivity compared to the other co-ligands tested.

Complexations of **L2** behaved better. From the complexations of **L2** to Ni(COD)$_2$ without co-ligand, or with phenylacetylene or acetophenone as co-ligand, a complex is proposed where nickel is only supported by **L2**. Isolation of this compound was unsuccessful, however. Complexations of **L2** to Ni(COD)$_2$ with PPh$_3$ or BPI resulted in the well-defined (**L2**)Ni(PPh$_3$) and (**L2**)Ni(BPI) complexes. For (**L2**)Ni(BPI) a crystal structure was obtained, which is very similar to the (^{Ph}dpbp)Ni(BPI) complex, showing no effect of the increase in bulk or change in electronic properties the PCy$_2$ group brings.

Both **L1** and **L2**, in combination with Ni(COD)$_2$, proved active in the [2+2+2] cyclotrimerization of methyl propiolate. No significant change in reactivity when compared to the ^{Ph}dpbp ligand was found however. The change in bulk and/or electronic properties of the phosphine arms does not influence the [2+2+2] cyclotrimerization of alkynes under the tried conditions.

The complex of (**L2**)Ni(BPI) proved inactive towards the activaton of H$_2$. It showed reactivity towards H$_2$SiPh$_2$, but the formed compound is unknown. It is proposed that the BPI ligand dissociates and a complex with the silane is formed.

In the hydrosilylation of alkenes and alkynes, **L1** and Ni(COD)$_2$ proved inactive under the tried conditions. The (**L2**)Ni(BPI) complex proved moderately active in the hydrosilylation of 1-octene, reaching 15% yield after 18 hours at RT with a catalyst loading of 1 mol%. The activity towards the hydrosilylation of diphenylacetylene proved higher, reaching a yield of 91% after 18 hours, using a catalyst loading of 2 mol% and doing the reaction in THF at RT. Still, when comparing to the literature, the reaction time is very long. (**L2**)Ni(BPI) proved inactive in the hydrosilylation of a terminal alkyne, phenylacetylene, under the tried reaction conditions.

5. Outlook

5.1. Optimization of ligand synthesis

The ligands **L1** and **L2** were synthesized with an overall yield of 16% and 4%, respectively, which is quite low if complexes with these ligands are going to be studied more intensively. Especially the synthesis of **L2** proved difficult and hard to reproduce. None of the reaction steps seem to reach full conversion and a column is required for the work-up, in which quite some product oxidizes. Optimizing the reaction conditions, *e.g.* longer reaction times, different solvents, might give a reaction with a higher conversion and thus less side-products, and potentially a simpler work-up is necessary.

A possible way to improve the reaction is to change the carbonyl source. The chlorine of the used DMCC is an excellent leaving group, while the -NMe$_2$ group is a very poor one. If this group is changed to a better leaving group, -OR for example, the last step of the reaction should be more facile[51]. The difference in leaving character between this group and the chlorine should stay big enough to prevent disubstitution.

To make the work-up simpler the phosphorus might be protected before the work-up. A protection with BH$_3$, which can be helpful for alkylphosphines[52], was attempted in our group before, but removal of the protecting borane proved difficult, most likely for steric reasons[25]. Protection of the phosphine using sulphur is another possibility, but the conditions are not very mild[53]. As Scheme 46 shows, first the phosphine is refluxed in the presence of elemental sulphur, in CS$_2$, to yield the protected phosphine. Deprotection is done by refluxing O.N. in a 2:1 mixture of MeOH and P(*t*-Bu)$_3$. CS$_2$ is very toxic, however, so a (de)protection protocol based on this is undesirable for personal safety reasons.

$$PR_3 \xrightarrow[\text{Reflux, 16 h}]{S,\ CS_2} R_3P=S \xrightarrow[\text{Reflux, 16 h}]{MeOH,\ P(t\text{-Bu})_3\ (2:1)} PR_3$$
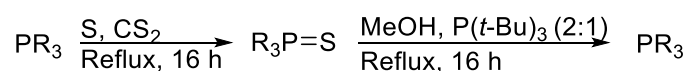
Scheme 46: Protection and deprotection of phosphines based on sulphur.

Simply allowing the phosphine to be oxidized and reducing after the work up can also be looked into, if a suitable reduction protocol can be found. Most reduction protocols are for triarylphosphines or diarylalkylphosphines only, and dialkylarylphosphines are not mentioned[54]. Another protocol, which mentions trialkylphosphines as well, require a distillation step[55], which will be hard, if not impossible, with the finished ligand.

5.2. Ligand modifications

Other phosphine arms can also be investigated. For one, the -PPh$_2$ group could be exchanged for a -P(*p*-Tol) group. This group has similar properties, electronic as well as steric, as the phenyl, but due to the -CH$_3$ group it is easier to monitor in NMR, and the -CH$_3$ helps with the solubility of the ligand. The -PCy$_2$ group can also be modified, changing the cyclohexyl to *e.g.* isopropyl or *t*-butyl groups. As seen in Table 4, this changes the electronic parameter v$_{CO}$ only slightly, so the phosphorus will still donate strongly to the nickel centre. What does change is the steric bulk around nickel, with *i*-propyl lowering the bulk and *t*-butyl increasing it compared to cyclohexyl. These ligands can be made using the method of synthesis of ^{Cy}PCO^{Ph}P.

R-Group	Cone angle (°)	v$_{CO}$ (cm^{-1})
Phenyl	145	2068.9
p-Tolyl	145	2066.7
Cyclohexyl	179	2056.4
i-Propyl	160	2059.2
t-Butyl	182	2056.1

Table 4: Cone angle and v$_{CO}$ for used and potential phosphine substituents, based on a PR$_3$ group[32].

Also, the ^{Cy}dpbp ligand could still be of interest. The two strongly donating -PCy$_2$ groups might allow for a complex without co-ligand, which is also helped by the increase in bulk. As no oversubstitution was observed in the synthesis route followed here, it might be applied to this ligand as well.

5.3. Coordination to other base metals

In this research, **L1** and **L2** were only complexated to Ni^0. Complexations with Ni^I or Ni^{II} can be of interest, as can other first row transition metals such as iron or cobalt. These have a lower electron density than Ni^0, a d^{10} metal. This means the ketone might be not coordinated, allowing for greater backbone flexibility. This proved to be useful for **L1**, when complexated to $Ni(COD)_2$ with phenylacetylene as a co-ligand, as the binding of the ketone prevented the formation of stable complexes with other co-ligands.

5.4. $^{Cy}PCO^{Ph}P$ complexes

An often-observed species in complexations with $^{Cy}PCO^{Ph}P$ and $Ni(COD)_2$ gives two doublets in ^{31}P-NMR at 17.5 ppm and 28.1 ppm. The exact nature of this species is unknown, but as it appears when using different co-ligand, or no co-ligand at all, it is proposed to be e a complex without co-ligand or a solvent adduct. To establish the nature of this species isolation is most likely required, which has not succeeded yet. If the complex can be obtained purely, more information can be acquired from NMR, and a crystal structure, if obtainable, would be very helpful in characterizing this species.

5.5. Reactivity of ($^{Cy}PCO^{Ph}P$)Ni(BPI) towards small molecules

(**L2**)Ni(BPI) proved inactive towards activation of H_2 in the tried conditions. If the isolation of the (**L2**)Ni complex proves successful, its reactivity towards the activation of H_2 can be investigated as well. For the hydrosilylation of alkynes with the (**L2**)Ni(BPI) complex the conditions can still be optimized. Hydrosilylation might be improved be screening different catalyst loadings, reaction temperatures or reaction times. Also, the substrate scope can be extended, as only the hydrosilylation of 1- octene and diphenylacetylene was investigated here. Different alkynes, both terminal or internal, or carbon-heteroatom bonds, such as imines and ketone, can also be investigated as substrates for hydrosilylation reactions. Other classes of small molecules can also be tested for reactivity towards (**L2**)Ni(BPI), such as alkyl halides (*e.g.* MeI).

6. Experimental

6.1. Materials

Unless otherwise stated, dry degassed solvents were used. Et_2O, toluene and hexane were purified using a MBRAUN MB SPS-800 solvent purification system. These solvents were degassed by bubbling N_2 through for at least 30 minutes and dried overnight over molecular sieves prior to usage. Dioxane and THF were distilled over sodium/benzophenone under N_2 atmosphere and bubbled through with N_2 for at least 30 minutes. These solvents were dried overnight over molecular sieves prior to usage. C_6D_6 and d_8-THF were degassed using the freeze-pump-thaw procedure and stored over molecular sieves prior to usage. Et_3N was degassed by bubbling N_2 through for at least 30 minutes and dried overnight over molecular sieves prior to usage.

All other chemicals were used as received from their supplier, unless stated otherwise.

6.2. Analysis methods

NMR spectra were recorded using a Varian 400 MHz or an Agilent 400 MHz NMR spectrometer, at 25 °C. ^1H, ^{13}C and ^{31}P NMR spectra were recorded at 400 MHz, 100 MHz and 162 MHz respectively. The chemical shifts are presented in ppm, referenced to the solvent residual peak[56], determined relative to TMS. Attenuated Total Reflectance (ATR) IR spectra were recorded using a Perkin Elmer Spectrum One FT-IR spectrometer. GC-MS measurements were executed using a Perkin Elmer Clarus 680 GC (column: PE, Elite 5MS, 15m x 0.25mm. ID x 0.25 µm), fitted with a Clarus SQ8T MS and analysed using TurboMass software. ESI-MS analysis was recorded with a Waters LCT Premier XE spectrometer. Elemental analysis was provided by Mikroanalytisches Laboratorium Koble, Müllheim an der Ruhr, Germany.

6.3. Synthesis methods

6.3.1. Ligand synthesis

Synthesis of (2-bromophenyl)diphenyl phosphine (7)
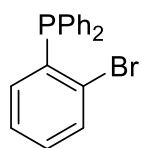
Based on a procedure by Moret *et al.*[18] 2-iodobromobenzene (6.8 ml, 53.7 mmol), diphenyl phosphine (10.09 g, 54.2 mmol), $Pd(PPh_3)_4$ (0.32 g, 0.28 mmol) and Et_3N (10.5 ml, 75.2 mmol) were dissolved in 100 ml dry, degassed toluene under N_2. After heating to 100°C for 18 hours the mixture was extracted with 80 ml degassed brine. The aqueous layer was washed with Et_2O (4x30ml) and MeOH (1x5ml). All organic layers were combined, dried over $MgSO_4$ and the solvent was evaporated. The remaining solid was washed with cold MeOH. The product was obtained (16.51 g, 48.39 mmol, 89%) as a pale-yellow solid after drying *in vacuo* overnight.

^{1}H NMR (400 MHz, C_6D_6, 25°C): δ_H 7.34 (Ar*H*, m, 5H), 7.04 (Ar*H*, m, 6H), 6.88 (Ar*H*, ddd, $^3J_{H,H}$ = 7.6 Hz, $^3J_{H,P}$ = 2.4 Hz, $^4J_{H,H}$ = 1.6 Hz, 1H), 6.76 (Ar*H*, dt, $^3J_{H,H}$ = 7.4 Hz, $^4J_{H,H}$ = 1.3 Hz, 1H), 6.67 (Ar*H*, dt, $^3J_{H,H}$ = 7.6 Hz, $^4J_{H,H}$ = 1.8 Hz, 1H).
^{31}P NMR (161 MHz, C_6D_6, 25°C) δ_P -4.7.
ATR-IR: v [cm^{-1}]: 3053, 1552, 1476, 1445, 1434, 1417, 1090, 1015, 754, 742, 694, 513, 488.
EI-MS: m/z: Calculated for [M]$^+$: 341, found 1.

Synthesis of (2-bromophenyl)di-*o*-tolylphosphine (8)
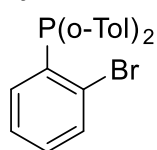
Dissolved 2-iodobromobenzene (6 ml, 46.7 mmol), di(*o*-tolyl)phosphine (8.9 g, 41.5 mmol), $Pd(PPh_3)_4$ (0.50 g, 0.43 mmol) and Et_3N (9 ml, 64.6 mmol) in 100 ml dry, degassed toluene under N_2. After heating to 100°C for 94 hours the mixture was extracted with 45 ml degassed brine. The aqueous layer was washed with Et_2O (3x20ml). All organic layers were combined, dried over $MgSO_4$ and the solvent was evaporated. The remaining solid was washed with cold. The product was obtained (15.35 g, 41.69 mmol, 94%) as a light-yellow solid after drying *in vacuo* overnight.

¹H NMR (400 MHz, C₆D₆, 25°C): δ_H 7.32 (Ar*H*, ddd, $^3J_{H,H}$ = 7.3 Hz, $^3J_{H,P}$ = 3.8 Hz, $^4J_{H,H}$ = 1.4 Hz, 1H), 6.96 (Ar*H*, m, 6H), 6.85 (Ar*H*, m, 3H), 6.69 (Ar*H*, dt, $^3J_{H,H}$ = 7.5 Hz, $^4J_{H,H}$ = 1.3 Hz, 1H), 6.63 (Ar*H*, dt, $^3J_{H,H}$ = 7.7 Hz, $^4J_{H,H}$ = 1.8 Hz, 1H), 2.36 (C*H₃*, d, $^4J_{H,P}$ = 1.3 Hz, 6H).
³¹P NMR (161 MHz, C₆D₆, 25°C) δ_P -19.6.
ATR-IR: ν [cm⁻¹]: 3054, 302, 2968, 2941, 2912, 1587, 1554, 1466, 1445, 1422, 1377, 1269, 1250, 1200, 1161, 1130, 1098, 1017, 746, 716.
EI-MS: m/z: Calculated for [M]⁺: 369, found 369.

Synthesis of 2-(di-o-tolylphosphino)-N,N-dimethylbenzamide (11)
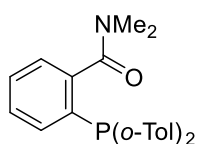
(2-bromophenyl)di-*o*-tolylphosphine (7.05 g, 19.1 mmol) was dissolved in 40 ml dry, degassed Et₂O under N₂ and cooled to -70°C. *n*-BuLi (1.6 M in hexane, 13.5 ml, 21.6 mmol) was added to the solution dropwise over 5 minutes while stirring. The solution was allowed to warm to RT and after 3 hours cooled back to -70°C. A solution of dimethyl carbamoyl chloride (2.33 g, 21.7 mmol) in 25 ml dry, degassed Et₂O was added dropwise over 5 minutes to the reaction mixture. The mixture was allowed to warm to RT again, while stirring for 20 hours. The reaction was cooled to 0°C and quenched with a solution of NH₄Cl (2.5 M in water, 30.5 ml) The aqueous layer was washed with Et₂O (3x15ml). The organic layers were combined, dried over MgSO₄ and the solvent was. The solid product was washed with cold Et₂O. The product was obtained (4.11 g, 11.4 mmol, 59%) as an orange solid after drying overnight in *vacuo*.

¹H NMR (400 MHz, C₆D₆, 25°C): δ_H 7.04 (Ar*H*, m, 3H), 6.98 (Ar*H*, dd, *J* = 7.4 Hz, *J* = 1.4 Hz, 2H), 6.93 (Ar*H*, m, 3H), 6.87 (Ar*H*, dd, *J* = 7.2 Hz, *J* = 1.3 Hz, 2H), 6.83 (Ar*H*, dd, *J* = 7.5 Hz, *J* = 1.4 Hz, 2H), 2.71 (N-C*H₃*, s, 3H), 2.36 (Ar-C*H₃*, d, $^3J_{H,P}$ = 1.3 Hz, 6H), 2.22 (N- C*H₃*, s, 3H).
¹³C NMR (100 MHz, C₆D₆, 25°C) : δ_C 169.9 (C=O, d, $^3J_{C,P}$ = 3.4 Hz), 144.7 (C-P, d, $^1J_{C,P}$ = 35.2 Hz), 142.2 (C-P, d, $^1J_{C,P}$ = 26.5 Hz), 135.0 (Ar 4°, d, $^2J_{C,P}$ = 11.7 Hz), 134.8 (Ar ,s), 133.9 (Ar 4°, d, $^2J_{C,P}$ = 15.4 Hz), 133.3 (Ar, s), 130.2 (Ar, d, $^3J_{C,P}$ = 4.6 Hz) 128.8 (Ar, s), 128.56 (Ar, s), 126.3 (Ar, d, $^3J_{C,P}$ = 8.0 Hz), 125.9 (Ar, s), 37.8 (N-Me, s), 33.8 (N-Me, s), 21.1 (Ar-*Me*, d, $^3J_{C,P}$ = 21.9 Hz).
³¹P NMR (161 MHz, C₆D₆, 25°C): δ_P -28.1.
ATR-IR: ν [cm⁻¹]: 3053, 2937, 1634, 1451, 1386, 1271, 1212, 1169, 1122, 1090, 1050, 779, 748.
EI-MS: m/z: Calculated for [M]⁺ : 362, found 362.

Synthesis of (2-(di-o-tolylphosphinophenyl)(2-(diphenylphosphino)phenyl)methanone (L1)
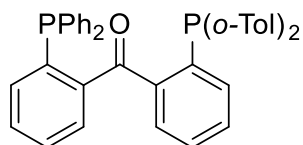
(2-bromophenyl)diphenyl phosphine (4.00 g, 11,7 mmol) was suspended in 30 ml dry, degassed Et₂O under N₂ and cooled to -70°C. *n*-BuLi (1.6M in hexane, 8.5 ml, 13.6 mmol) was added to the solution dropwise over 5 minutes while stirring. The solution was allowed to warm to RT and after 3 hours cooled back to -70°C. 2-(di-o-tolylphosphino)-N,N-dimethylbenzamide (4.29 g, 11.9 mmol) was dissolved in 9 ml dry, degassed THF, and added dropwise to the reaction mixture, over 5 minutes. The reaction was kept at -70°C for 10 minutes, after which it was warmed to RT and left stirring overnight (20 hours). The reaction was cooled to 0°C and quenched with a solution of NH4Cl (2.5 M in water, 30.5 ml) The aqueous layer was washed with Et2O (3x15ml). The organic layers were combined, dried over MgSO₄ and the solvent was evaporated. The resulting mixture was purified using column chromatography, using a column packed with neutral alumina and PE:EtOAc (20:1) as eluent. The product was obtained as a bright yellow solid after evaporating the solvent (2,20 g, 3.80 mmol, 33%).

¹H NMR: (400 MHz, C₆D₆, 25°C): δ_H 7.31 (Ar*H*, m, 4H), 7.17 (Ar*H*, m, 4H), 7,00 (Ar*H*, m, 10H), 6.93 (Ar*H*, m, 2H), 6.87 (Ar*H*, t, $^3J_{H,H}$ = 7.4 Hz, 2H), 6.80 (Ar*H*, dt, $^3J_{H,H}$ = 7.6 Hz, $^4J_{H,P}$ = 1.4 Hz, 2H), 6.74 (Ar*H*, dt, $^3J_{H,H}$ = 7.4 Hz, $^4J_{H,P}$ = 1.4 Hz, 1H), 6.66 (Ar*H*, dt, $^3J_{H,H}$ = 7.5 Hz, $^4J_{H,P}$ = 1.3 Hz, 1H), 2.32 (Ar-C*H₃*, d, $^4J_{H,P}$ = 1.4 Hz, 6H).
¹³C NMR: (100 MHz, C₆D₆, 25°C) : δ_C 196.9 (C=O, t, $^3J_{C,P}$ = 3.4 Hz), 144.6 (Ar, d, $^2J_{C,P}$ = 25.5 Hz), 144.2 (Ar, d, $^2J_{C,P}$ = 24.9 Hz), 142.5 (C-P, d, $^1J_{C,P}$ =27.4 Hz), 139.3 (dd, $^1J_{C,P}$ =24.8 Hz, $^5J_{C,P}$ =1.5 Hz), 138.4 (C-P, d, ^{1}

$J_{C,P}$ =12.6 Hz), 137.7 (C-P, dd, $^1 J_{C,P}$ =21.8 Hz, $^5 J_{C,P}$ =1.8 Hz), 136.0 (Ar, d, $^3 J_{C,P}$ =12.1 Hz), 134.9 (Ar, m), 133.9 (Ar, d, $^2 J_{C,P}$ =20.3 Hz), 133.4 (Ar, s), 130.7 (Ar, dt, $^3 J_{C,P}$=5.0 Hz, $^5 J_{C,P}$ =1.5 Hz), 130.4 (Ar, d, $^3 J_{C,P}$ =8.8 Hz), 130.1 (Ar, d, $^3 J_{C,P}$ =4.6 Hz), 128.42 (Ar, s), 128.2 (Ar, s), 128.1 (Ar, d, $^4 J_{C,P}$ =4.1 Hz), 125.9 (Ar, s), 21.2 (Me, d, $^3 J_{C,P}$ =22.9 Hz)
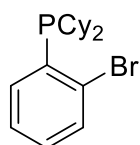
^{31}P NMR: (161 MHz, C_6D_6, 25°C): δ_P -8,5 (d, $^6 J_{P,P}$ = 4.3 Hz), -25,2 (d, $^6 J_{P,P}$ = 4,3 Hz).

ATR-IR: ν [cm^{-1}]: 3051, 1658, 1583, 1451, 1433, 1296, 1161, 1121, 1027, 928, 743, 717

HRMS (ESI, CH_3CN, $AgNO_3$): Calculated [M+Ag]$^+$: 687.077. Found [M+Ag]$^+$: 687.0983.

EA: Calculated: C: 80.95 %, H: 5.57 %. Found: C: 81.12 %, H: 5.81 %

Synthesis of (2-bromophenyl)di-cyclohexyl phosphine (9)

Based on a procedure by Buchwald et al[33]. D*i*PPF (0.33 g, 0.78 mmol), Pd(OAc)$_2$ (0.19 g, 0.85 mmol) and Cs_2CO_3 (10.4 g, 31.9 mmol) were combined in a Schlenk flask and put under vacuum for 30 minutes. 40 ml of dry, degassed dioxane was added under N_2 to form an orange suspension, which quickly turned brown. After stirring for 1 hour, 2-Iodobromobenzene (7.49 g, 26.4 mmol) and dicyclohexylphosphine (4.97 g, 25.9 mmol) were added and the mixture was heated to 80°C for 22 hours. After allowing the mixture to cool down, 30 ml Et_2O was added and the mixture was filtered over a neutral alumina plug and over celite. The solvent was removed *in vacuo* to obtain a white solid (4.5 g, 12.7 mmol, 49%). Characterization values of ^{1}H and ^{31}P NMR, ATR-IR and EI-MS correspond to literature[33].

^{1}H NMR (400 MHz, C_6D_6, 25°C): δ_H 7.49 (Ar*H*, ddd, $^3 J_{H,H}$ = 7.6 Hz, $^3 J_{H,P}$ = 3.0 Hz, $^4 J_{H,H}$ = 1.2 Hz, 1H), 7.25 (Ar*H*, td, $^3 J_{H,H}$ = 7.6 Hz, $^3 J_{H,H}$ = 1.5 Hz, 1H), 6.95 (Ar*H*, td, $^3 J_{H,H}$ = 7.6 Hz, $^3 J_{H,H}$ = 1.2 Hz, 1H), 6.73 (Ar*H*, td, $^3 J_{H,H}$ = 7.6 Hz, $^4 J_{H,H}$ = 1.5 Hz, 1H), 2.04-0.98 (Cy*H*, m, 22H)

^{31}P NMR (161 MHz, C_6D_6, 25°C) δ_P 0.7.

ATR-IR: ν [cm^{-1}]: 2920, 2847, 1445, 1414, 1262, 1091, 1018, 1002, 799, 740.

EI-MS: m/z: Calculated for [M]$^+$: 352, found 352.

Synthesis of 2-(dicyclohexylphosphaneyl)-N,N-dimethylbenzamide (12)
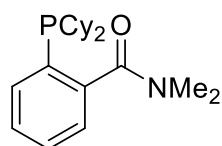
(2-bromophenyl)di-cyclohexyl phosphine (2.4 g, 6.68 mmol) was added to a dried Schlenk flask and which was evacuated for 30 minutes. Under N2 atmosphere, 20 ml of dry, degassed Et_2O was added and the solution was cooled to -60°C. *t*-BuLi (1.6 M in hexane, 10.5 ml, 16.8 mmol) was added dropwise to the solution over the course of 5 minutes. A white precipitate formed in the orange solution. The solution was allowed to warm for 1 hour while stirring, then cooled back to -60°C. under N_2, Dimethyl carbamoyl chloride (0.66 ml, 0.72 g, 6.70 mmol) was put in a dried Schlenk flask and dissolved in 10 ml dry, degassed Et_2O. The solution was degassed by bubbling N_2 through for 20 minutes, after which it was slowly transferred to the reaction flask over the course of 5 minutes. The mixture was allowed to warm to RT and left stirring overnight. After cooling the reaction to 0°C, 10 ml of a dry, degassed 2.5 M solution of NH_4Cl was added. The aqueous phase was washed with Et_2O (3x 10 ml). The organic layers were combined and dried over $MgSO_4$. The solvents were removed *in vacuo*. The compound was used without further purifications for the next step.

Synthesis of 2-(diphenylphosphaneyl)-N,N-dimethylbenzamide (10)
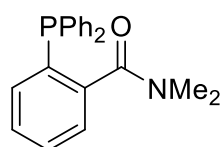
(2-bromophenyl)di-phenyl phosphine (10.0 g, 29.3 mmol) was added to a dried Schlenk flask and was evacuated for 30 minutes. Under N_2, 40 ml of dry, degassed Et_2O was added. The solution was cooled to -60°C, and *n*-BuLi (1.6 M in hexane, 21.0 ml, 33.6 mmol) was added slowly to the solution over the course of 5 minutes. A white precipitate formed in the orange solution. The solution was allowed to warm for 1 hour while stirring, then cooled back to -60°C. Under N_2, Dimethyl carbamoyl chloride (2.8 ml, 3.3 g, 30.3 mmol) was put in a dried Schlenk flask and dissolved in 20 ml dry, degassed Et_2O. The solution was bubbled through for it 20 minutes with N_2, after which it was transferred to the reaction flask. The mixture was allowed to warm to RT and left stirring

overnight. After cooling the reaction to 0°C, NH_4Cl (2.5M in water, 45 ml) was added. The organic layer was separated and extracted 2 times with 10 ml of water. The aqueous phase was washed with Et_2O (3x 20 ml). The organic layers were combined and dried over $MgSO_4$. The solvents were removed *in vacuo*. The resulting mixture was purified using column chromatography, using a column packed with neutral alumina, PE:EtOAc (20:1) as eluent. After removing the solvent *in vacuo,* the product was obtained as a yellow glue (6.0 g, 18.0 mmol, 61%).

^{1}H NMR: (400 MHz, C_6D_6, 25°C): δ_H 7.40 (ArH, td, $^3J_{H,H}$ = 7.6 Hz, $^4J_{H,P}$ = 2.1 Hz 4H), 7.23 (ArH, m, 1H), 7,11 (ArH, m, 1H), 7.07-7.00 (ArH, m, 6H), 6.98 (ArH, m, 1H), 6.91 (ArH, td, $^3J_{H,H}$ = 7.4 Hz, $^4J_{H,P}$ = 1.4 Hz, 2H), 2.79 (NCH_3, s, 1H), 2.32 (NCH_3, s, 1H)

^{31}P NMR: (161 MHz, C_6D_6, 25°C): δ_P -11.4

Synthesis of (2-(di-cyclohexylphosphinophenyl)(2-(diphenylphosphino)phenyl)methanone, L2
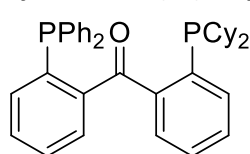
(2-bromophenyl)dicyclohexyl phosphine (6.21 g, 17.6 mmol) was dissolved in 40 ml dry, degassed Et_2O under N_2 and cooled to -70°C. *t*-BuLi (1.6M in hexane, 22.0 ml, 35.2 mmol) was added to the solution dropwise while stirring over the course of 5 minutes. The solution was allowed to warm to -20°C and after 1 hour cooled back to -70°C. 2-(di-phenylphosphino)-N,N-dimethylbenzamide (5.85 g, 17.5 mmol) was dissolved in 30 ml dry, degassed Et_2O, and added to the reaction mixture over the course of 5 minutes. The reaction was kept at -70°C for 10 minutes, after which it was warmed to RT and stirred for 96 hours. The reaction was cooled to 0°C and quenched with a solution of NH_4Cl (2.5 M in water, 30.5 ml) The aqueous layer was washed with Et_2O (3x15ml). The organic layers were combined, dried with $MgSO_4$ and the solvent was evaporated. The resulting mixture was purified using column chromatography, with a column packed with neutral alumina and PE:EtOAc (20:1) as eluent. The solvents were removed *in vacuo* and after washing with Et_2O the product was obtained as a bright yellow solid (1.40 g, 2.49 mmol, 14%).

^{1}H NMR (400 MHz, C_6D_6, 25°C): δ_H 7.56 (ArH, t, J = 7.1 Hz, 3H), 7.43 (ArH, m, 1H), 7.39 (ArH, dd, J = 7.6 Hz, J = 3.7 Hz, 1H), 7.28 (ArH, dd, J = 7.6 Hz, J = 3.4 Hz, 1H), 7.12 (ArH and C_6D_6, m, 7H), 6.99 (ArH, t, J = 7.4 Hz, 1H), 6.93 (ArH, t, J = 7.4 Hz, 1H), 6.87 (ArH, t, J = 7.4 Hz, 1H), 1.80 (CH, CH_2, m, 4H). 1.57 (CH_2, m, 8H), 1.07 (CH_2, m, 11H)

^{13}C NMR (100 MHz, C_6D_6, 25°C): δ_C 189.1 (C=O, d, $^3J_{C,P}$ = 6.1 Hz), 149.6 (Ar 4°, dd, $^1J_{C,P}$ = 31.4 Hz, $^5J_{C,P}$ = 1.2 Hz), 142.7 (Ar 4°, dd, $^1J_{C,P}$ = 17.3 Hz, $^5J_{C,P}$ = 1.8 Hz), 142.2 (Ar 4°, dd, $^2J_{C,P}$ = 29.3 Hz, $^4J_{C,P}$ = 1.8 Hz), 139.8 (Ar 4°, d, $J_{C,P}$ = 12.4 Hz), 135.5 (Ar 4°, d, $J_{C,P}$ = 0.9 Hz), 135.3 (Ar 3°, m), 134.7 (Ar 3°, d, $^2J_{C,P}$ = 20.5 Hz), 133.1 (Ar 3°, d, $^2J_{C,P}$ = 30.2 Hz), 131.6 (Ar 3°, s), 128.6 (Ar 3°, m), 127.5 (Ar 3°, s), 34.3 (CH, d, $^1J_{C,P}$ =15.1 Hz), 30.5 (CH_2, d, $^3J_{C,P}$ = 16.5 Hz), 29.7 (CH_2, d, $^2J_{C,P}$ = 29.2 Hz), 27.4 (CH_2, m), 26.7 (CH_2, s)

^{31}P NMR (161 MHz, C_6D_6, 25°C): δ_P -2.4 (d, $^6J_{P,P}$ = 5.3 Hz), -10.2 (broad s).

HRMS (ESI, CH_3CN, $AgNO_3$): Calculated [M+Ag]$^+$: 671.1605. Found [M+Ag]$^+$: 671.1808.

6.3.2. Complexation reactions

Attempted Complexation of L1 with Ni(COD)$_2$ in THF

L1 (47.6 mg, 82 µmol), Ni(COD)$_2$ (23.6 mg, 86 µmol) were weighed in a glovebox and dissolved in 3 ml THF. The solution was stirred for 1 minute and turned black immediately. The solvent was removed *in vacuo*, and the remaining solid was dissolved in 0.3 ml THF. 1.5 ml hexane was added and put in the fridge overnight. The black suspension was filtered using a pipette filtration and washed with cold hexane. The resulting black solid was analysed using NMR.

^{31}P NMR (161 MHz, C_6D_6, 25°C): δ_P 25.2 (s), 21.5 (s), -19.8 (s), -23.6 (s)

^{1}H NMR and **^{31}P NMR** spectra are shown in appendix B10 and C10 respectively.

Attempted Complexation of L1 with Ni(COD)$_2$ in the presence of BPI

L1 (11.2 mg, 19.4 µmol), Ni(COD)$_2$ (4.8 mg, 17.4 µmol) and BPI (3.3 mg, 18.2 µmol) were weighed in a glovebox and dissolved in C_6D_6. The black solution was followed *in situ* using NMR.

^{31}P NMR (161 MHz, C_6D_6, 25°C): δ_P 20.1 (broad s), 12.8 (Broad d, $J_{P,P}$ = 104 Hz), 6.9 (Broad d, $J_{P,P}$ = 104 Hz), 1.2 (Broad s)

^{1}H NMR and **^{31}P NMR** spectra are shown in appendix B11 and C11 respectively.

Attempted complexation of 3 equiv. L1 with 2 equiv. Ni(COD)$_2$ in THF

L1 (14.7 mg, 25.4 µmol) and Ni(COD)$_2$ (4.5 mg, 16.4 µmol) were weighed in a glovebox and dissolved in THF. The solution was stirred for 1 minute and turned black immediately . Precipitation of a black solid was observed after vapour diffusion of HMDSO into a toluene solution of the crude product. The black precipitate was filtered, dried *in vacuo* of and analysed using NMR.

^{31}P NMR (161 MHz, C$_6$D$_6$, 25°C) : δ_P 20.1 (s), 12.8 (d, J=104.0 Hz), 6.8 (d, J=104.0 Hz), 1.2 (s) -8,5 (d, $^6J_{P,P}$ = 4.3 Hz), -25,2 (d, $^6J_{P,P}$ = 4,3 Hz).

^{1}H NMR and **^{31}P NMR** spectra are shown in in appendix B12 and C12 respectively.

Attempted Complexation of L1 with Ni(COD)$_2$ in the presence of PPh$_3$

L1 (49.5 mg, 85.6 µmol), Ni(COD)$_2$ (23.5 mg, 85.4 µmol) and PPh$_3$ (22.5 mg, 89.6 µmol) were weighed in a glovebox and dissolved in THF. The solution was stirred for 1 minute and turned black immediately. The solvent was then evaporated and precipitation of a black solid was observed via vapour diffusion of HMDSO into a toluene solution of the crude product. The black precipitate was filtered of, dried *in vacuo* and analysed using NMR.

^{31}P NMR (161 MHz, C$_6$D$_6$, 25°C): δ_P 34.7 (s), 33.1 (s), 17.2 (s), 7.8 (s), 1.8 (s), -8,5 (d, $^6J_{P,P}$ = 4.3 Hz), -22.4 (m), -25,2 (d, $^6J_{P,P}$ = 4,3 Hz).

^{1}H NMR and **^{31}P NMR** spectra are shown in appendix B13 and C13 respectively.

Attempted Complexation of L1 with Ni(COD)$_2$ in the presence of Phenylacetylene

L1 (10.7 mg, 18.5 µmol), Ni(COD)$_2$ (4.9 mg, 18 µmol) and Phenylacetylene (2.3 mg, 23 µmol) were weighed in a glovebox and dissolved in C$_6$D$_6$ and the black solution was followed *in situ* with NMR.

^{31}P NMR (161 MHz, C$_6$D$_6$, 25°C: δ_P 35.3 (d, $J_{P,P}$ = 27.9 Hz), 25.1 (d, $J_{P,P}$ = 27.9 Hz)

^{1}H NMR and **^{31}P NMR** spectra are shown in appendix B14 and C14 respectively.

Complexation of L2, Ni(COD)$_2$ and PPh$_3$ (17)
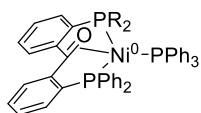
L2 (10.3 mg, 18.3 mmol), Ni(COD)$_2$ (4.5 mg, 16 mmol) and PPh$_3$ (4.4 mg, 17 mmol) were weighed in a glovebox and dissolved in 0.8 ml C$_6$D$_6$. Crystallization was achieved using solvent evaporation with toluene as solvent, hexane as antisolvent.

^{31}P NMR (161 MHz, C$_6$D$_6$, 25°C): δ_P 39.0 (dd, $J_{P,P}$ = 17 Hz, $J_{P,P}$ = 36Hz), 29.4 (dd, $J_{P,P}$ = 17 Hz, $J_{P,P}$ = 66 Hz), 10.8 (dd, $J_{P,P}$ = 35 Hz, $J_{P,P}$ = 65 Hz).

^{1}H NMR (400 MHz, C$_6$D$_6$, 25°C): δ_H 9.90 (N*H*, s, 1H), 8.36 (Ar*H*, m, 2H), 7.98 (Ar*H*, d, $J_{P,H}$ = 7.4 Hz, 2H), 7.82 Ar*H,* t, $J_{P,H}$ = 7.9 Hz, 2H), 7.77-7.67 (Ar*H*, m, 3H), 7.44-7.3 (Ar*H*, m, 2H), 7.15-6.83 (ArH, m, 16H), 1.97-0.63 (Cy*H*, m, 22H)

^{13}C NMR (100 MHz, C$_6$D$_6$, 25°C): δ_C 168.3 (*C*=N, dd, $^3J_{P,C}$ = 7.1 Hz, $^3J_{P,C}$ = 4.8 Hz), 158.4 (Ar*C*, d, $J_{P,C}$ = 35.4 Hz), 156.6 (Ar*C*, d, $J_{P,C}$ = 33.3 Hz), 139.6 (Ar*C*, d, $J_{P,C}$ = 2.8 Hz), 139.3 (Ar*C*, d, $J_{P,C}$ = 2.9 Hz), 138.8 (Ar*C*, d, $J_{P,C}$ = 14.4 Hz), 138.4 (Ar*C*, d, $J_{P,C}$ = 28.9 Hz) 138.7 (Ar*C*, m), 134.4 (Ar*C*, s), 134.0 (Ar*C*, d, $J_{P,C}$ = 15.0 Hz) 133.1 (Ar*C*, d, $J_{P,C}$ = 13.4 Hz), 130.8 (Ar*C*, dd, $J_{P,C}$ = 6.3 Hz, $J_{P,C}$ = 2.4 Hz), 129.4 (Ar*C*, s), 129.0 (Ar*C*, s), 128.8 (Ar*C*, d, $J_{P,C}$ = 3.6 Hz), 128.6 (Ar*C*, s), 127.5 (Ar*C*, d, $J_{P,C}$ = 15.9 Hz), 127.2 (Ar*C*, s) 126.3 (Ar*C*, dd, $J_{P,C}$ = 18.5 Hz, $J_{P,C}$ = 4.0 Hz), 125.4 (Ar*C*, d, $J_{P,C}$ = 15.2 Hz) 118.1 (*C*=O, dd, $^3J_{P,C}$ = 5.4 Hz, $^3J_{P,C}$ = 3.9 Hz), 37.2 (*C*H, d, $J_{P,C}$ =12.8 Hz), 29.6 (*C*H$_2$, d, $J_{P,C}$ =7.8 Hz), 29.1 (*C*H$_2$, d, $J_{P,C}$ =3.3 Hz), 28.6 (*C*H$_2$, d, $J_{P,C}$ =7.1 Hz)

Complexation of L2, Ni(COD)$_2$ and BPI (18)
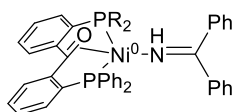
L2 (10.0 mg, 17.7 mmol), Ni(COD)$_2$ (4.3 mg, 16 mmol) and BPI (4.3 mg, 24 mmol) were weighed in a glovebox and dissolved in 0.8 ml C$_6$D$_6$. Crystallization was achieved using vapour diffusion with toluene as solvent, hexane as antisolvent.

^{31}P NMR (161 MHz, C$_6$D$_6$, 25°C): δ_P 35.08 (d, $^6J_{P,P}$ = 82 Hz), 7.72 (d, $^6J_{P,P}$ = 83 Hz).

¹H NMR (400 MHz, C₆D₆, 25°C): δ$_H$ 8.02 (Ar*H*, d, *J*$_{P,H}$ = 7.2 Hz, 1H), 7.86 (Ar*H*, t, *J*$_{P,H}$ = 7.9 Hz, 2H), 7.78 (Ar*H*, m, 4H), 7.58 Ar*H,* t, *J*$_{P,H}$ = 6.3 Hz, 1H), 7.40 (Ar*H*, m, 3H), 7.27 (Ar*H*, , t, *J*$_{P,H}$ = 5.6 Hz, 1H), 7.15-6.90 (Ar*H*, m, 18H), 2.10-0.46 (Cy*H*, m, 22H)

Attempted complexation of L2, Ni(COD)₂ and Phenylacetylene

L2 (10.0 mg, 17.7 mmol), Ni(COD)₂ (4.3 mg, 16 mmol) and phenylacetylene (1.6 mg, 16 mmol) were weighed in a glovebox and dissolved in 1 ml C₆H₆. The solvent was evaporated *in vacuo* and the resulting mixture washed with HMDSO. After drying *in vacuo* the remaining black solid was analysed by NMR.

³¹P NMR (161 MHz, C₆D₆, 25°C): δ$_P$ 28.2 (d, ⁶*J*$_{P,P}$ = 89 Hz), 17.5 (d, ⁶*J*$_{P,P}$ = 89 Hz).

¹H NMR, **¹³C NMR** and **³¹P NMR** spectra are shown in appendix B17, C17 and D6 respectively.

Attempted complexation of L2, Ni(COD)₂ and acetophenone

L2 (10.0 mg, 17.7 mmol), Ni(COD)₂ (4.3 mg, 16 mmol) and acetophenone (1.9 mg, 15 mmol) were weighed in a glovebox and dissolved in 1 ml C₆H₆. The solvent was evaporated *in vacuo* and the resulting mixture washed with HMDSO. After drying *in vacuo* the remaining black solid was analysed by NMR.

³¹P NMR (161 MHz, C₆D₆, 25°C): δ$_P$ 44.0, 28.2 (d, *J*$_{P,P}$ = 89 Hz), 17.5 (d, *J*$_{P,P}$ = 90 Hz), 3.5.

³¹P NMR spectrum is shown in appendix C19

Attempted complexation of L2 and Ni(COD)₂

L2 (14.0 mg, 24.8 mmol), Ni(COD)₂ (6.0 mg, 22 mmol) were weighed in a glovebox and dissolved in 1 ml C₆H₆. The solvent was evaporated *in vacuo* and the resulting mixture washed with HMDSO. After drying *in vacuo* the remaining black solid was analysed by NMR.

³¹P NMR (161 MHz, C₆D₆, 25°C): δ$_P$ 44.0, 28.2 (d, *J*$_{P,P}$ = 89 Hz), 17.5 (d, *J*$_{P,P}$ = 90 Hz), 3.4.

³¹P NMR spectrum is shown in appendix C18.

6.3.3. Activation of small molecules

Attempted reaction of 18 with H₂

In a glovebox, **18** (10 mg, 12.4 μmol) was dissolved in C₆D₆ and transferred the solution to a J. Young type NMR tube. N₂ was replaced with H₂ gas (approx. 1 atm.) using a freeze-pump-thaw cycle (3x). m. The reaction was followed *in situ* over time at RT during which no changes in NMR were detected. Heating the reaction at 70°C O.N. does not produce any changes.

¹H NMR, and **³¹P NMR** spectra are shown in appendix B18 and C20 respectively

Reaction of 18 with H₂SiPh₂

In a glovebox, **18** (5 mg, 6.2 μmol) and H₂SiPh₂ (1.16 μl, 1.15 mg, 6.2 μmol) were dissolved in 0.8 ml C₆D₆. The dark green solution was analysed using NMR after 1 and 6 hours before adding H₂SiPh₂ (1.16 μl, 1.15 mg, 6.2 μmol). After letting the mixture react O.N. the yellow mixture was again analysed using NMR.

³¹P and ¹H NMR spectra are shown in appendix B19 and C21

6.3.4. Catalytic comparison in alkyne cyclotrimerization

Cyclotrimerization of methyl propiolate with L1 and Ni(COD)₂

In a glovebox, **L1** (11.0 mg, 19 μmol) and methyl propiolate (290 mg, 3.45 mmol) were dissolved in 4 ml Toluene. The solution was then added to Ni(COD)₂ (5.2 mg, 19 μmol). The reaction was left stirring for 16 hours. The work up was performed by adding 10 ml water, removing the organic phase and extracting with Et₂O (3x5 ml). The organic layers were combined, dried over MgSO₄, filtered and dried *in vacuo*. The resulting colourless oil was analysed using NMR. Isomeric ratios are reported according to ¹H-NMR. NMR values correspond to literature
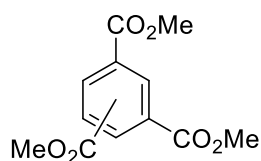
¹H NMR (400 MHz, C$_6$D$_6$, 25°C) of the major product: δ$_H$ 8.52 (ArH, d, ⁴$J_{H,H}$ = 1.6 Hz, 1H), 7.91 (ArH, t, ³$J_{H,H}$ = 8.0 Hz, ⁴$J_{H,H}$ = 1.6 Hz, 1H) 7.37 (ArH, d, ³$J_{H,H}$ = 8.0 Hz, 1H), 3.53 (CH_3, s, 3H), 3.44 (CH_3, s, 3H), 3.39 (CH_3, s, 3H)
¹H NMR spectrum is shown in appendix B20

Cyclotrimerization of methyl propiolate with L2 and Ni(COD)$_2$
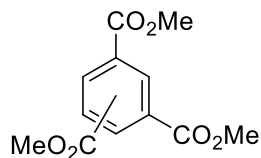
In a glovebox, **L2** (10 mg, 18 μmol) and Ni(COD)$_2$ (4.9 mg, 18 μmol) were dissolved in 2 ml C$_6$H$_6$. Methyl propiolate (334 mg, 3.97 mmol) was dissolved in 2 ml C$_6$H$_6$ and added slowly to the catalyst mixture. The reaction was left stirring for 16 hours. The work up was performed by adding 2 ml water, removing the organic phase and extracting with Et$_2$O (3x2 ml). The organic layers were combined, dried over MgSO$_4$, filtered and dried *in vacuo*. The resulting brown oil was analysed using NMR. Isomeric ratios are reported according to ¹H-NMR. NMR values correspond to literature

¹H NMR (400 MHz, C$_6$D$_6$, 25°C) of the major product: δ$_H$ 8.52 (ArH, d, ⁴$J_{H,H}$ = 1.6 Hz, 1H), 7.91 (ArH, t, ³$J_{H,H}$ = 8.0 Hz, ⁴$J_{H,H}$ = 1.6 Hz, 1H) 7.37 (ArH, d, ³$J_{H,H}$ = 8.0 Hz, 1H), 3.53 (CH_3, s, 3H), 3.44 (CH_3, s, 3H), 3.39 (CH_3, s, 3H)
¹H NMR spectrum is shown in appendix B21

6.3.5. Hydrosilylation reactions

Hydrosilylation with H$_2$SiPh$_2$ of 1-octene with L1 and Ni(COD)$_2$

In a glovebox, $^{o\text{-Tol}}$PCO^{Ph}P (8 mg, 13.8 μmol) and Ni(COD)$_2$ (3.8 mg, 13.8 μmol) were dissolved in 1 ml C$_6$H$_6$, giving a black solution. After adding H$_2$SiPh$_2$ (257 μl, 255 mg, 1.38 mmol) and 1-octene (217 μl, 155 mg, 1.38 mmol) the resulting dark yellow mixture was left stirring for 17 hours. The work up was performed by adding 2 ml water, removing the organic phase and extracting with Et$_2$O (3x2 ml). The organic layers were combined, dried over MgSO$_4$, filtered and dried *in vacuo*. The resulting brown oil was analysed using NMR. Conversion of H$_2$SiPh$_2$ and yield of (E)-(1,2-diphenylvinyl)diphenylsilane were calculated according to NMR by adding mesitylene as internal standard and comparison with literature.
¹H NMR spectrum is shown in appendix B23

Hydrosilylation with H$_2$SiPh$_2$ of 1-octene with 18

In a glovebox, **18** (5 mg, 6.2 μmol) was dissolved in 1 ml C$_6$D$_6$. After adding H$_2$SiPh$_2$ (185 μl, 184 mg, 1.00 mmol) and 1-octene (156 μl, 112 mg, 1.00 mmol) the resulting orange mixture was left stirring for 17 hours. The work up was performed by adding 2 ml water, removing the organic phase and extracting with Et$_2$O (3x2 ml). The organic layers were combined, dried over MgSO$_4$, filtered and dried *in vacuo*. The resulting brown oil was analysed using NMR. Conversion of H$_2$SiPh$_2$ and yield of (E)-(1,2-diphenylvinyl)diphenylsilane were calculated according to NMR by adding mesitylene as internal standard and comparison with literature.
¹H NMR spectrum is shown in appendix B24

Hydrosilylation with H$_2$SiPh$_2$ of diphenylacetylene with 18

In a glovebox, **18** (5 mg, 6.2 μmol) and H$_2$SiPh$_2$ (1.16 μl, 1.15 mg, 6.2 μmol) were dissolved in 1 ml C$_6$D$_6$, giving a dark green solution. After adding H$_2$SiPh$_2$ (116 μl, 115 mg, 623 μmol) and diphenylacetylene (111 mg, 623 μmol) the reaction was left overnight. The work up was performed by adding 2 ml water, removing the organic phase and extracting with Et$_2$O (3x2 ml). The organic layers were combined, dried over MgSO$_4$, filtered and dried *in vacuo*. The resulting orange oil was analysed using NMR. Conversion of H$_2$SiPh$_2$ and yield of (E)-(1,2-diphenylvinyl)diphenylsilane were calculated according to NMR by adding mesitylene as internal standard and comparison with literature.
¹H NMR spectrum is shown in appendix B22

Hydrosilylation with H_2SiPh_2 of phenylacetylene using 18

In a glovebox, H_2SiPh_2 (152 mg, 0.82 mmol) and phenylacetylene (82 µl, 76 mg, 0.75 mmol) were dissolved in 2 ml C_6H_6 and added to **18** (3 mg, 3.73 µmol). The yellow solution was stirred for 18 hours, after which it turned green. The work up was performed by adding 2 ml water, removing the organic phase and extracting with Et_2O (3x2 ml). The organic layers were combined, dried over $MgSO_4$, filtered and dried *in vacuo*. The resulting brown oil was analysed using NMR.
^{1}H NMR spectrum is shown in appendix B25

Solvent optimization of the hydrosilylation with H_2SiPh_2 of diphenylacetylene

In a glovebox, H_2SiPh_2 (76 µl, 75 mg, 406 mmol) and diphenylacetylene (92 mg, 516 mmol) were dissolved in 2 ml solvent and added **18** (3 mg, 3.73 µmol). The yellow solution was stirred for 18 hours, after which it turned green. The work up was performed by adding 2 ml water, removing the organic phase and extracting with Et_2O (3x2 ml). The organic layers were combined, dried over $MgSO_4$, filtered and dried *in vacuo*. The resulting brown oil was analysed using NMR. Conversion of H_2SiPh_2 and yield of (E)-(1,2-diphenylvinyl)diphenylsilane were calculated according to NMR by adding mesitylene as internal standard and comparison with literature.
^{1}H NMR spectra are shown in appendix B26-B29

7. Acknowledgements

During my project I had help and support of numerous people, who I would like to thank here.

First, I'd like to thank **Alessio** for being my daily supervisor. I am thankful I could be a part of 'Alessio's Army'. During my project you taught me a lot of new skills on the lab and about writing scientifically. I also really appreciated the way you came up with new suggestions or tips when my project was not running smoothly.

Thank you, **Dr. Marc-Etienne Moret**, for being my first supervisor, and allowing me to do my research at OCC. I learned a lot during the work discussions, making me think about my results in a way I had not considered before.

Thank you, **Prof. Bert Klein-Gebbink** for being my second supervisor. Also from you I learned a lot during the work discussions, and I appreciated the more, in my mind, out of the box solutions you came up with for encountered problems.

I would like to thank **Johann** and **Thomas** for help with the NMR, ESI-MS and general lab issues, but also for the stories told during coffee breaks about 'the old days'.

I would like to thank the whole **OCC Group** for the very friendly environment on the lab, in the office but also during the social activities such as borrels and the bbq. The lunch and coffee breaks would not mostly have felt like Friday afternoon without you. I will remember my time at the group fondly. I would like to thank the other students as well: **Roel** and **Raoul**, also part of 'Alessio's Army'; **Elena, Bram, Yoni** and **Laurens**, I am slightly sorry for distracting you when I got bored; **Hidde**, **Cody** and **Joost**, thanks for the help when I started in the group.

I would also like to thank my parents and friends for their general support.

8. References

(1)   Busacca, C. A.; Fandrick, D. R.; Song, J. J.; Senanayake, C. H. *Adv. Synth. Catal.* **2011**, *353* (11–12), 1825–1864.

(2)   Report, M. *The Global Catalyst Market*; 2015.

(3)   Crabtree, R. H. *The Organometallic Chemistry Of The Transition Metals*, 6th editio.; Wiley, 2014.

(4)   Johansson Seechurn, C. C. C.; Kitching, M. O.; Colacot, T. J.; Snieckus, V. *Angewandte Chemie - International Edition*. Wiley-Blackwell May 21, 2012, pp 5062–5085.

(5)   Suzuki, A. *Angew. Chemie Int. Ed.* **2011**, *50* (30), 6722–6737.

(6)   Peris, E.; Crabtree, R. H. *Coord. Chem. Rev.* **2004**, *248*, 2239–2246.

(7)   Stahl, S. S.; Labinger, J. A.; Bercaw, J. E. *Angew. Chemie Int. Ed.* **1998**, *37* (16), 2180–2192.

(8)   Van Der Vlugt, J. I. *Eur. J. Inorg. Chem.* **2012**, No. 3, 363–375.

(9)   Commodity and Metal Prices, Metal Price Charts - InvestmentMine http://www.infomine.com/investment/metal-prices/ (accessed Aug 9, 2017).

(10)   Iron Ore | Today's Spot Price Charts - Market Index https://www.marketindex.com.au/iron-ore (accessed Sep 24, 2018).

(11)   It's Elemental - The Periodic Table of Elements http://education.jlab.org/itselemental/index.html (accessed Aug 9, 2017).

(12)   Ragsdale, S. W. *JBC* **2009**, *284* (28), 18571–18575.

(13)   Luca, O. R.; Konezny, S. J.; Blakemore, J. D.; Colosi, D. M.; Saha, S.; Brudvig, G. W.; Batista, V. S.; Crabtree, R. H. *New J. Chem* **2012**, *36*, 38.

(14)   Jeffrey, J. C.; Rauchfuss, T. B. *Inorg. Chem.* **1979**, *18* (10), 2658–2666.

(15)   Adams, G. M.; Weller, A. S. *Coord. Chem. Rev.* **2018**, *355*, 150–172.

(16)   Christian Müller; Rene J. Lachicotte, and; Jones*, W. D. **2002**.

(17)   Braunschweig, H.; Dewhurst, R. D.; Schneider, A. *Chem. Rev.* **2010**, *110* (7), 3924–3957.

(18)   Saes, B. W. H.; Verhoeven, D. G. A.; Lutz, M.; Klein Gebbink, R. J. M.; Moret, M. E. *Organometallics* **2015**, *34* (12), 2710–2713.

(19)   Barrett, B. J.; Iluc, V. M. *Inorg. Chem.* **2014**, *53* (14), 7248–7259.

(20)   Langer, R.; Leitus, G.; Ben-David, Y.; Milstein, D. *Angew. Chemie - Int. Ed.* **2011**, *50* (9), 2120–2124.

(21)   Semproni, S. P.; Hojilla Atienza, C. C.; Chirik, P. J. *Chem. Sci.* **2014**, *5* (5), 1956–1960.

(22)   Harman, W. H.; Peters, J. C. *J. Am. Chem. Soc.* **2012**, *134* (11), 5080–5082.

(23)   Macmillan, S. N.; Harman, W. H.; Peters, J. C. **2014**.

(24)   Verhoeven, D. G. A.; van Wiggen, M. A. C.; Kwakernaak, J.; Lutz, M.; Klein Gebbink, R. J. M.; Moret, M. E. *Chem. - A Eur. J.* **2018**, *24* (20), 5163–5172.

(25)   Van Alten, R. S. A study towards alkyl substituted diphosphine ligands with an envisioned redox non-innocent character, 2015.

(26) Saes, B. W. H. Nickel Complexes of Diphosphine-Ketone Ligand: Oxidation-State Dependent Coordination, 2014.

(27) Barbato, C.; Baldino, S.; Ballico, M.; Figliolia, R.; Magnolia, S.; Siega, K.; Herdtweck, E.; Strazzolini, P.; Chelucci, G.; Baratta, W. *Organometallics* **2018**, *37* (1), 65–77.

(28) Jing, Q.; Sandoval, C. A.; Wang, Z.; Ding, K. *European J. Org. Chem.* **2006**, No. 16, 3606–3616.

(29) Sung, S.; Boon, J. K.; Lee, J. J. C.; Rajabi, N. A.; Macgregor, S. A.; Krämer, T.; Young, R. D. *Organometallics* **2017**, *36* (8), 1609–1617.

(30) Orsino, A. F. *Synthesis and Reactivity of Nickel Complexes bearing a Cooperative Diphosphine Ketone Ligand*; 2017.

(31) Orsino, A. F. In *PhD Thesis Chapter 2*; 2018; pp 1–47.

(32) Tolman, C. a. *Chem. Rev.* **1977**, *77* (3), 313–348.

(33) Murata, M.; Buchwald, S. L. In *Tetrahedron*; 2004; Vol. 60, pp 7397–7403.

(34) Clevenger, A. L.; Stolley, R. M.; Staudaher, N. D.; Al, N.; Rheingold, A. L.; Vanderlinden, R. T.; Louie, J. *Organometallics* **2018**, *37* (19), 3259–3268.

(35) Orsino, A. **2017**.

(36) Sanderson, R. T. (Robert T. *Chemical bonds and bond energy*; Academic Press, 1976.

(37) Manan, R. S.; Kilaru, P.; Zhao, P. *J. Am. Chem. Soc.* **2015**, *137* (19), 6136–6139.

(38) Broere, D. L. J.; Ruijter, E. *Synthesis (Stuttg).* **2012**, *44*, 2639–2672.

(39) Winter, M. J. In *The Metal-Carbon Bond: Vol. 3 (1985)*; John Wiley & Sons, Ltd.: Chichester, UK; pp 259–294.

(40) Uyeda, C.; Steiman, T. J.; Pal, S. *Synlett* **2016**, *27* (6), 814–820.

(41) Jackson, E. P.; Montgomery, J. *J. Am. Chem. Soc.* **2015**, *137* (2), 958–963.

(42) Berding, J.; Van Paridon, J. A.; Van Rixel, V. H. S.; Bouwman, E. *Eur. J. Inorg. Chem.* **2011**, *2011* (15), 2450–2458.

(43) Kwakernaak, J. S. Synthesis of cobalt complexes with a diphosphine-ketone ligand and its application for silane activation and hydrosilylation reactions, 2017.

(44) Verhoeven, D. G. A. Base Metal Complexes of Ketone and Imine Ligands, 2018.

(45) Langkopf, E.; Schinzer, D. *Chem. Rev.* **1995**, *95* (5), 1375–1408.

(46) Chaulagain, M. R.; Mahandru, G. M.; Montgomery, J. *Tetrahedron* **2006**, *62* (32), 7560–7566.

(47) Bouwman, E. *Handb. Homog. Hydrog.* **2006**, 93–109.

(48) Steiman, T. J.; Uyeda, C. *J. Am. Chem. Soc.* **2015**, *137* (18), 6104–6110.

(49) Mo, Z.; Xiao, J.; Gao, Y.; Deng, L. *J. Am. Chem Soc* **2014**, *136*, 24.

(50) Zuo, Z.; Yang, J.; Huang, Z. *Angew. Chemie Int. Ed.* **2016**, *55* (36), 10839–10843.

(51) Clayden, J.; Greeves, N.; Warren, S. *Organic Chemistry*; 2001.

(52) Tang, Z.; Otten, E.; Reek, J. N. H.; van der Vlugt, J. I.; de Bruin, B. *Chem. - A Eur. J.* **2015**, *21* (36), 12683–12693.

(53)   Kreiter, R. Triarylphosphines with nucleophilic substituents for the construction of multimetallic and dendritic assemblies, 2006.

(54)   Li, P.; Wischert, R.; Métivier, P. *Angew. Chemie Int. Ed.* **2017**, *56* (50), 15989–15992.

(55)   Fritzsche, H.; Hasserodt, U.; Korte, F. Reduction of phosphine oxides, December 10, 1964.

(56)   Gottlieb, H. E.; Kotlyar, V.; Nudelman, A. *J. Org. Chem.* **1997**, *62* (21), 7512–7515.

9. Appendices

A. IR spectra
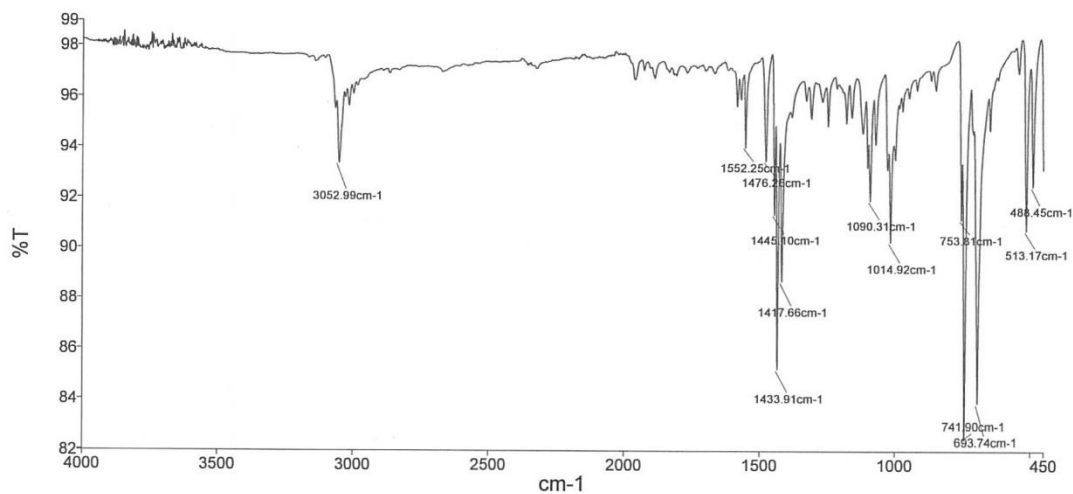
*Figure A 1: ATR-IR spectrum of (2-bromophenyl)diphenylphosphine (**7**)*
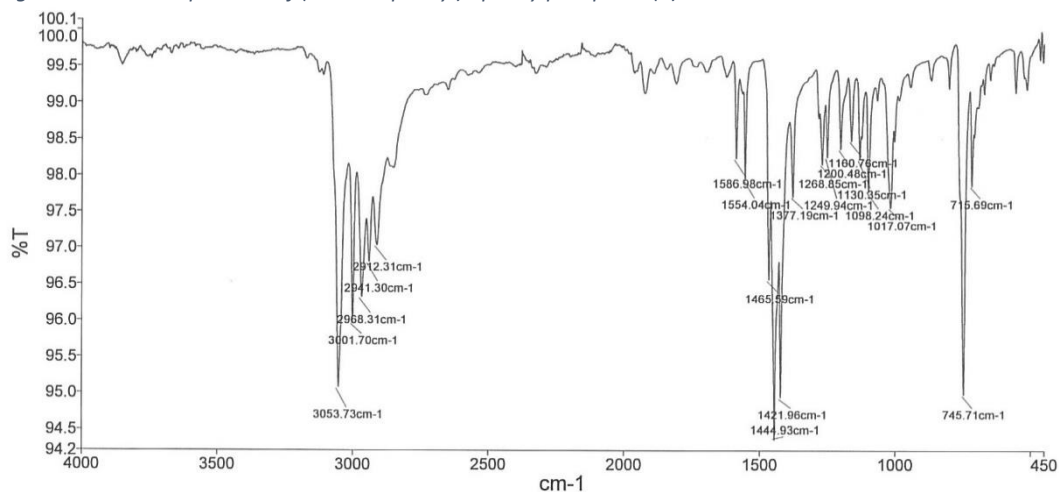
*Figure A 2: ATR-IR spectrum of (2-bromophenyl)di(o-tolyl)phosphane (**8**)*
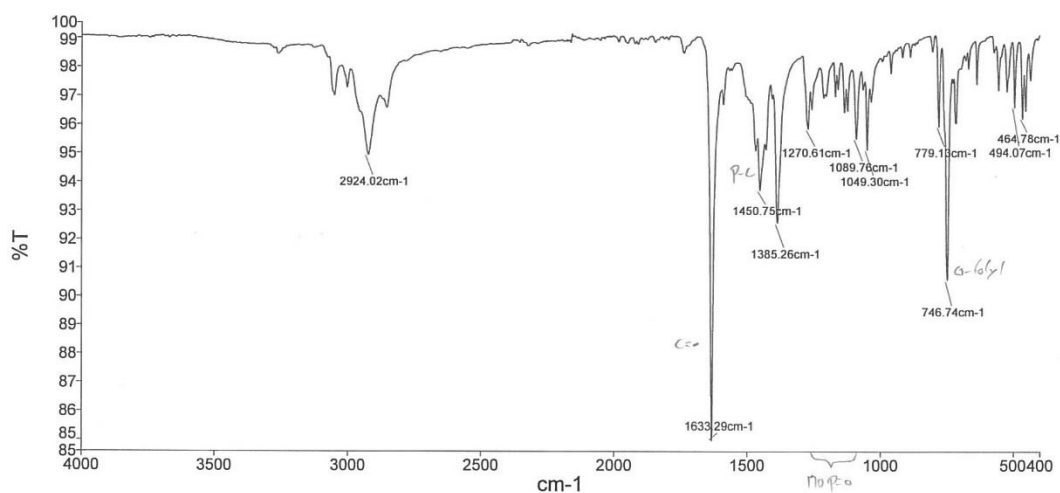
*Figure A 3: ATR-IR spectrum of 2-(di(o-tolyl)phosphaneyl)-N,N-dimethylbenzamide (**11**)*
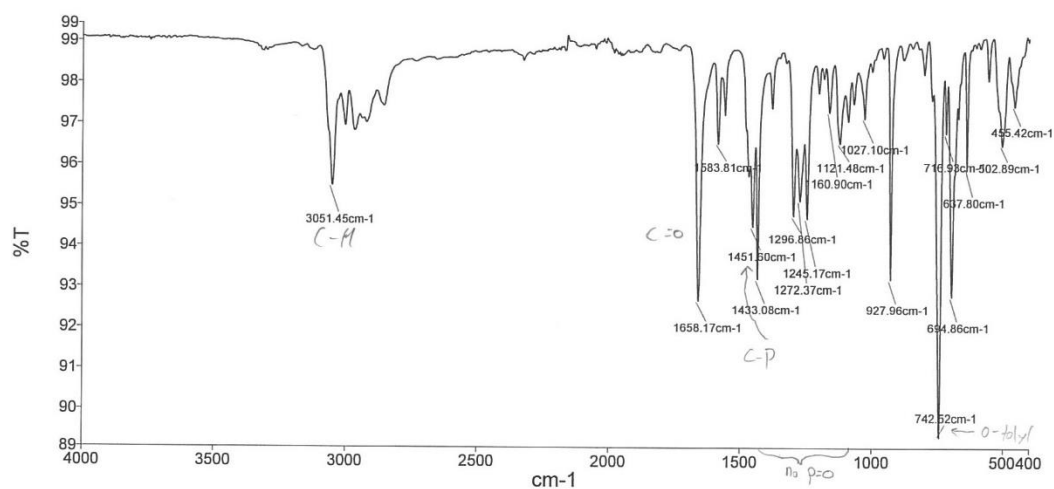
Figure A 4: ATR-IR spectrum of 1, (2-(di-o-tolylphosphaneyl)phenyl)(2-(diphenylphosphaneyl)phenyl)methanone (L1)
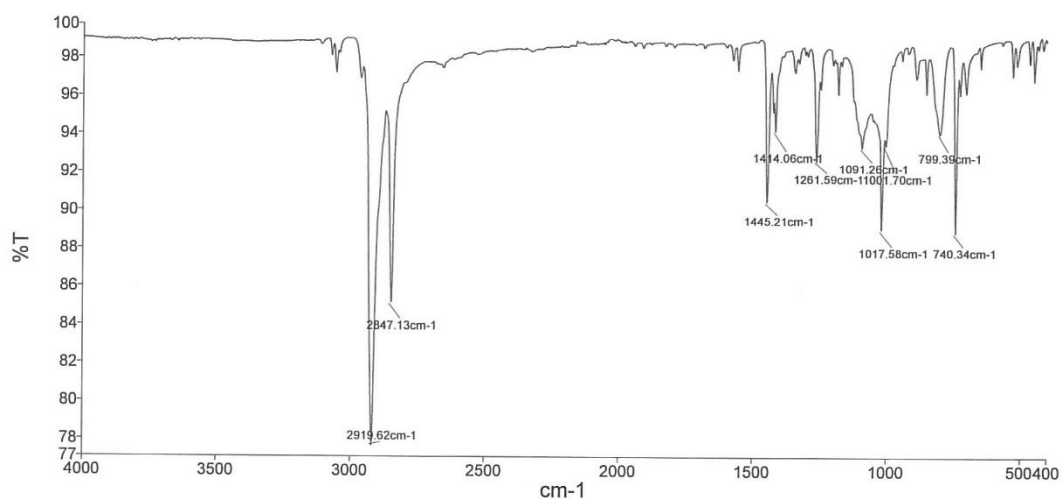
Figure A 5: ATR-IR spectrum of (2-bromophenyl)dicyclohexylphosphane (9)

B. ¹H-NMR Spectra
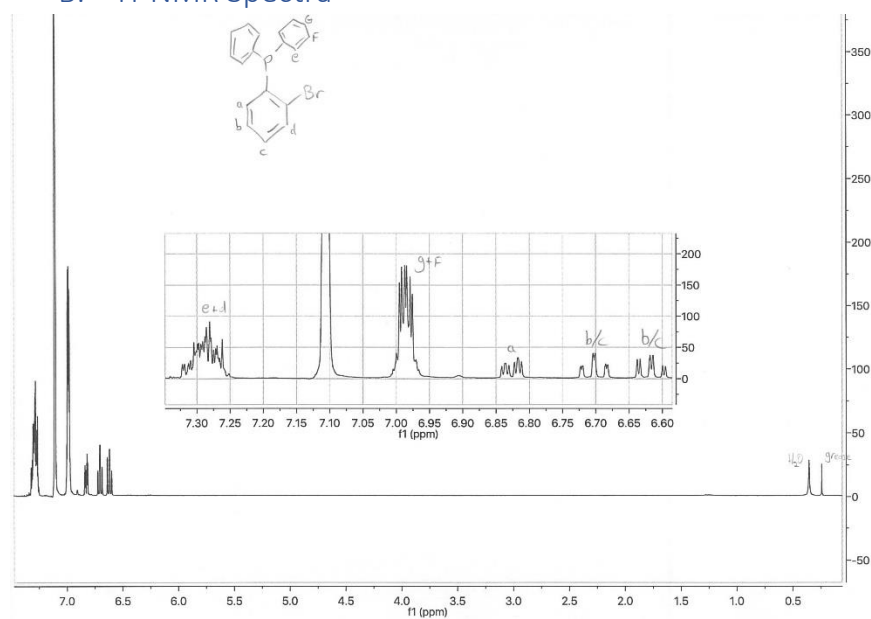
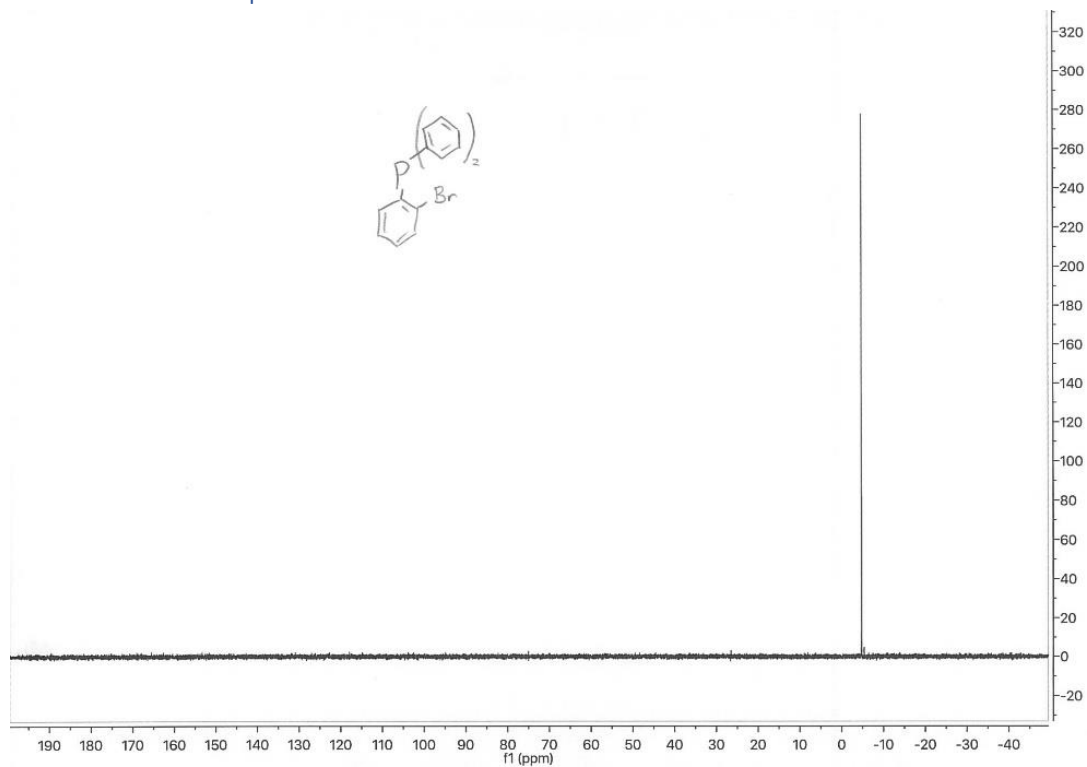*Figure B 1: ¹H-NMR spectrum in C₆D₆ of (2-bromophenyl)diphenylphosphane (7)*
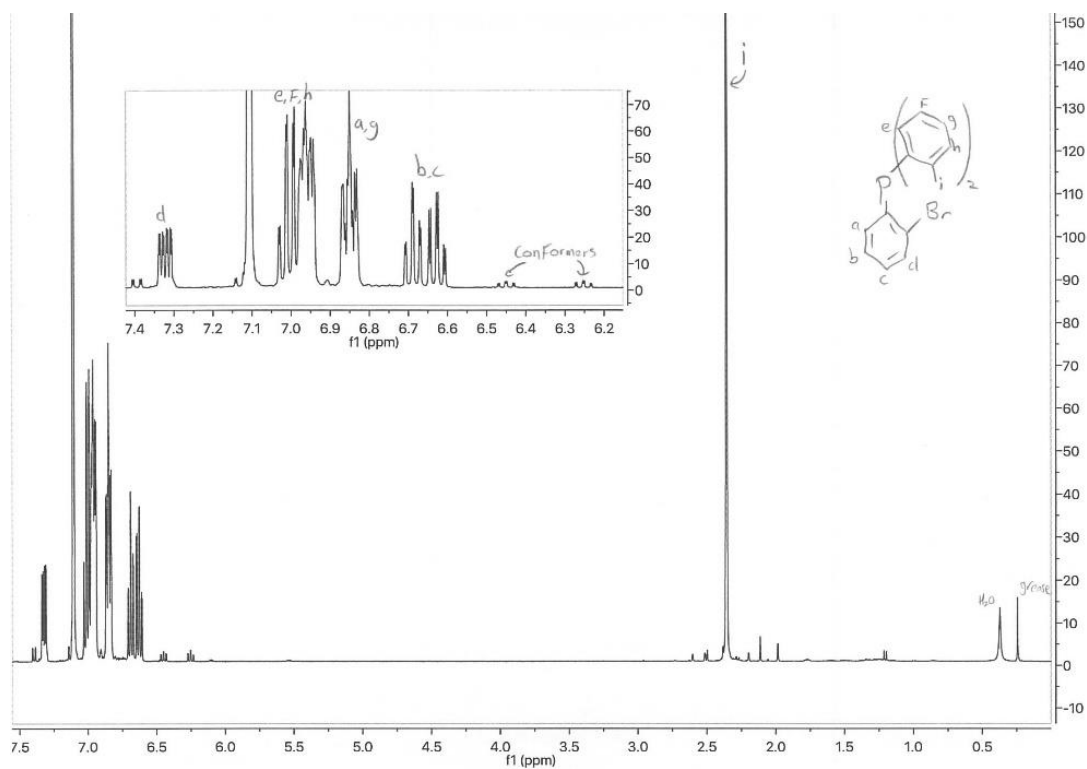
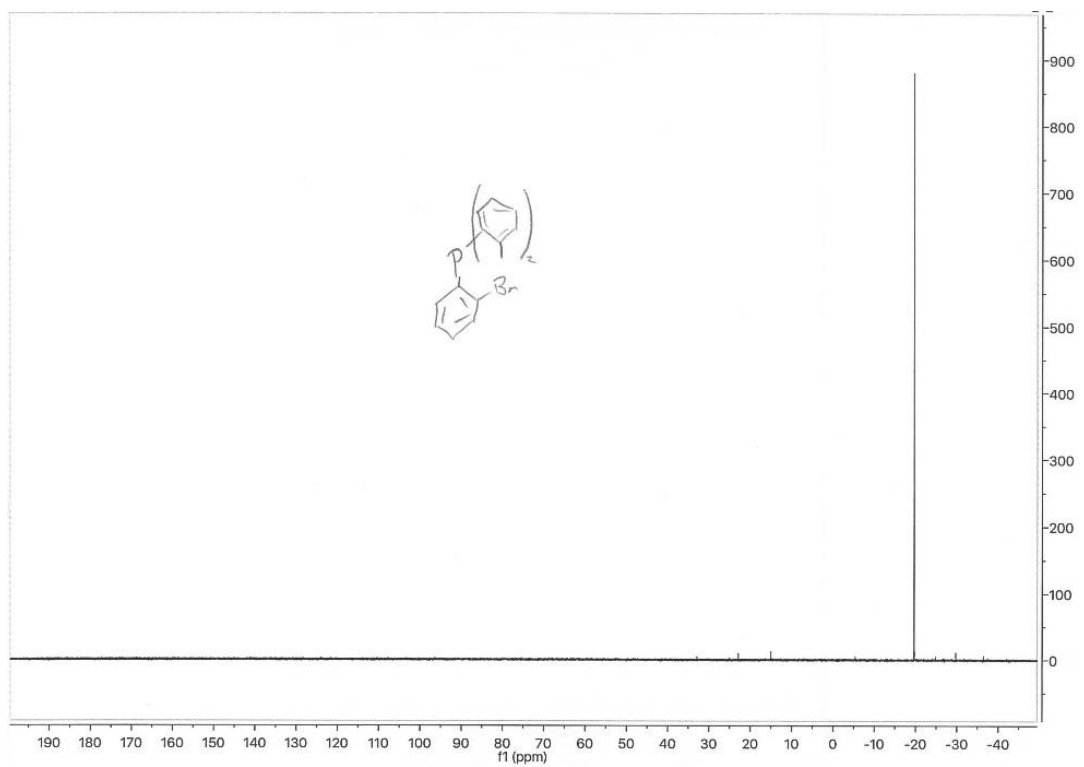*Figure B 2: ^{1}H-NMR spectrum in C_6D_6 of (2-bromophenyl)di(o-tolyl)phosphane (**8**)*
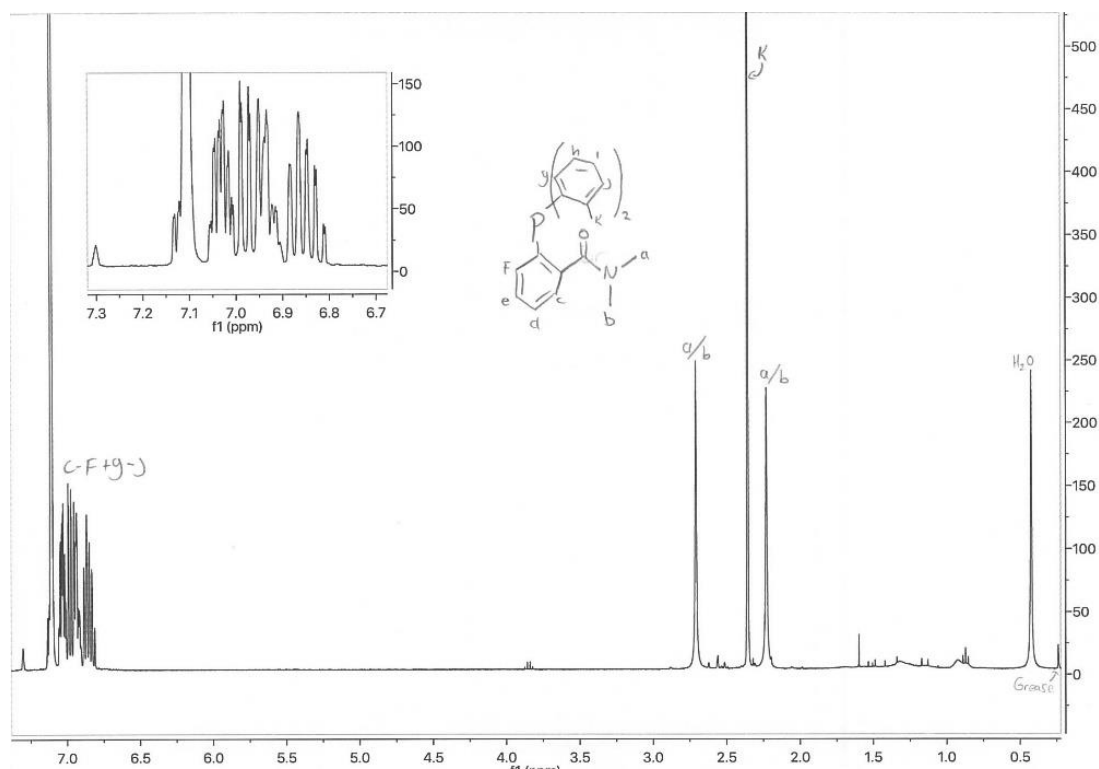
*Figure B 3: ^{1}H-NMR spectrum of 2-(di(o-tolyl)phosphaneyl)-N,N-dimethylbenzamide (**11**)*
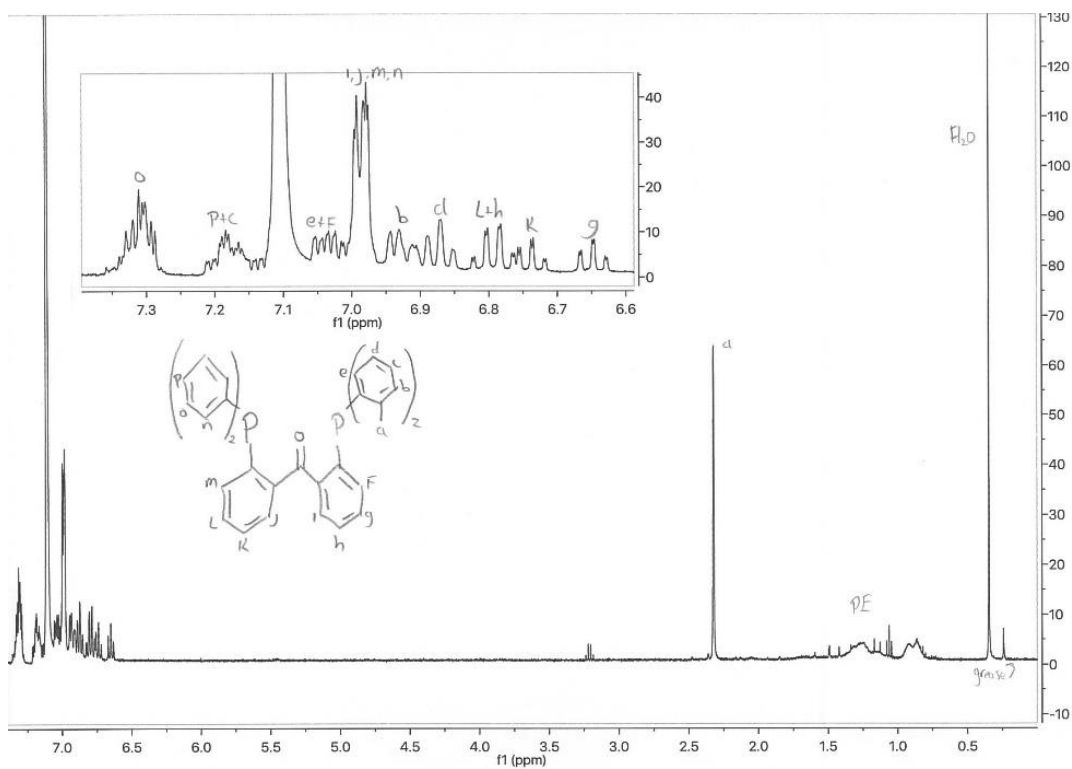
Figure B 4: ¹H-NMR spectrum in C₆D₆ of 1, (2-(di-o-tolylphosphaneyl)phenyl)(2-(diphenylphosphaneyl)phenyl)methanone (L1)
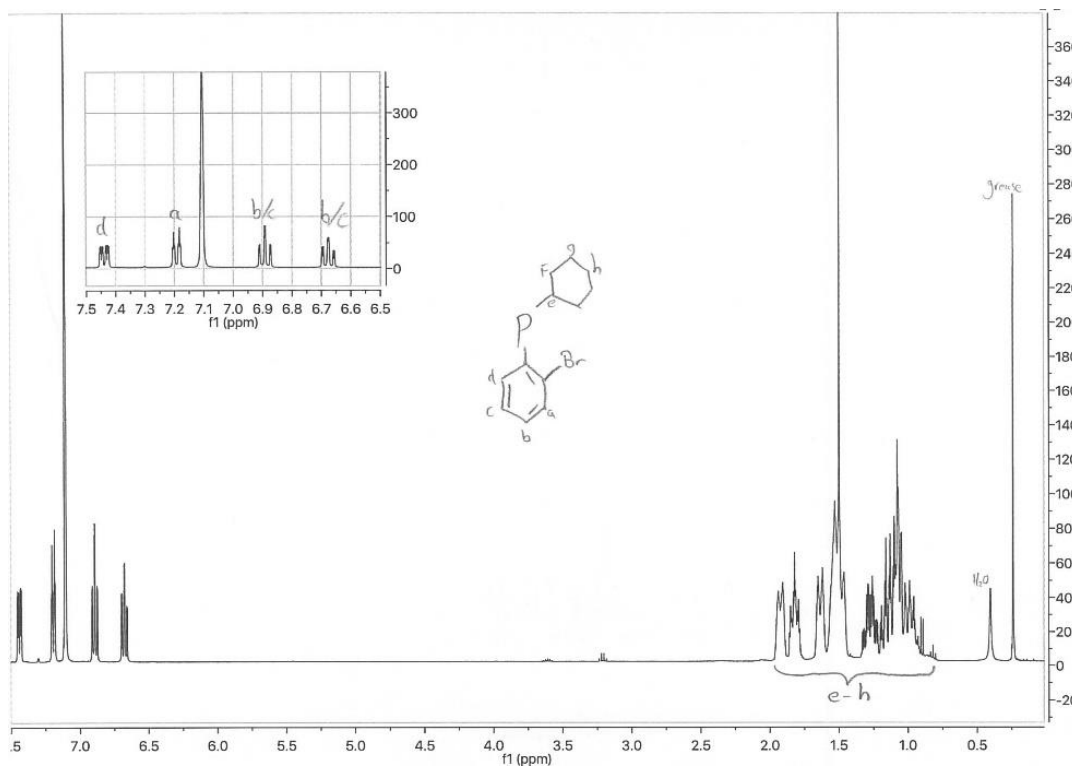
Figure B 5: ¹H-NMR spectrum in C₆D₆ of (2-bromophenyl)dicyclohexylphosphane (9)
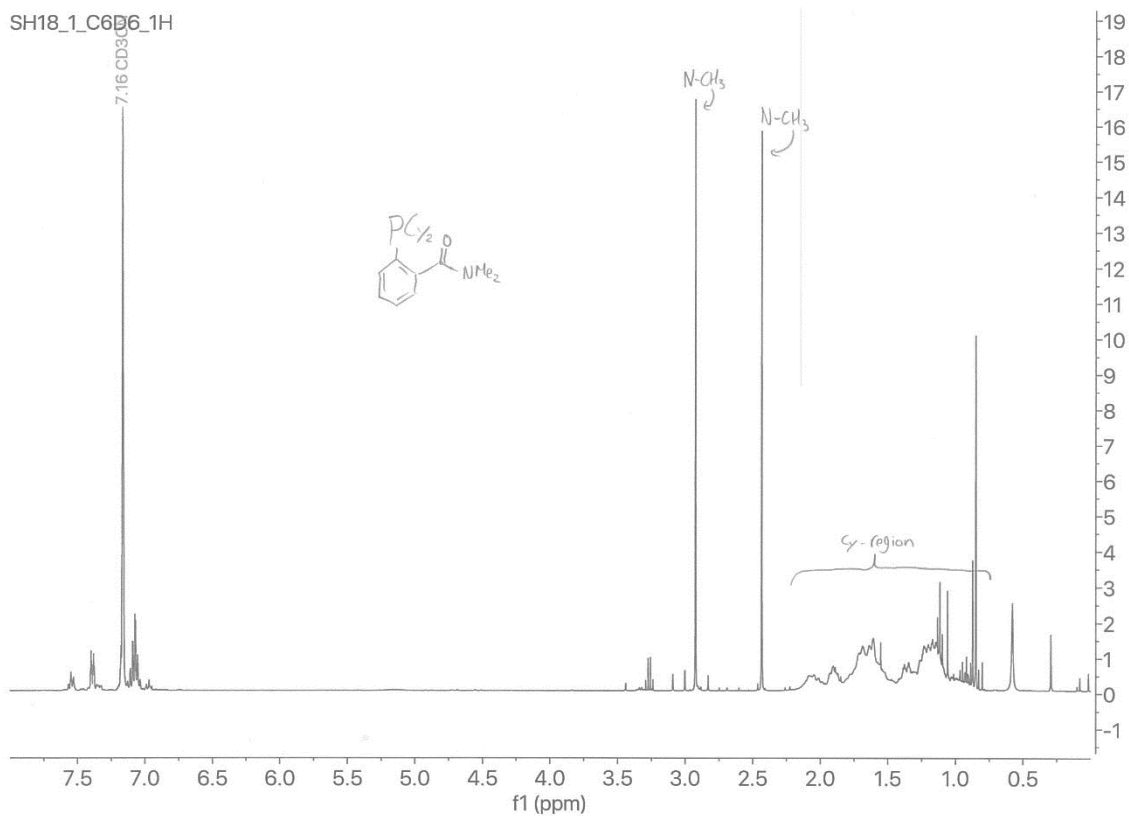
*Figure B 6: ^{1}H-NMR spectrum in C$_6$D$_6$ of the crude mixture of the synthesis 2-(dicyclohexylylphosphaneyl)-N,N-dimethylbenzamide (**12**)*
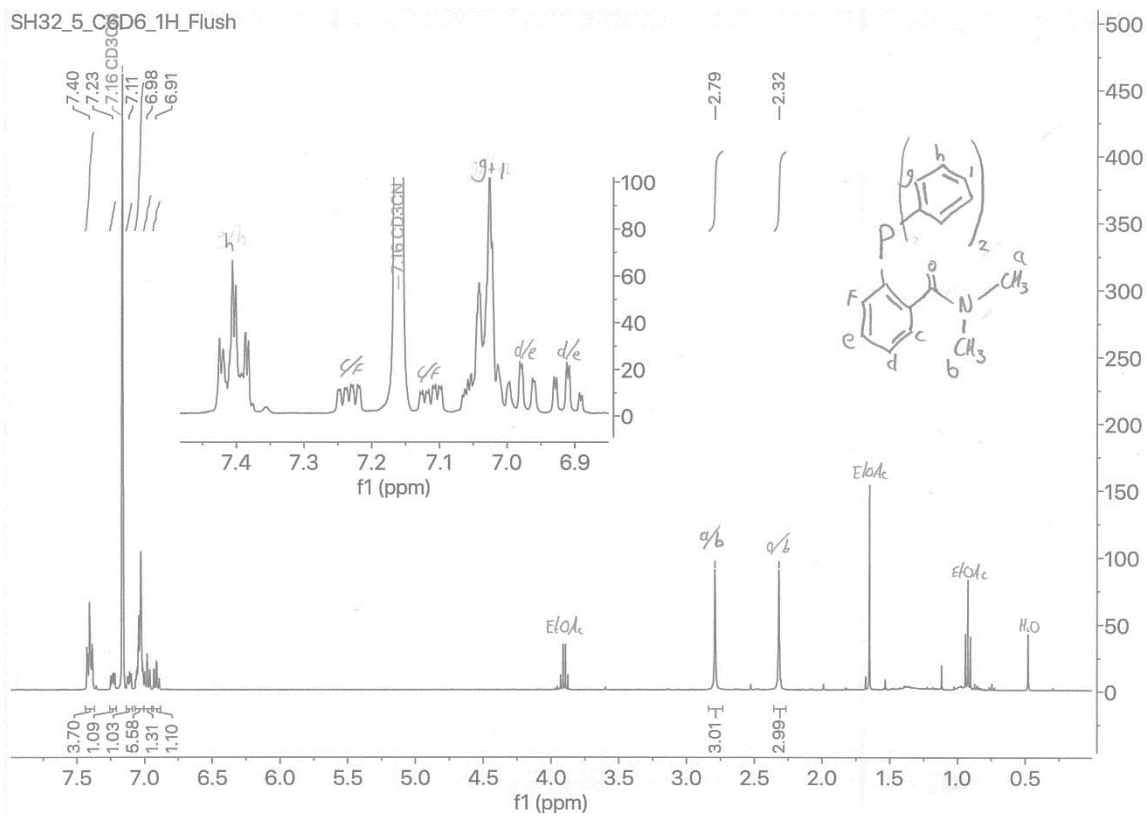
*Figure B 7: ^{1}H-NMR spectrum in C$_6$D$_6$ of 2-(diphenylphosphaneyl)-N,N-dimethylbenzamide (**10**)*
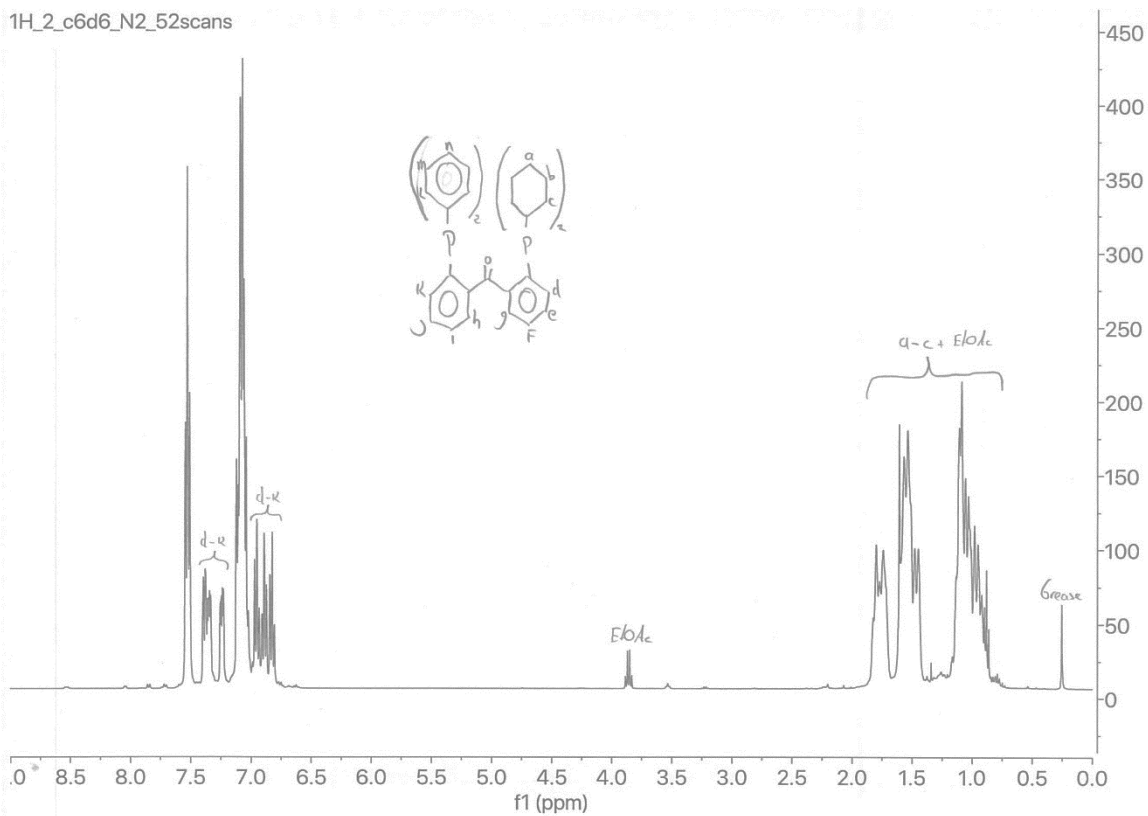
*Figure B 8: ^{1}H-NMR spectrum in C_6D_6 of (2-(dicyclohexylphosphaneyl)phenyl)(2-(diphenylphosphaneyl)phenyl)methanone, $^{o-Tol}PCO^{Ph}P$ (**L2**)*
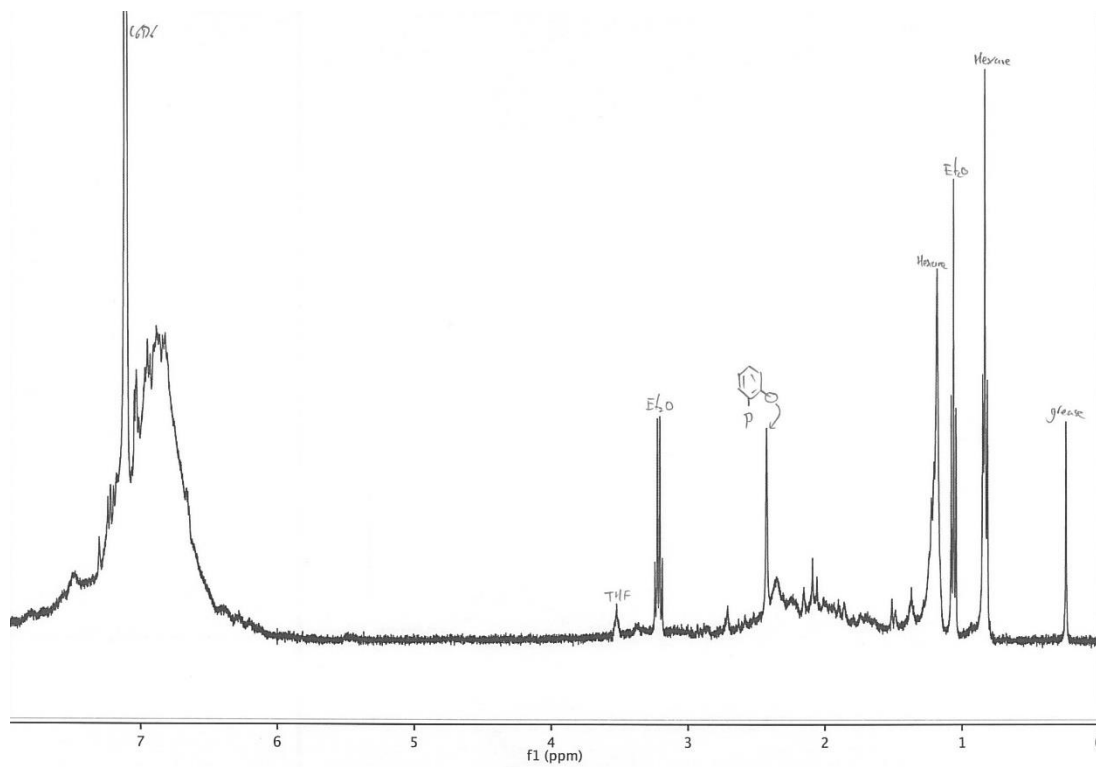
*Figure B 9: ^{1}H-NMR spectrum in C_6D_6 of a 1:1 mixture of **L1** and Ni(cod)$_2$*
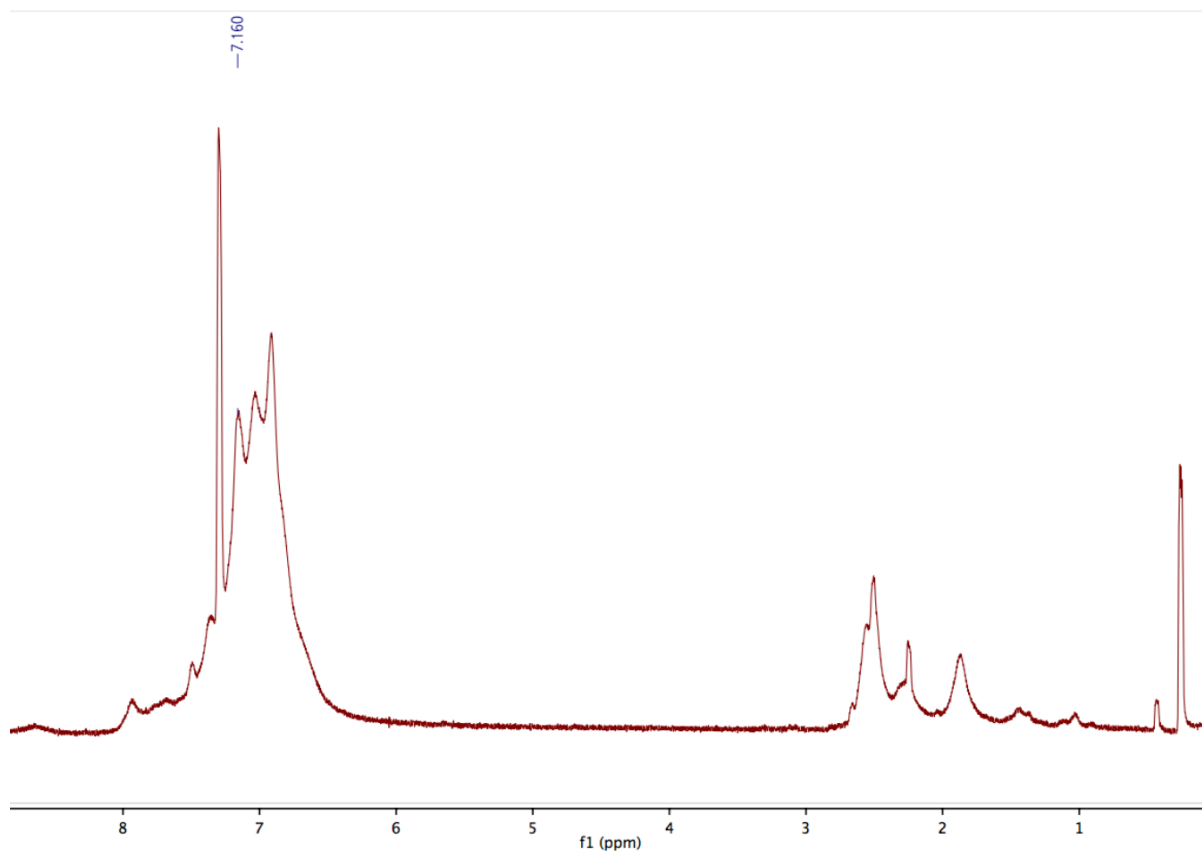
*Figure B 10:¹H-NMR spectrum of the complexation of **L1**, Ni(COD)₂ in toluene.*
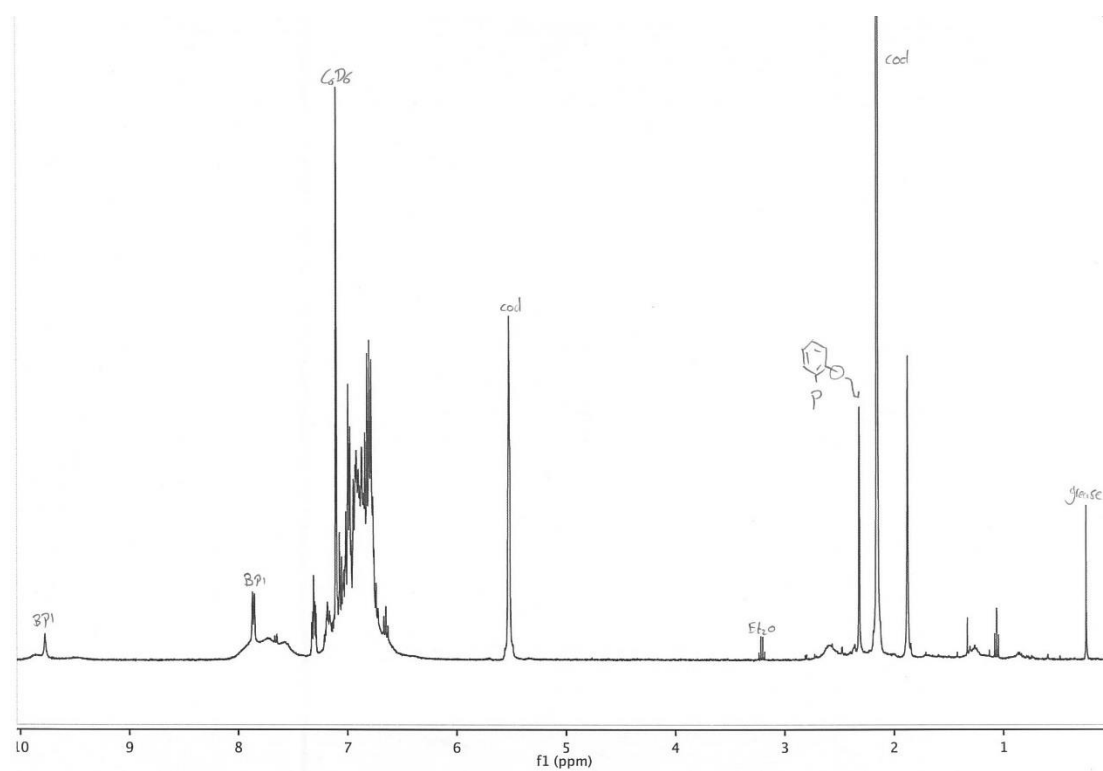
*Figure B 11: ¹H-NMR spectrum in C₆D₆ of a 1:1:1 mixture of **L1**, Ni(cod)₂ and BPI*
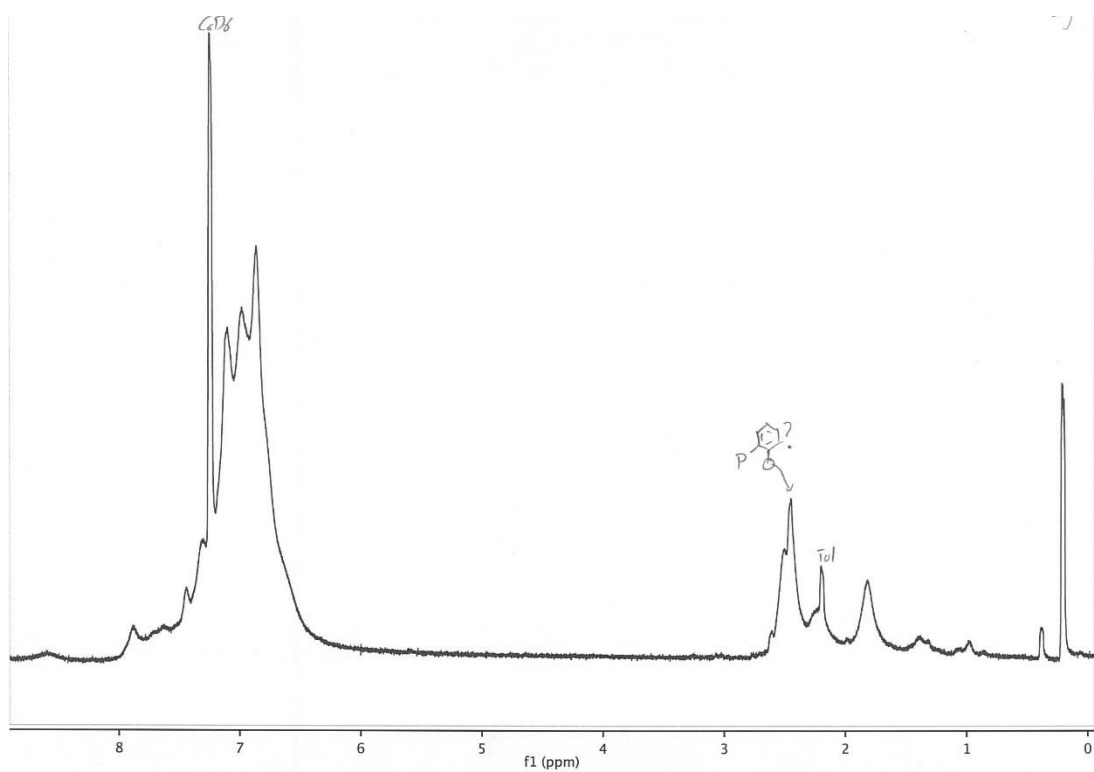
Figure B 12: ^{1}H-NMR spectrum in C$_6$D$_6$ of a 3:2 mixture of **L1** and Ni(cod)$_2$
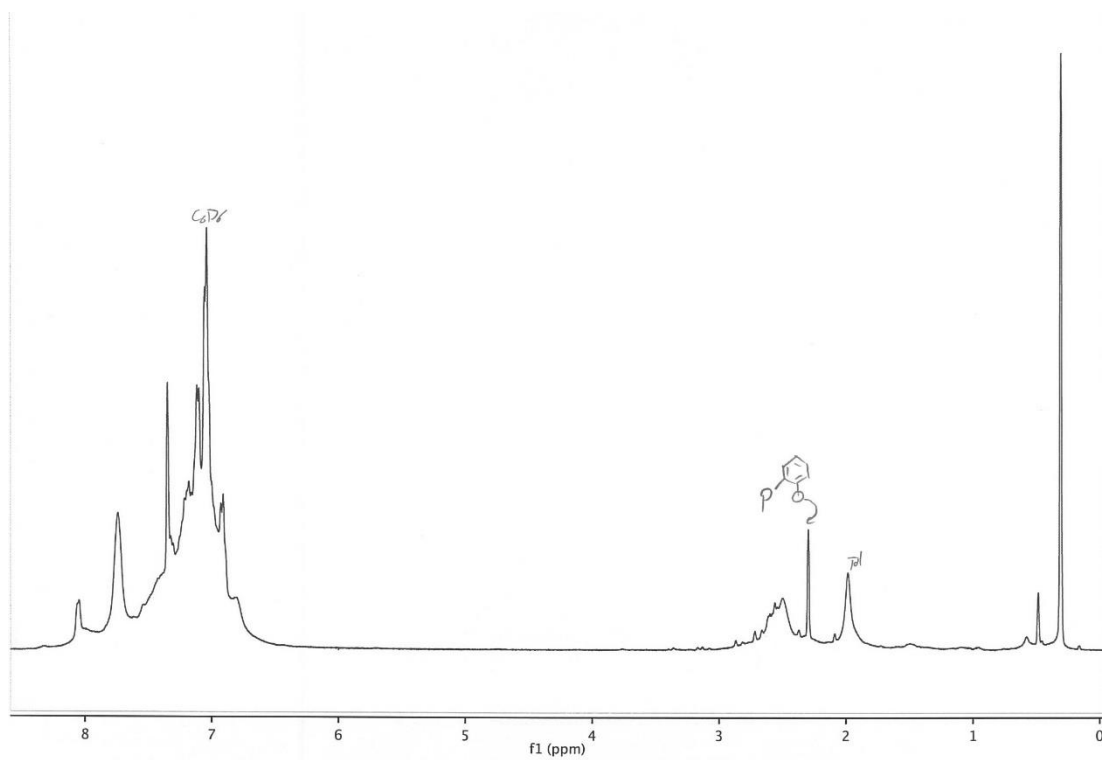
Figure B 13: ^{1}H-NMR spectrum in C$_6$D$_6$ of a 1:1:1 mixture of **L1**, Ni(cod)$_2$ and PPh$_3$
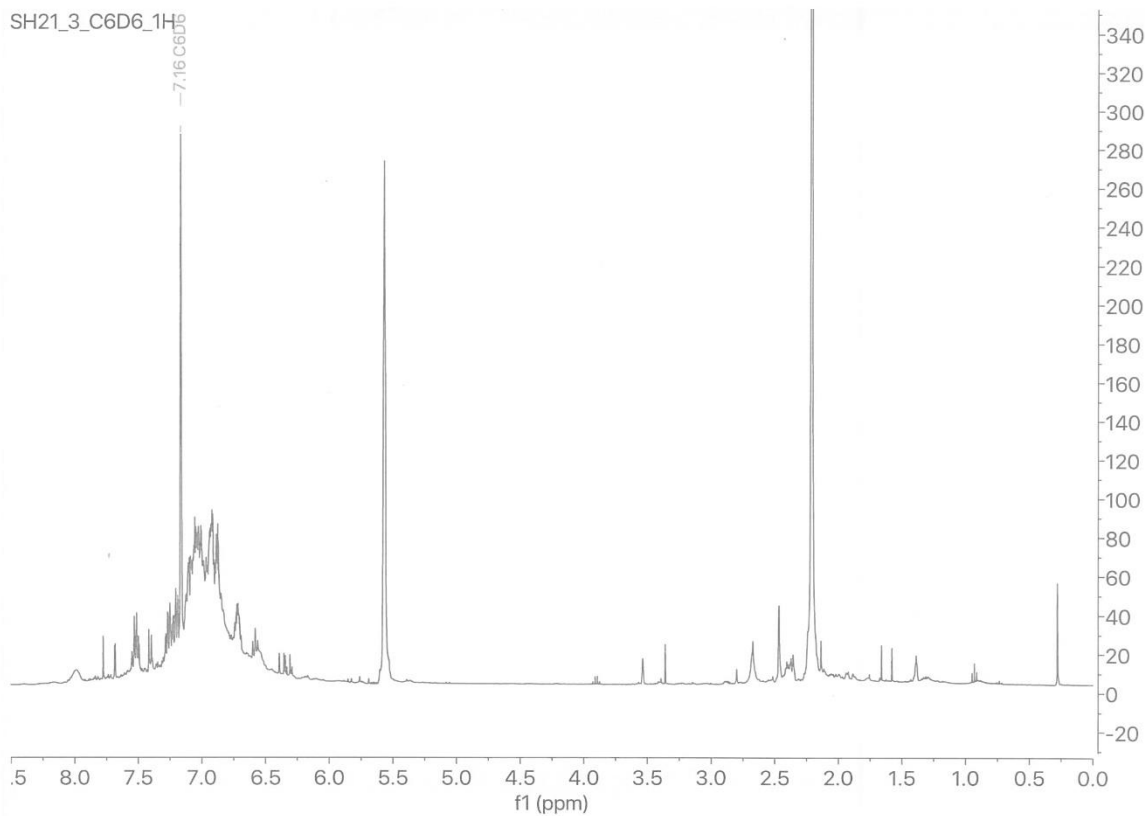
*Figure B 14: 1H-NMR spectrum in C6D6 of a 1:1:1 mixture of **L1**, Ni(cod)2 and phenylacetylene*
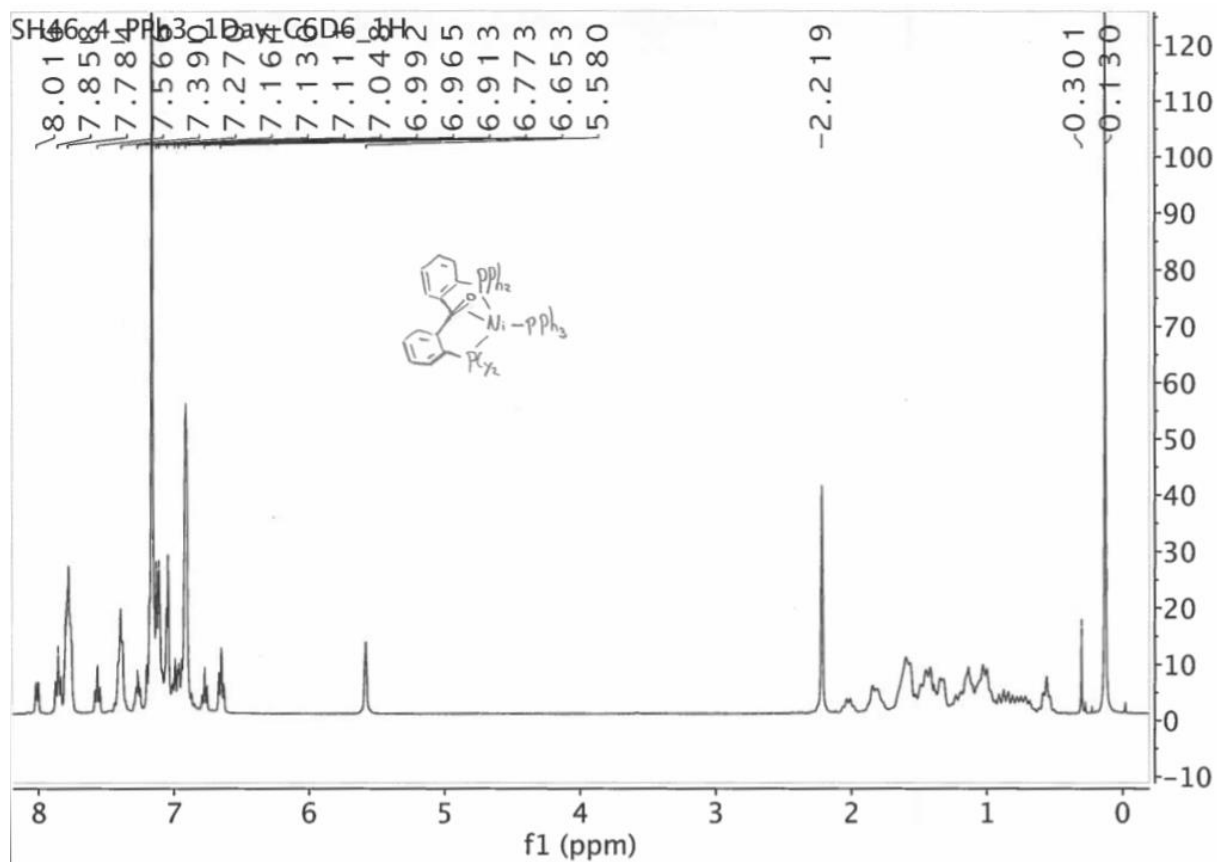
*Figure B 15: ¹H-NMR spectrum in C₆D₆ of **17***
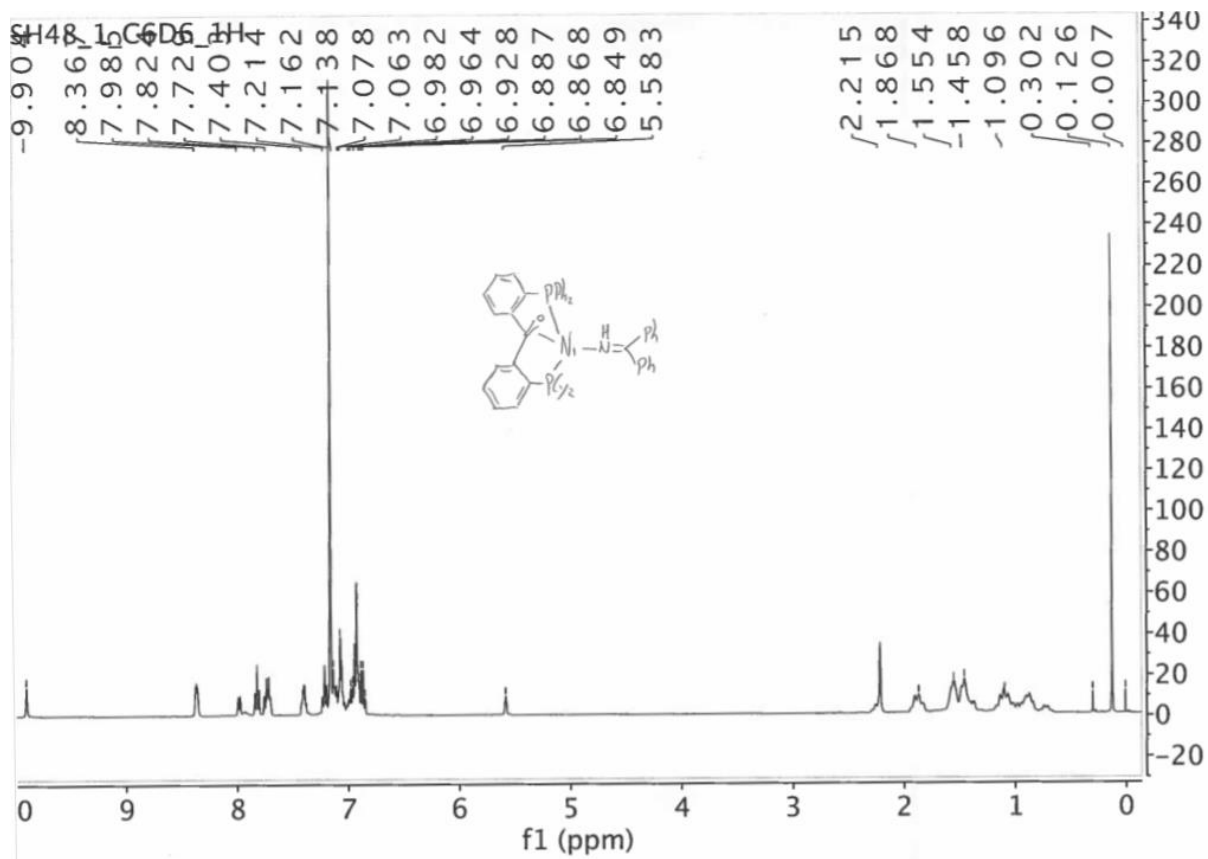
Figure B 16: ^{1}H-NMR spectrum in C_6D_6 of **18**
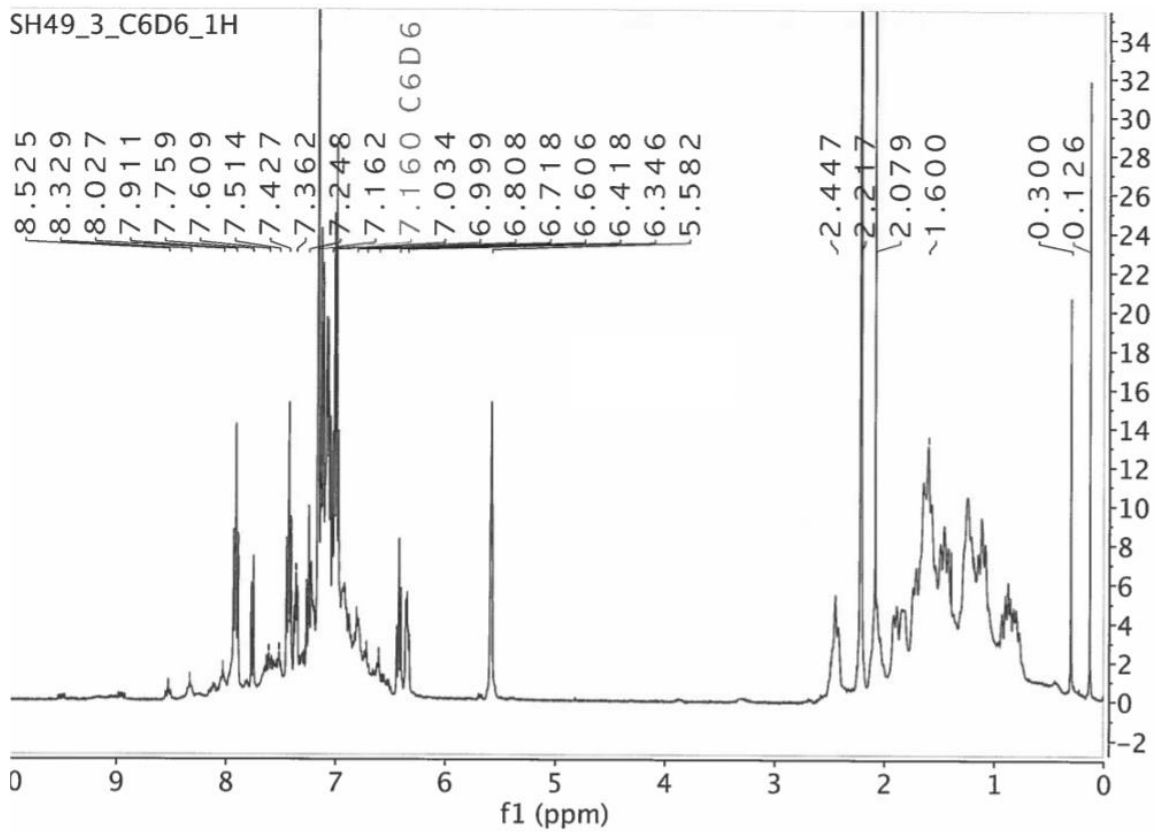
Figure B 17: ^{1}H-NMR spectrum in C_6D_6 of the complexation with Ni(COD)$_2$, **L2** and phenylacetylene
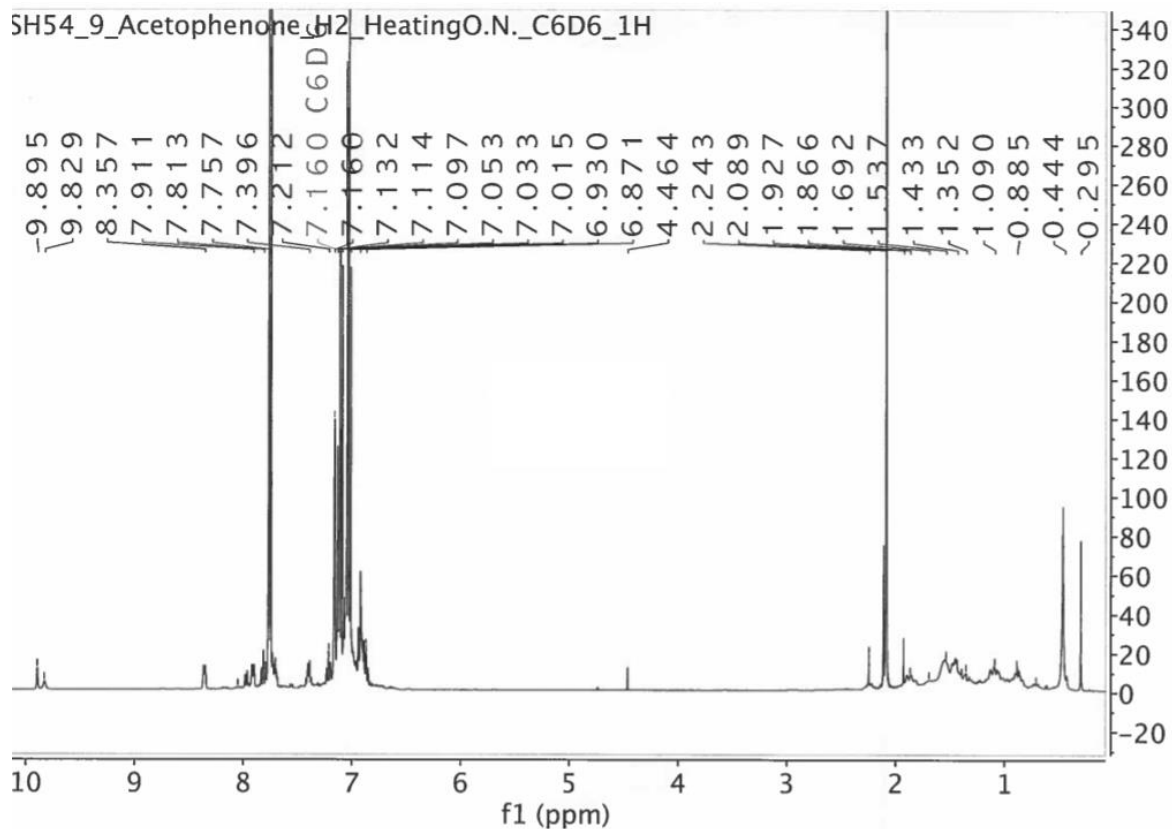
*Figure B 18: ¹H-NMR spectrum in C_6D_6 of the attempted hydrogenation of acetophenone with **18** and H_2*
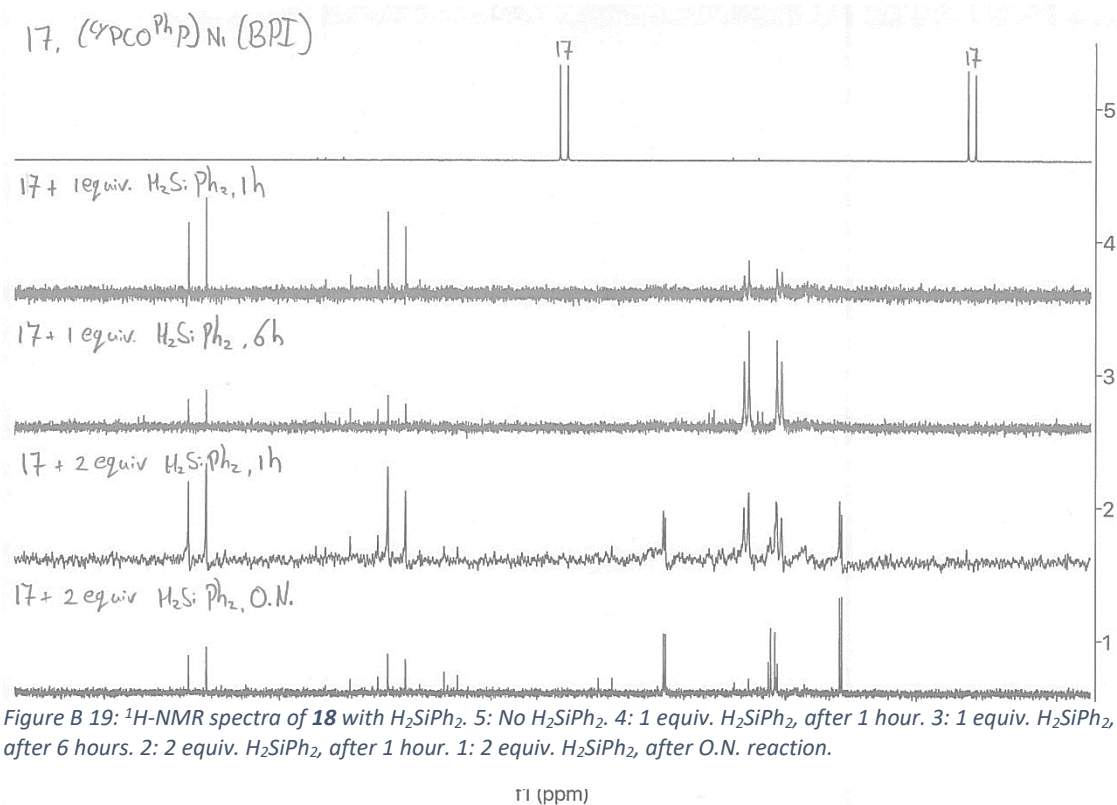
*Figure B 19: ¹H-NMR spectra of **18** with H_2SiPh_2. 5: No H_2SiPh_2. 4: 1 equiv. H_2SiPh_2, after 1 hour. 3: 1 equiv. H_2SiPh_2, after 6 hours. 2: 2 equiv. H_2SiPh_2, after 1 hour. 1: 2 equiv. H_2SiPh_2, after O.N. reaction.*
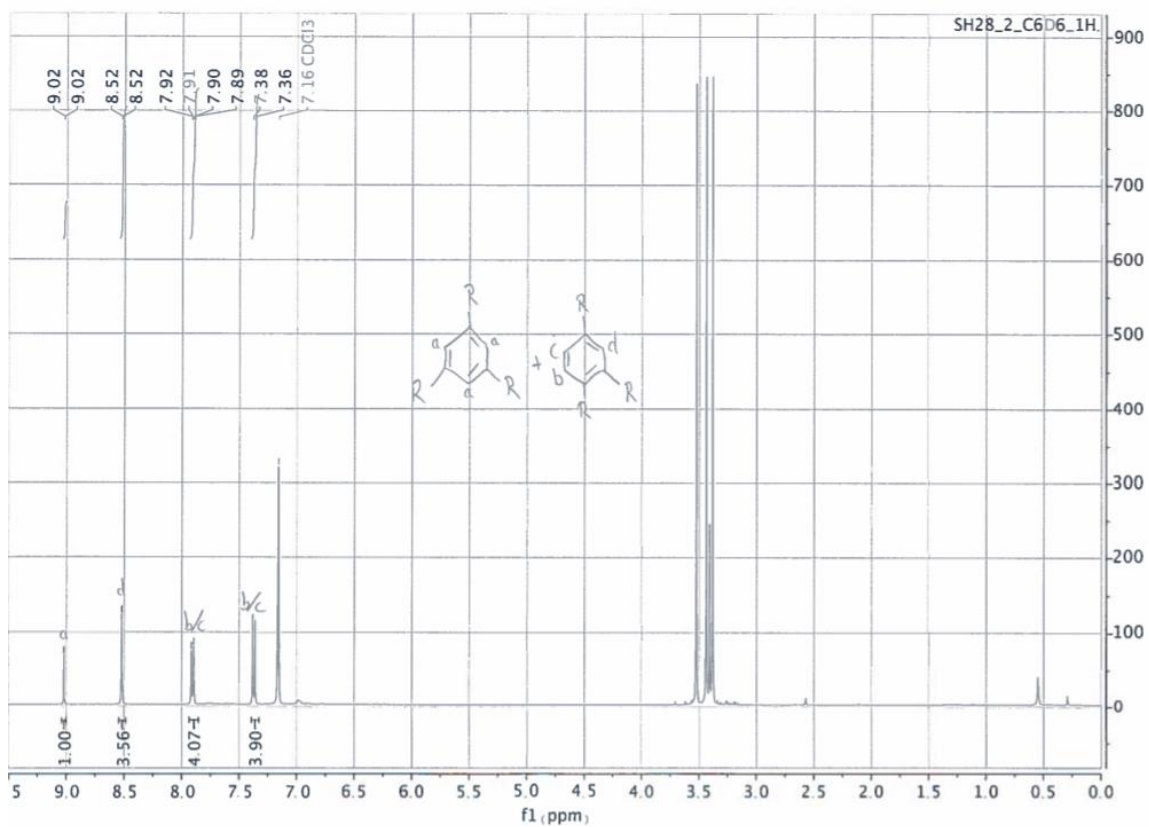
*Figure B 20: ^{1}H-NMR spectrum of the [2+2+2] cyclotrimerization product of methylpropiolate, using a catalyst mixture of Ni(COD)$_2$ and **L1**. R = -COOMe.*
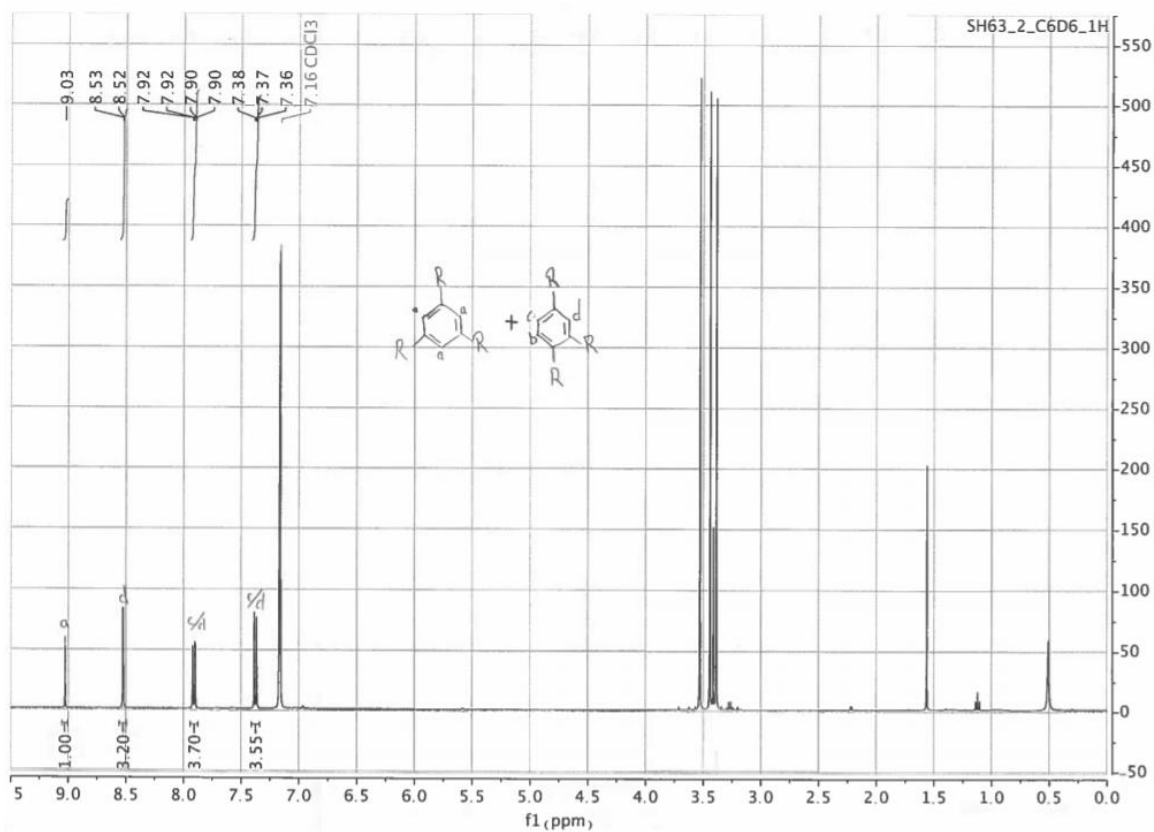
*Figure B 21: ^{1}H-NMR spectrum of the [2+2+2] cyclotrimerization product of methylpropiolate, using a catalyst mixture of Ni(COD)$_2$ and **L2** . R = -COOMe.*
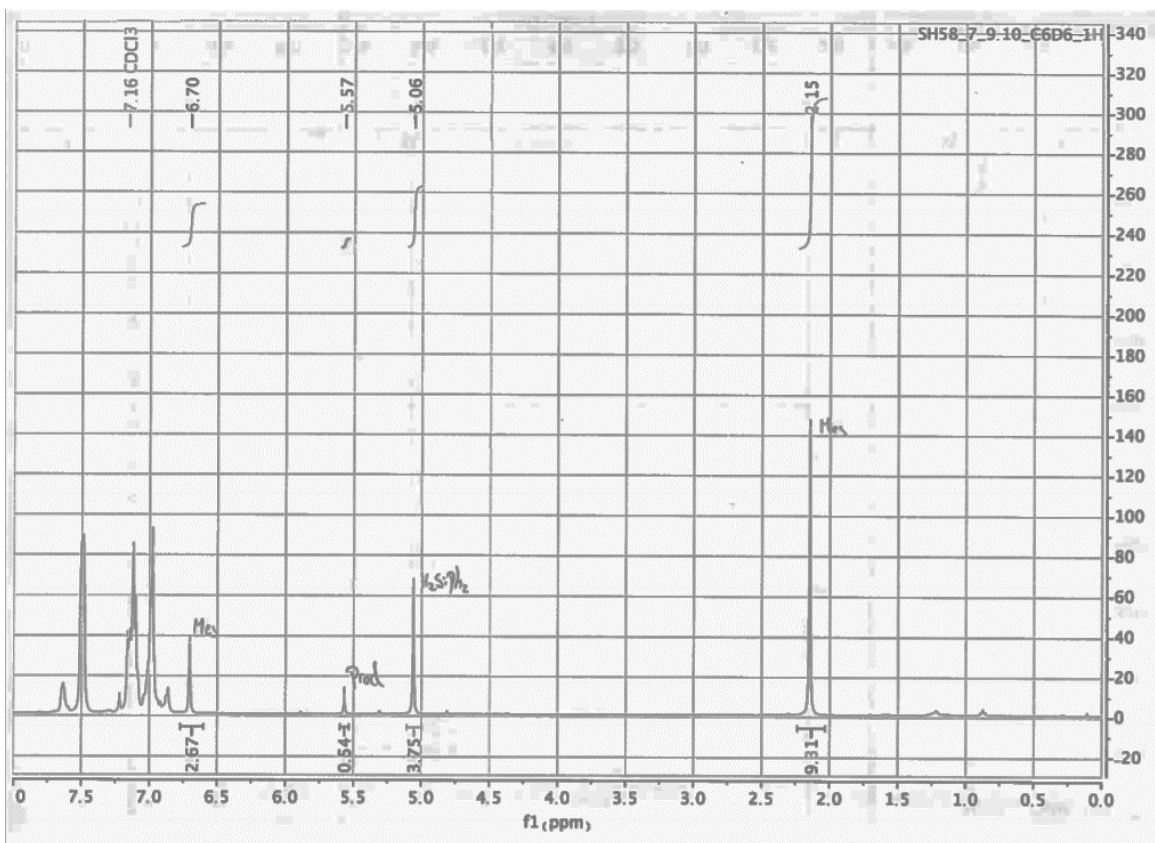
*Figure B 22: ¹H-NMR spectrum of the hydrosilylation of diphenylacetylene with diphenylsilane, using **18***
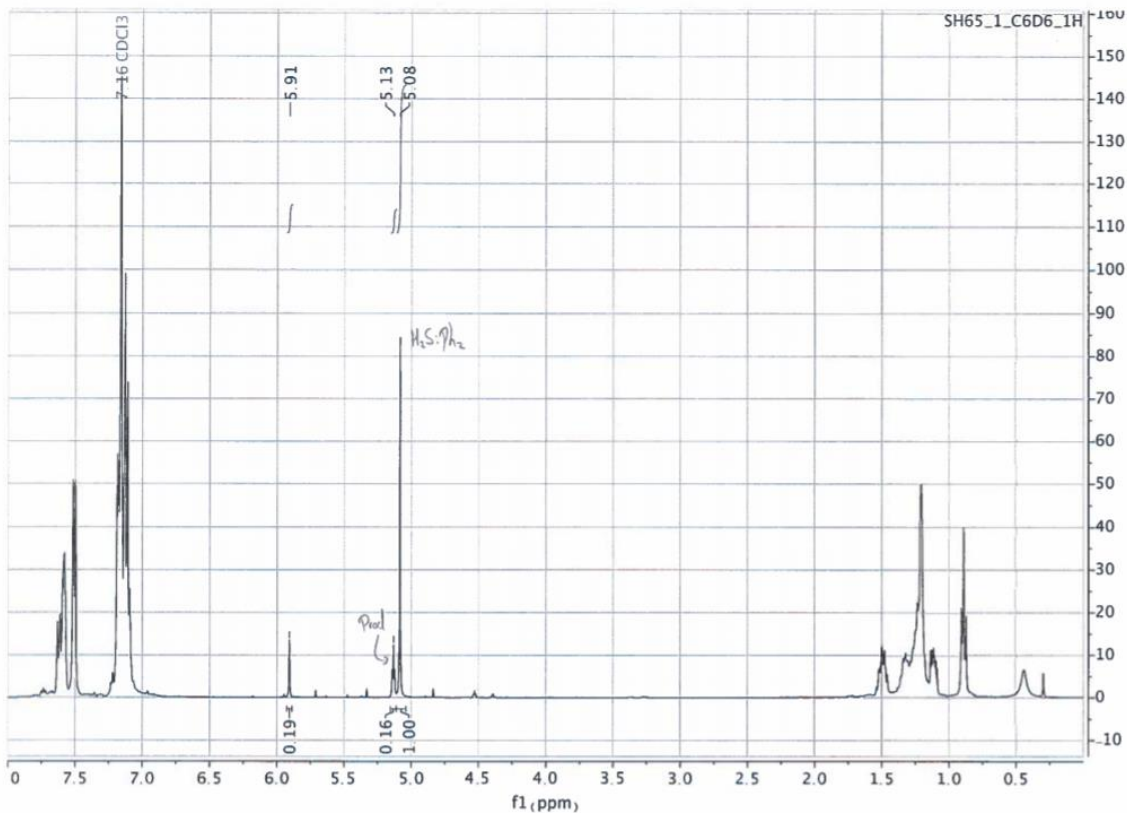
*Figure B 23: ¹H-NMR spectrum of the hydrosilylation of 1-octene with diphenylsilane , using a catalyst mixture of Ni(COD)₂ and **L1**.*
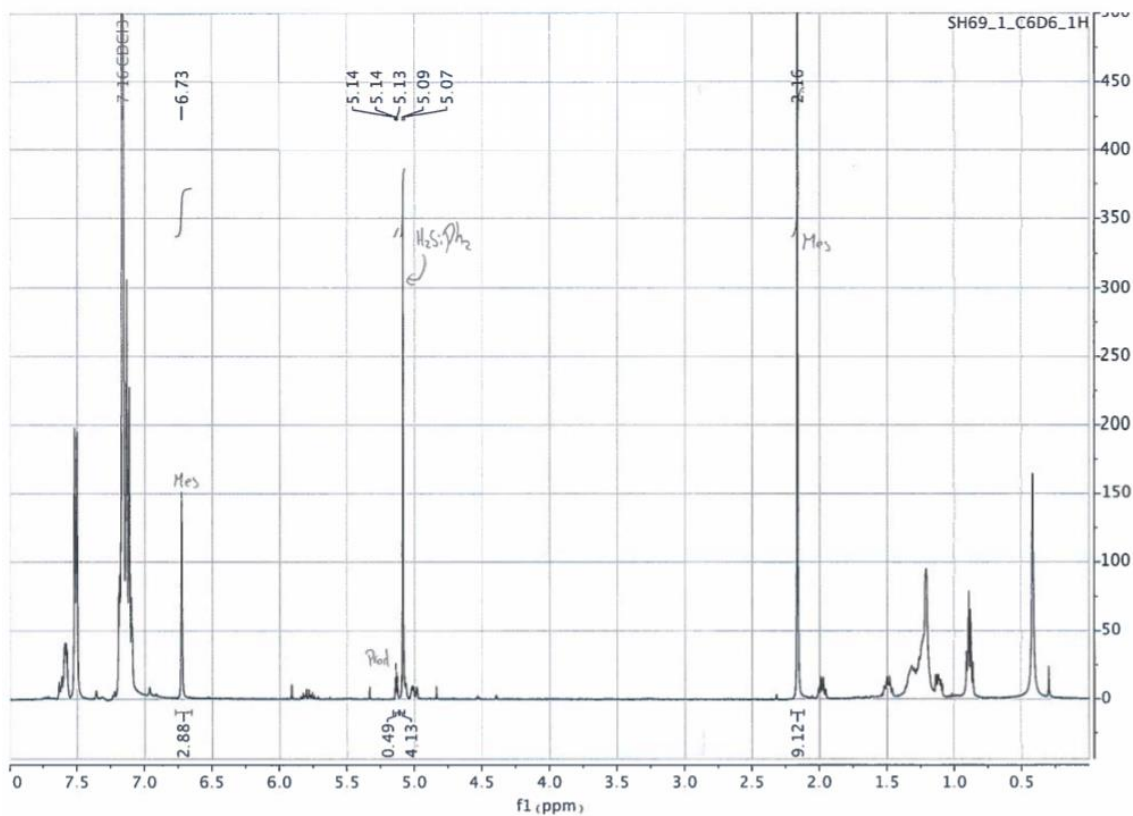
*Figure B 24: ¹H-NMR spectrum of the hydrosilylation of 1-octene with diphenylsilane, using **18**.*
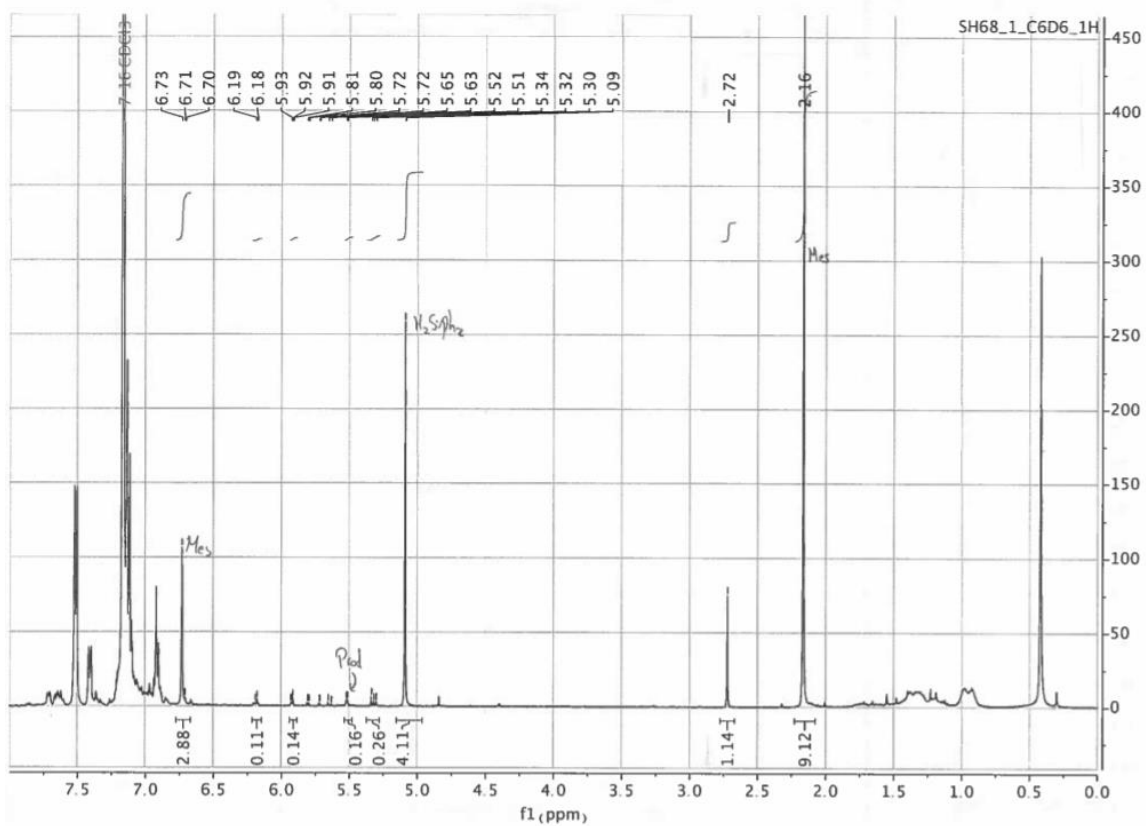
*Figure B 25: ¹H-NMR spectrum of the hydrosilylation of phenylacetylene with diphenylsilane. using **18**.*
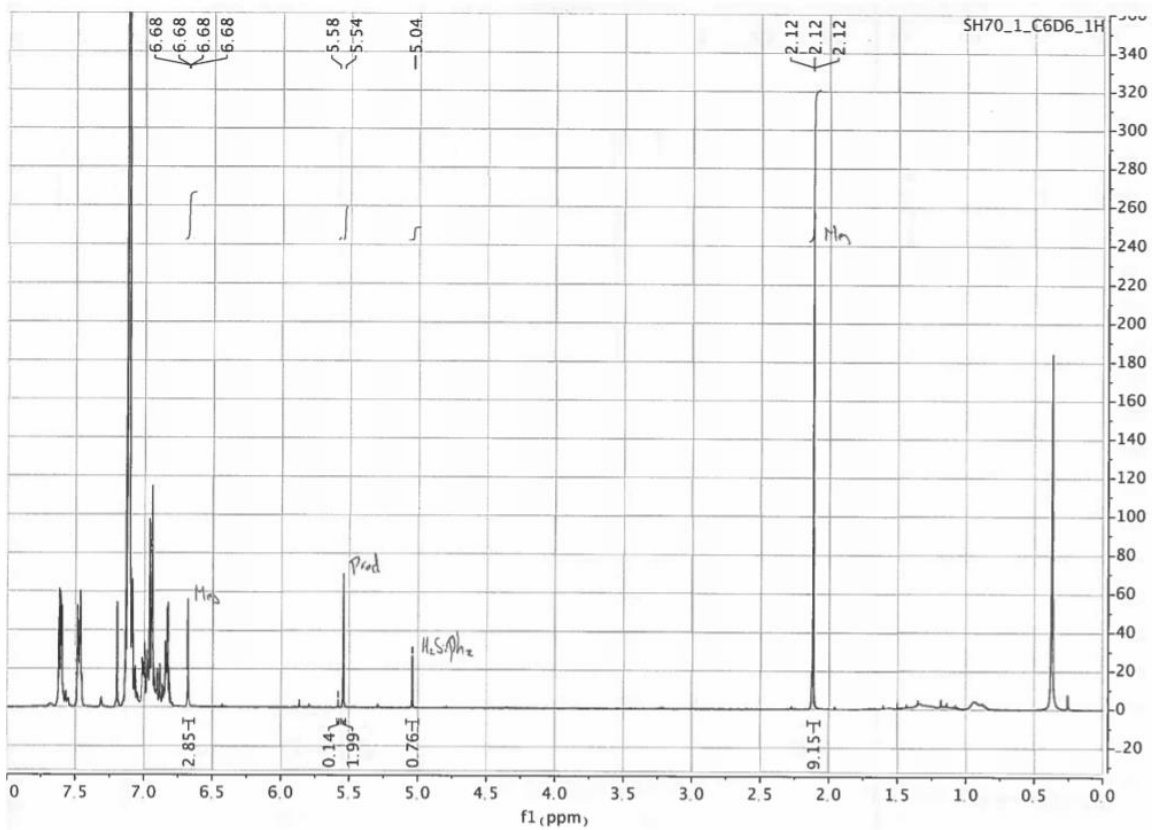
*Figure B 26: ^{1}H-NMR spectrum of the hydrosilylation in benzene of diphenylacetylene with H$_2$SiPh$_2$, using **18**.*
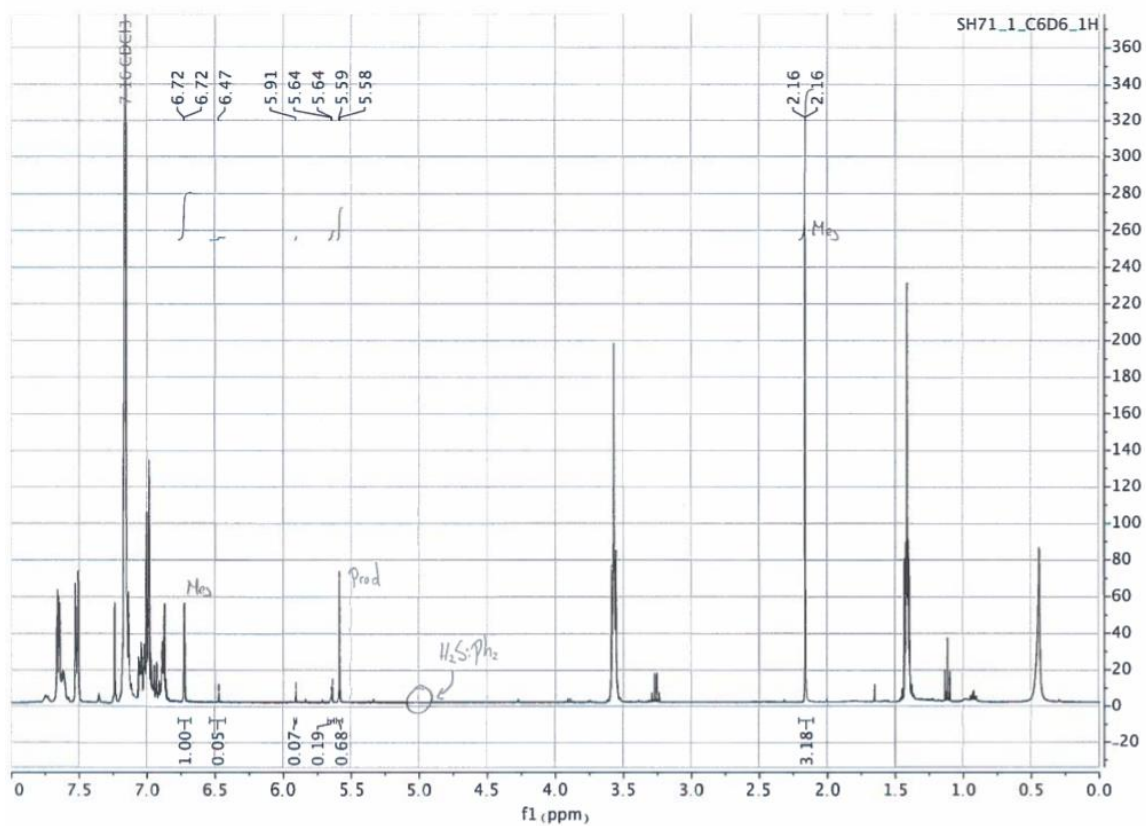
*Figure B 27: ^{1}H-NMR spectrum of the hydrosilylation in THF of diphenylacetylene with H$_2$SiPh$_2$, using **18**.*
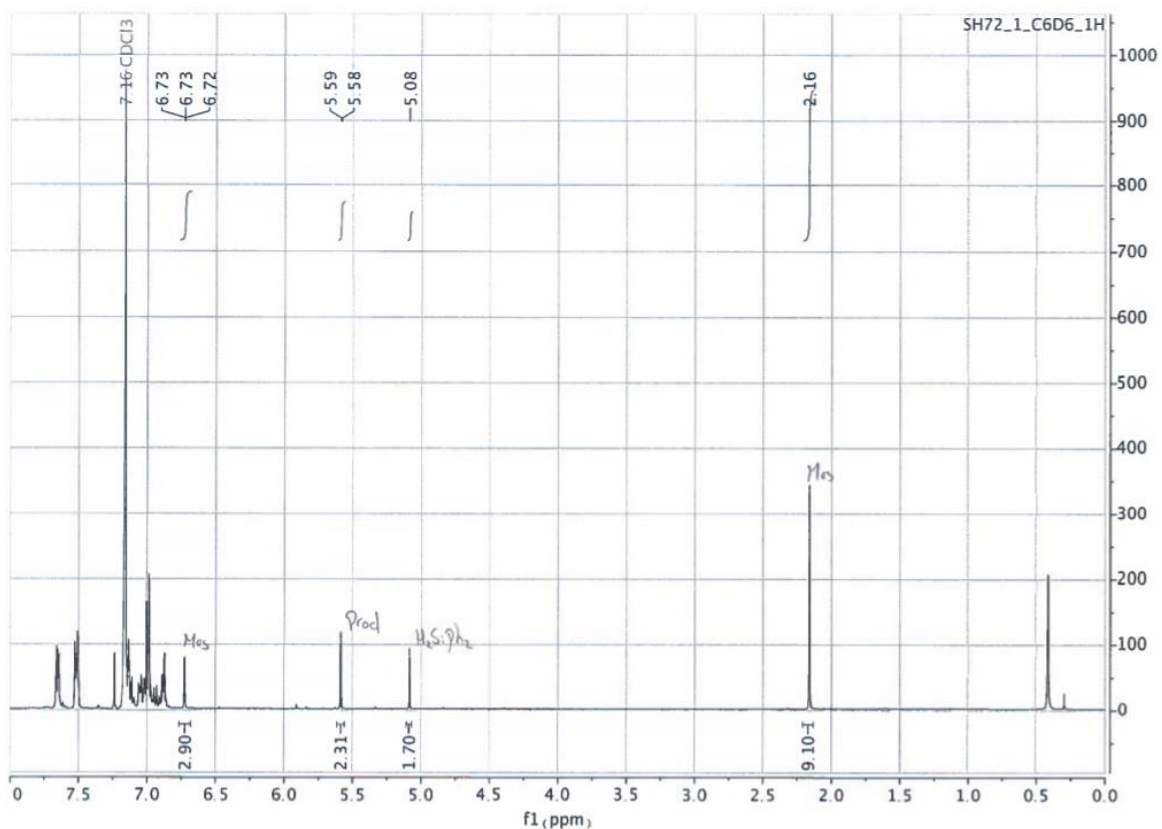
*Figure B 28: ^{1}H-NMR spectrum of the hydrosilylation in Et$_2$O of diphenylacetylene with H$_2$SiPh$_2$, using **18**.*
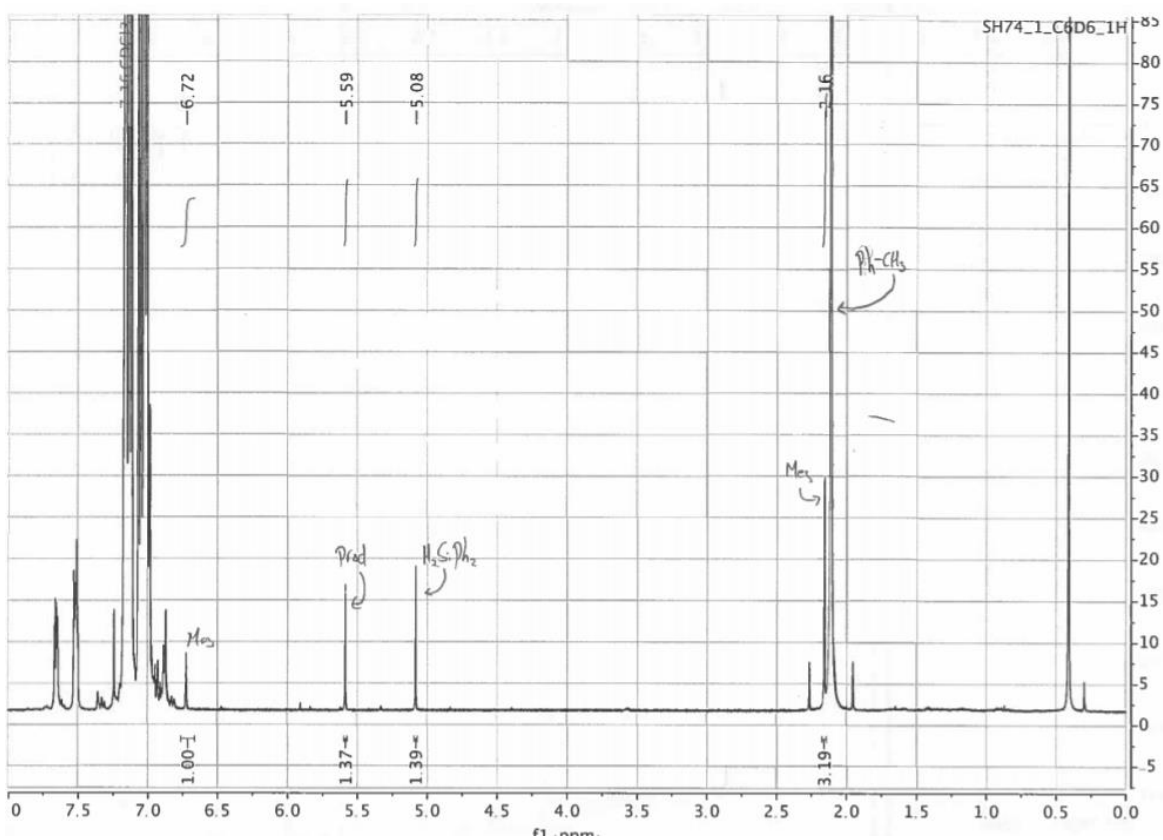
*Figure B 29: ^{1}H-NMR spectrum of the hydrosilylation in toluene of diphenylacetylene with H$_2$SiPh$_2$, using **18**.*

C. ^{31}P-NMR spectra

Figure C 1: ^{31}P -NMR spectrum in C_6D_6 of (2-bromophenyl)diphenylphosphane (**7**).

Figure C 2: ^{31}P -NMR spectrum in C_6D_6 of (2-bromophenyl)di(o-tolyl)phosphane (**8**).
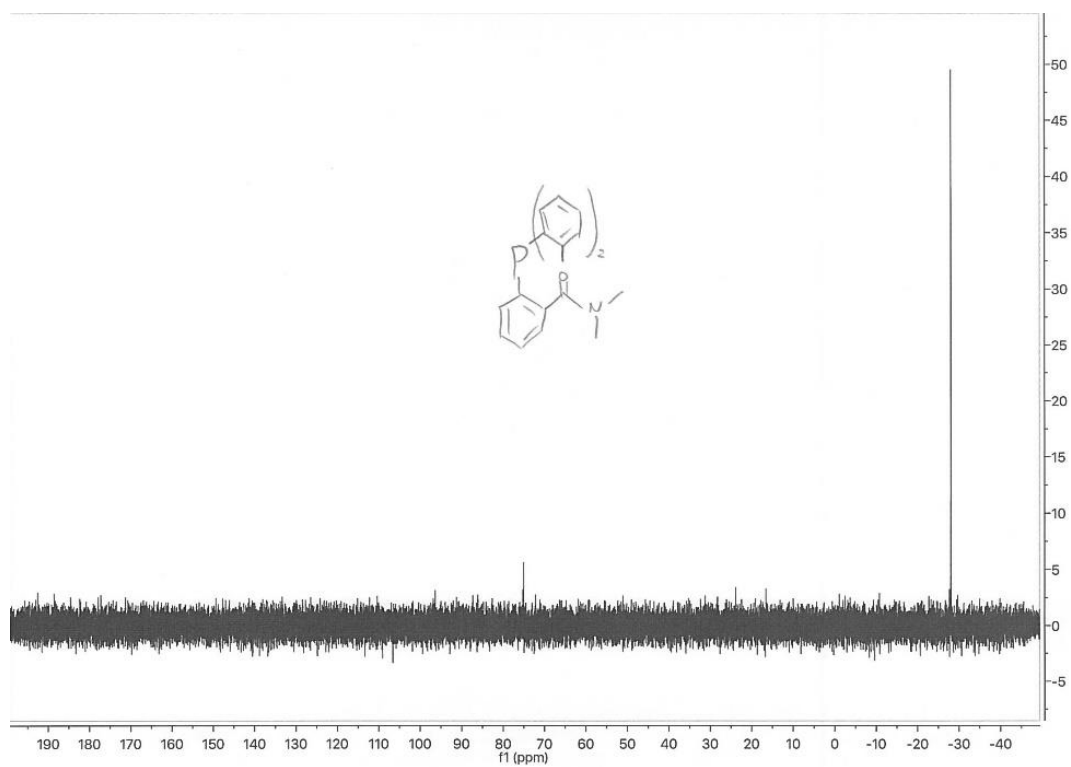
*Figure C 3: ^{31}P -NMR spectrum in C_6D_6 of 2-(di(o-tolyl)phosphaneyl)-N,N-dimethylbenzamide (**11**).*
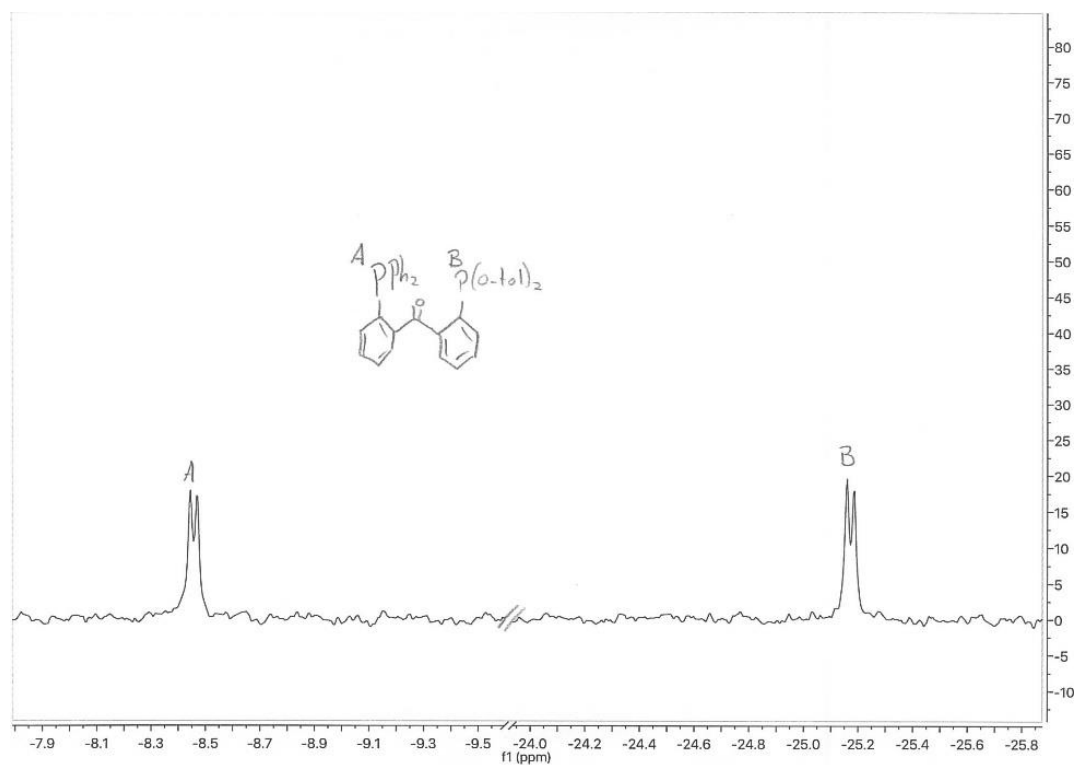
*Figure C 4: ^{31}P -NMR spectrum in C_6D_6 of **1**, (2-(di-o-tolylphosphaneyl)phenyl)(2-(diphenylphosphaneyl)phenyl)methanone (**L1**)*
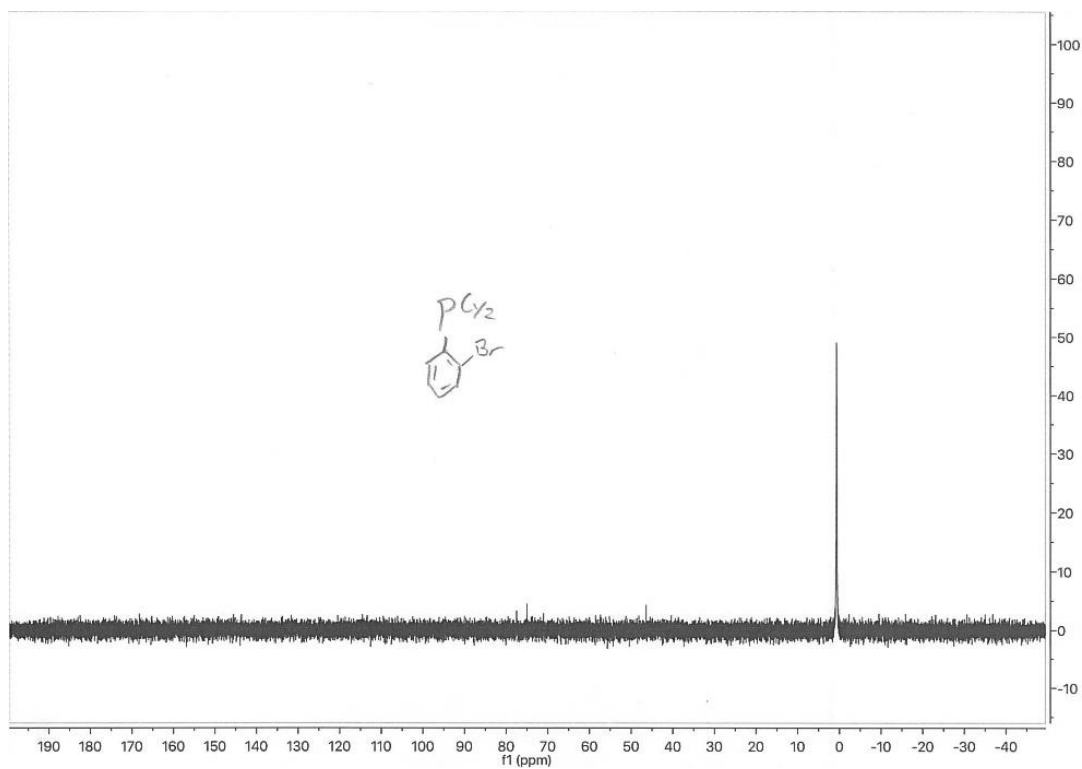
*Figure C 5: ^{31}P-NMR spectrum in C_6D_6 of (2-bromophenyl)dicyclohexylphosphane (**9**).*
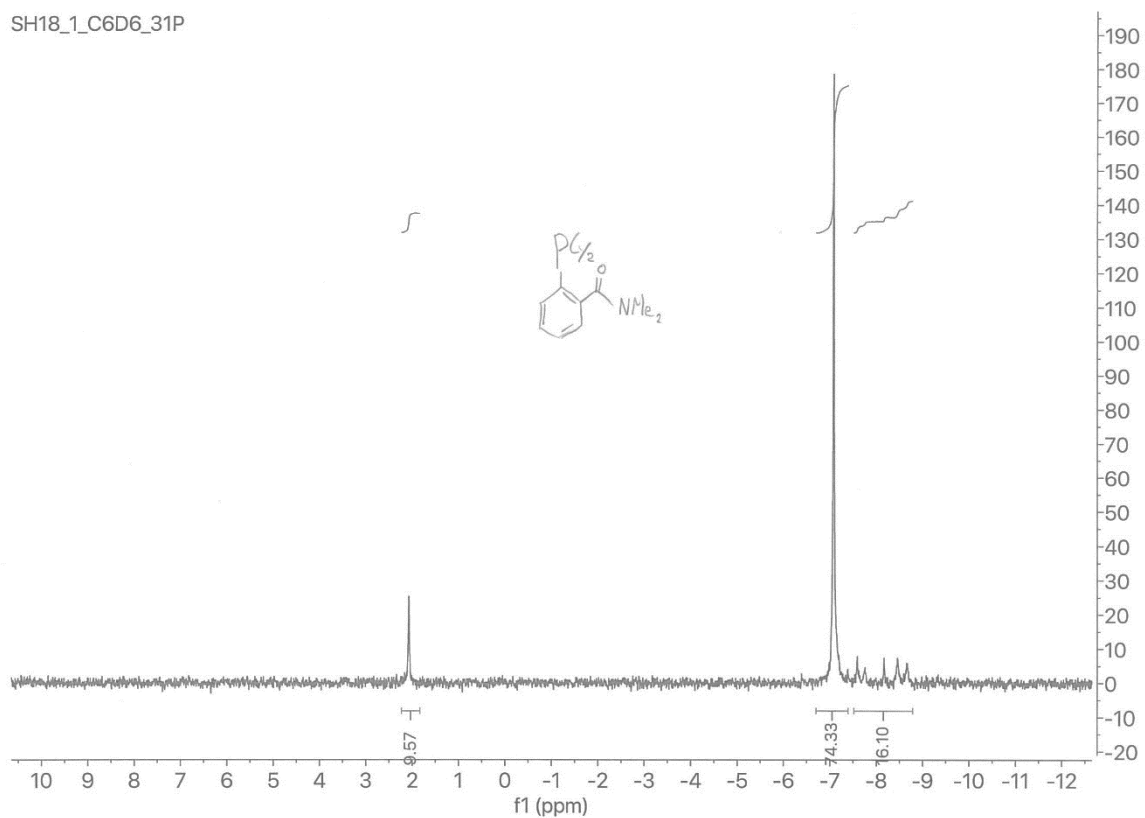
*Figure C 6: ^{31}P-NMR spectrum of the crude mixture of the synthesis of 2-(dicyclohexylphosphaneyl)-N,N-dimethylbenzamide (**10**).*

SH32_5_C6D6_31P_Flush

−−11.36
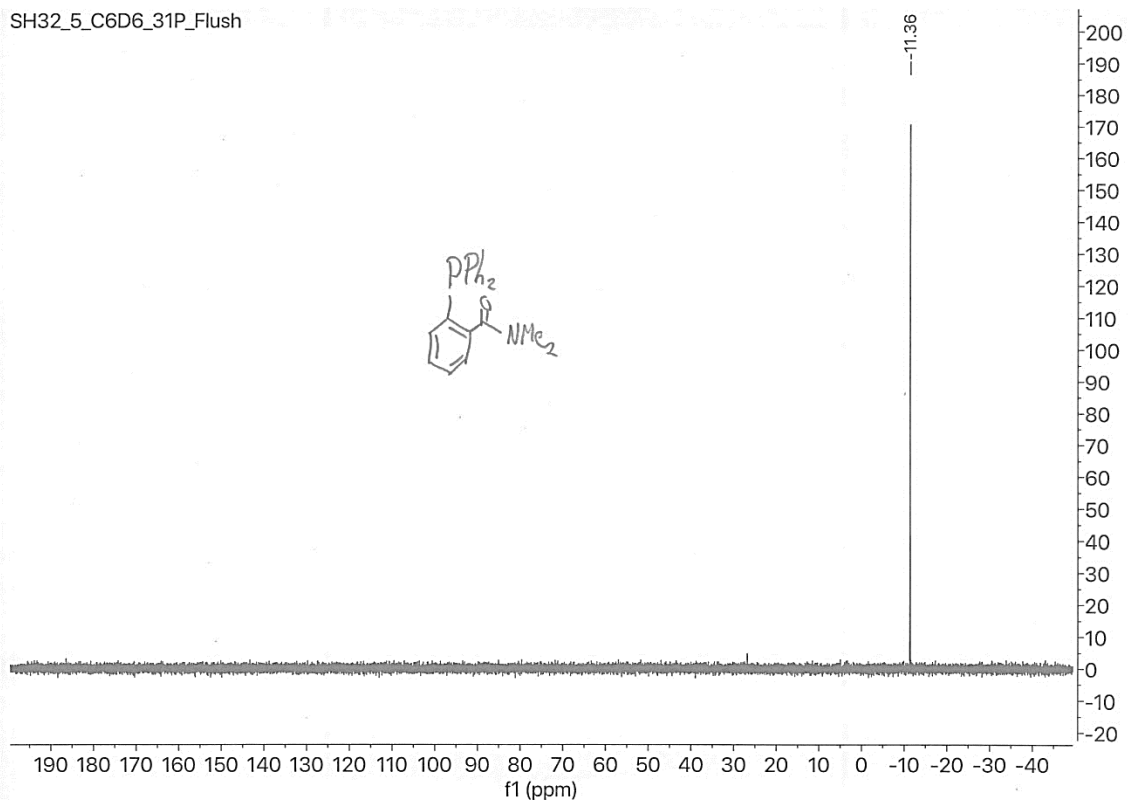
Figure C 7: ^{31}P-NMR spectrum of 2-(diphenylphosphaneyl)-N,N-dimethylbenzamide (11).

31P_2_c6d6_N2_128scans

−−2.38
−−10.21
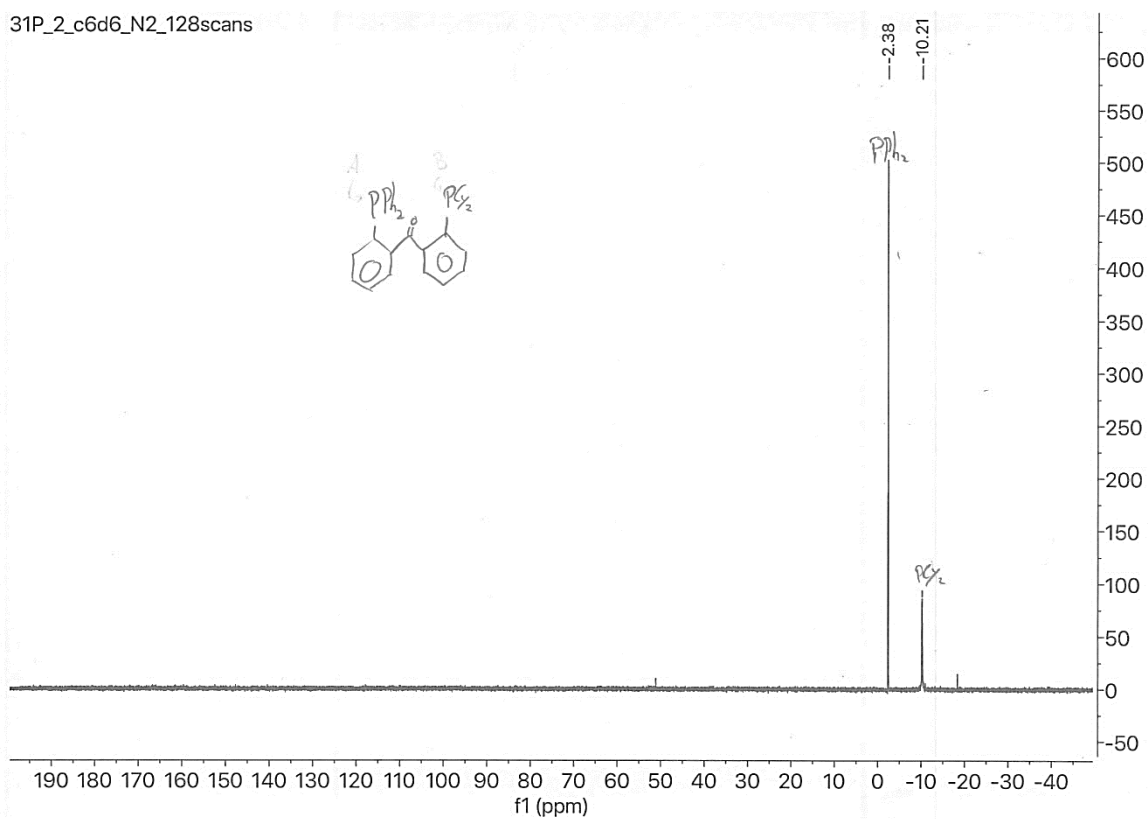
Figure C 8: ^{31}P-NMR spectrum of (2-(dicyclohexylphosphaneyl)phenyl)(2-(diphenylphosphaneyl)phenyl)methanone, (L2).
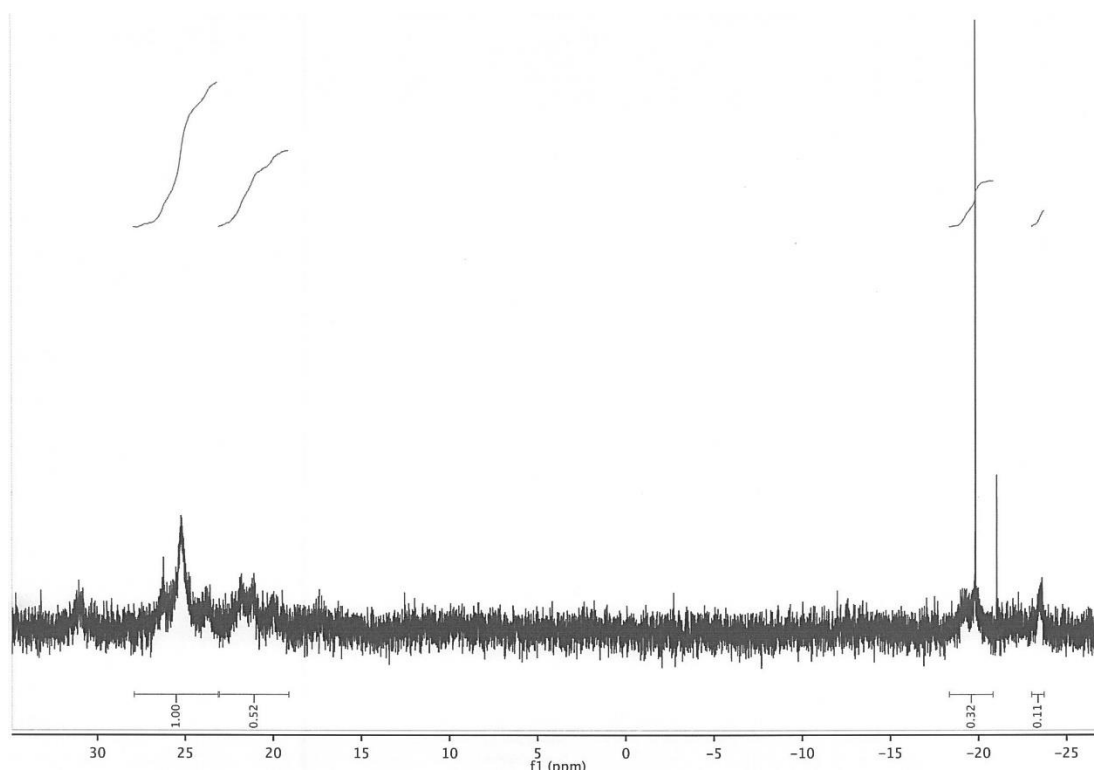
*Figure C 9: ^{31}P-NMR spectrum in C_6D_6 of a 1:1 mixture of **L1** and Ni(cod)$_2$*
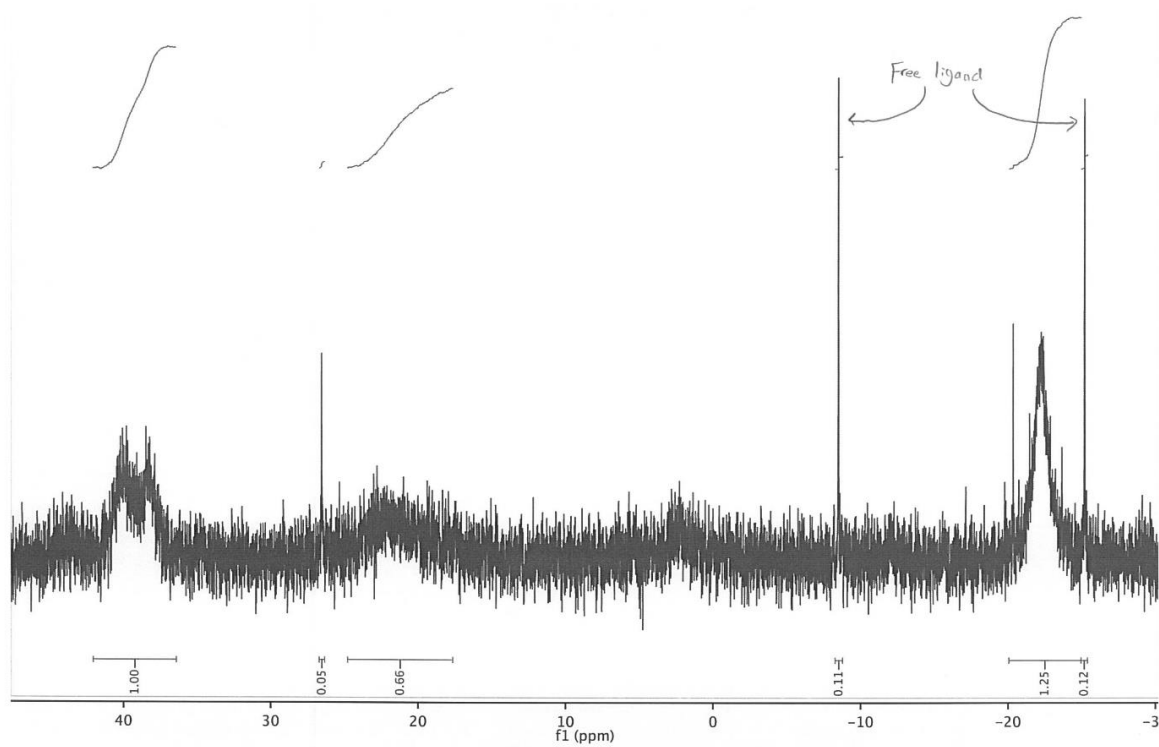
*Figure C 10: ^{31}P-NMR spectrum of the complexation of **L1** and Ni(COD)$_2$ in toluene.*
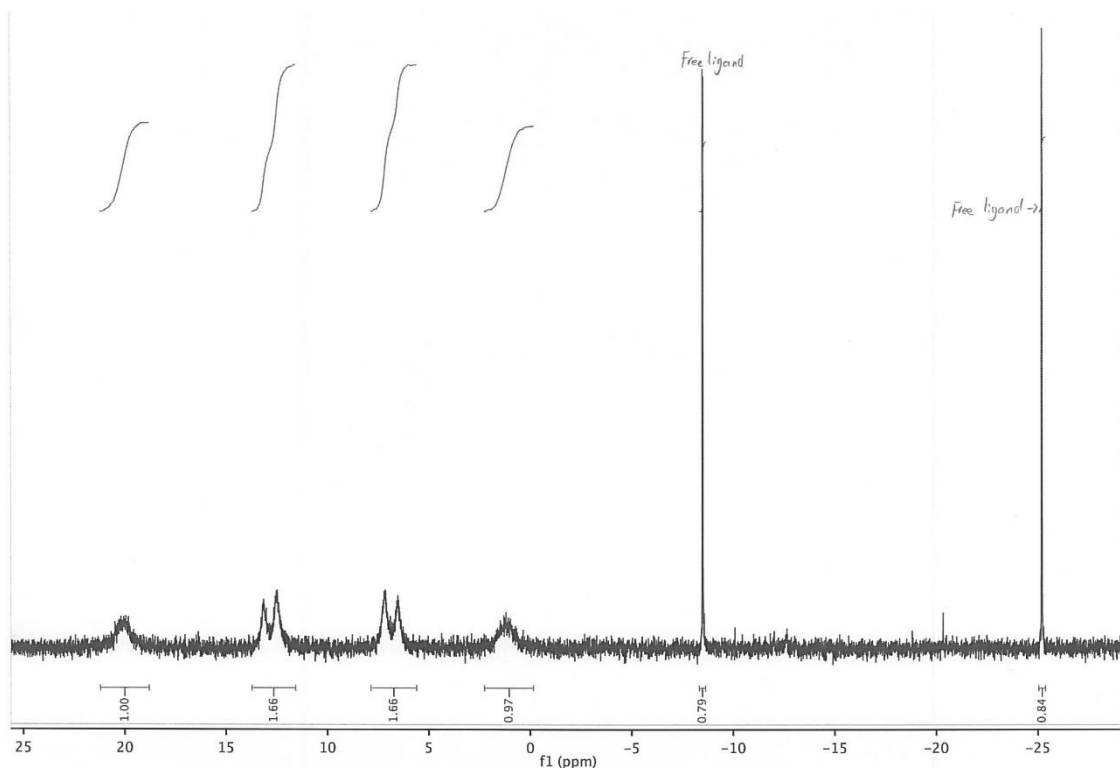
*Figure C 11: ^{31}P-NMR spectrum in C$_6$D$_6$ of a 1:1:1 mixture of **L1**, Ni(cod)$_2$ and BPI*
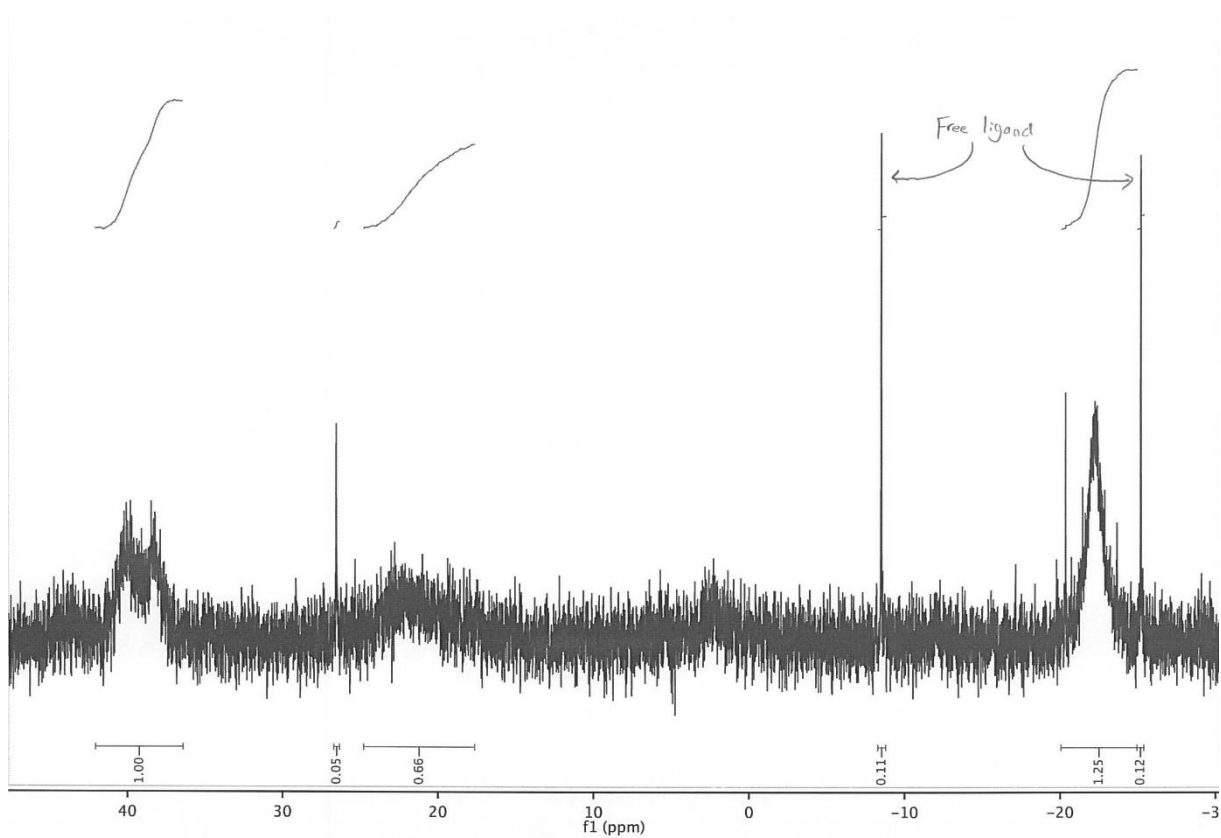
*Figure C 12: ^{31}P-NMR spectrum in C$_6$D$_6$ of a 3:2 mixture of **L1** and Ni(cod)$_2$*
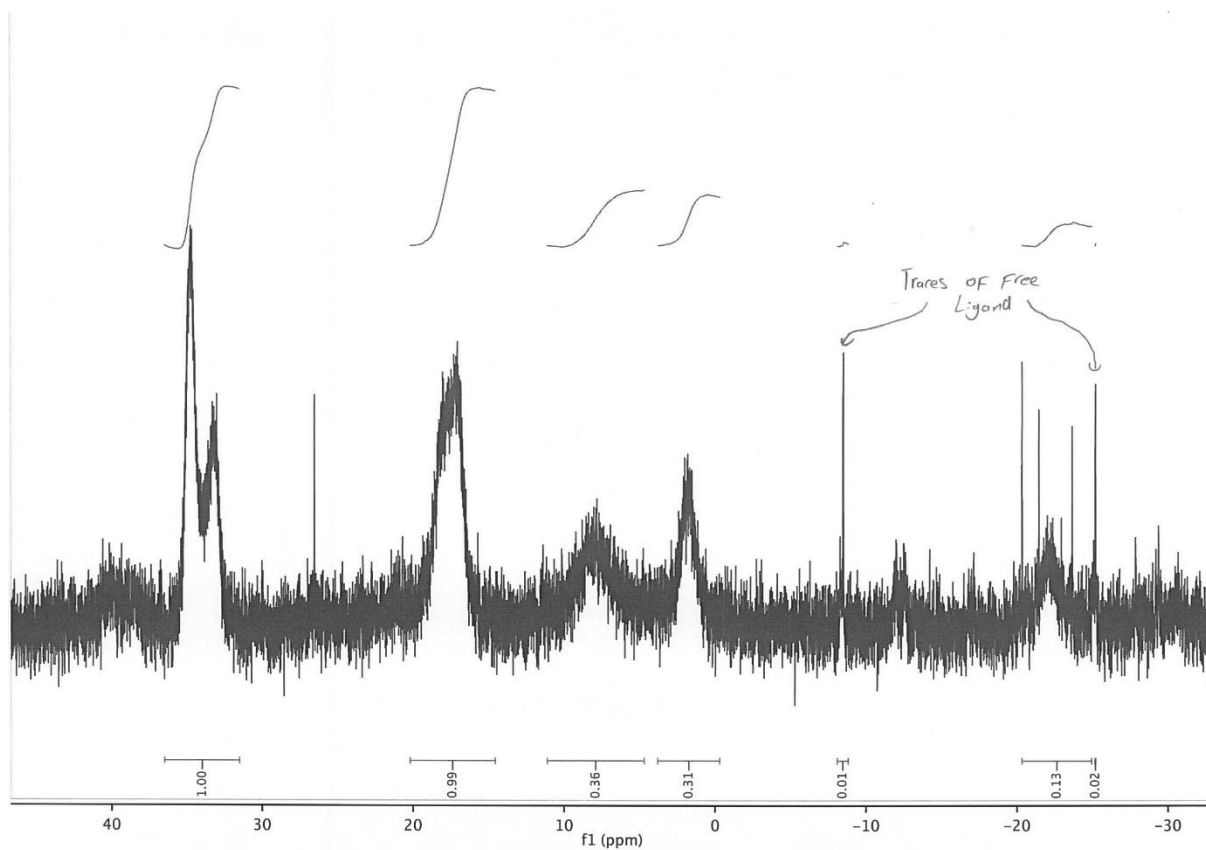
*Figure C 13: ^{31}P-NMR spectrum in C_6D_6 of a 1:1 mixture of **L1**, Ni(cod)$_2$ and PPh$_3$*
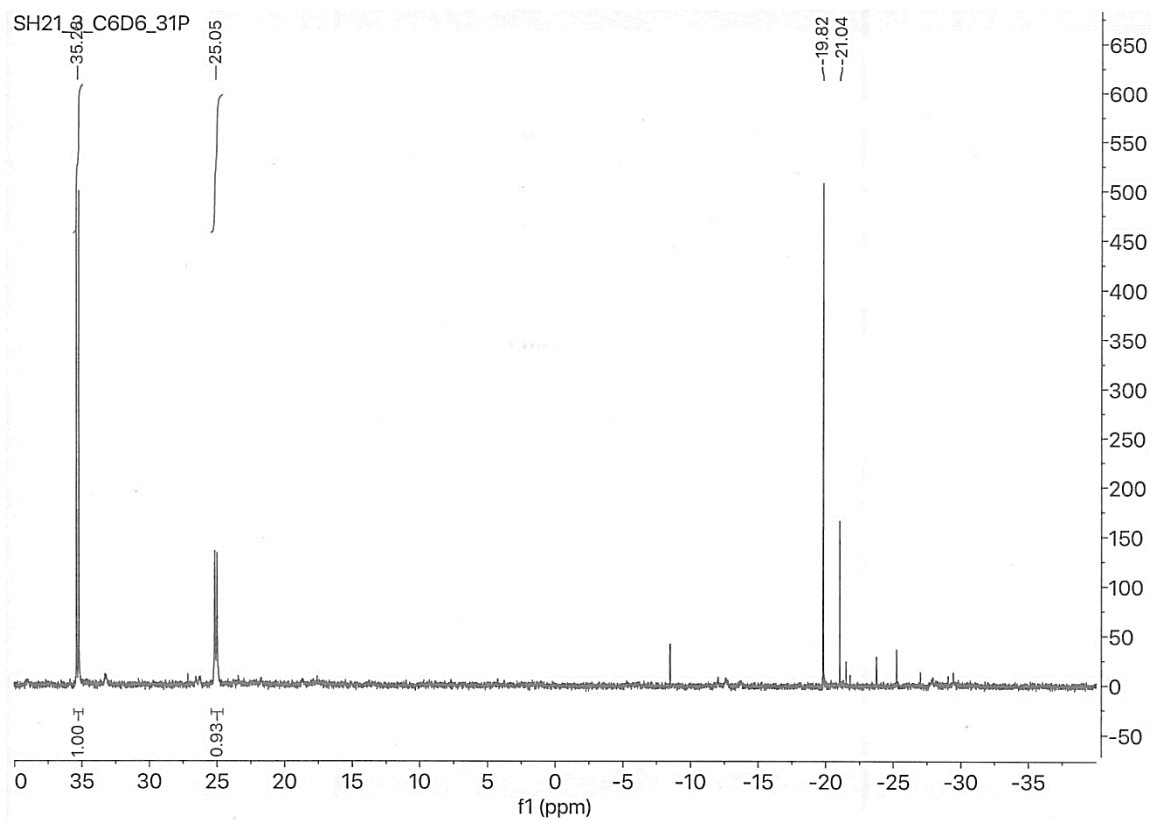
*Figure C 14: ^{31}P-NMR spectrum of the complexation in C_6D_6 of **L1**, Ni(COD)$_2$ and phenylacetylene*
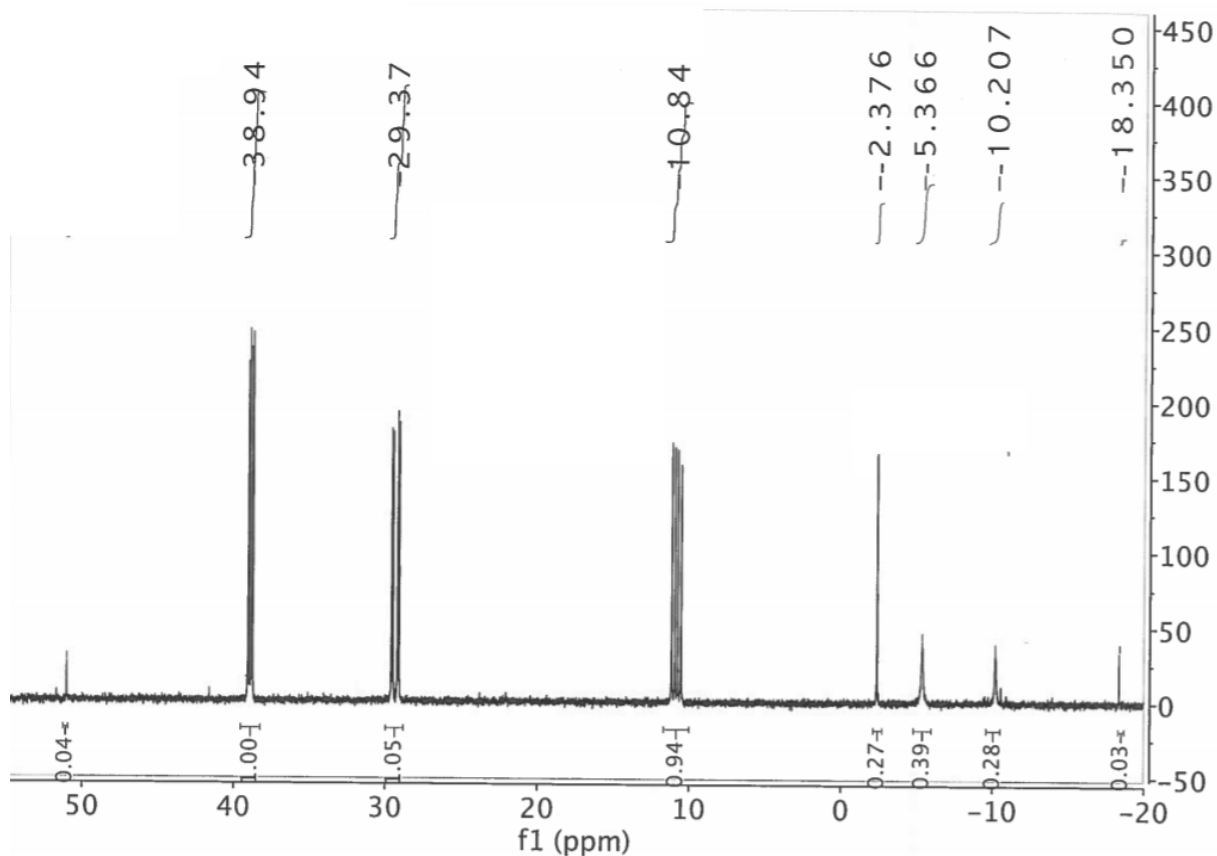
*Figure C 15: ^{31}P-NMR spectrum of **17** in benzene*
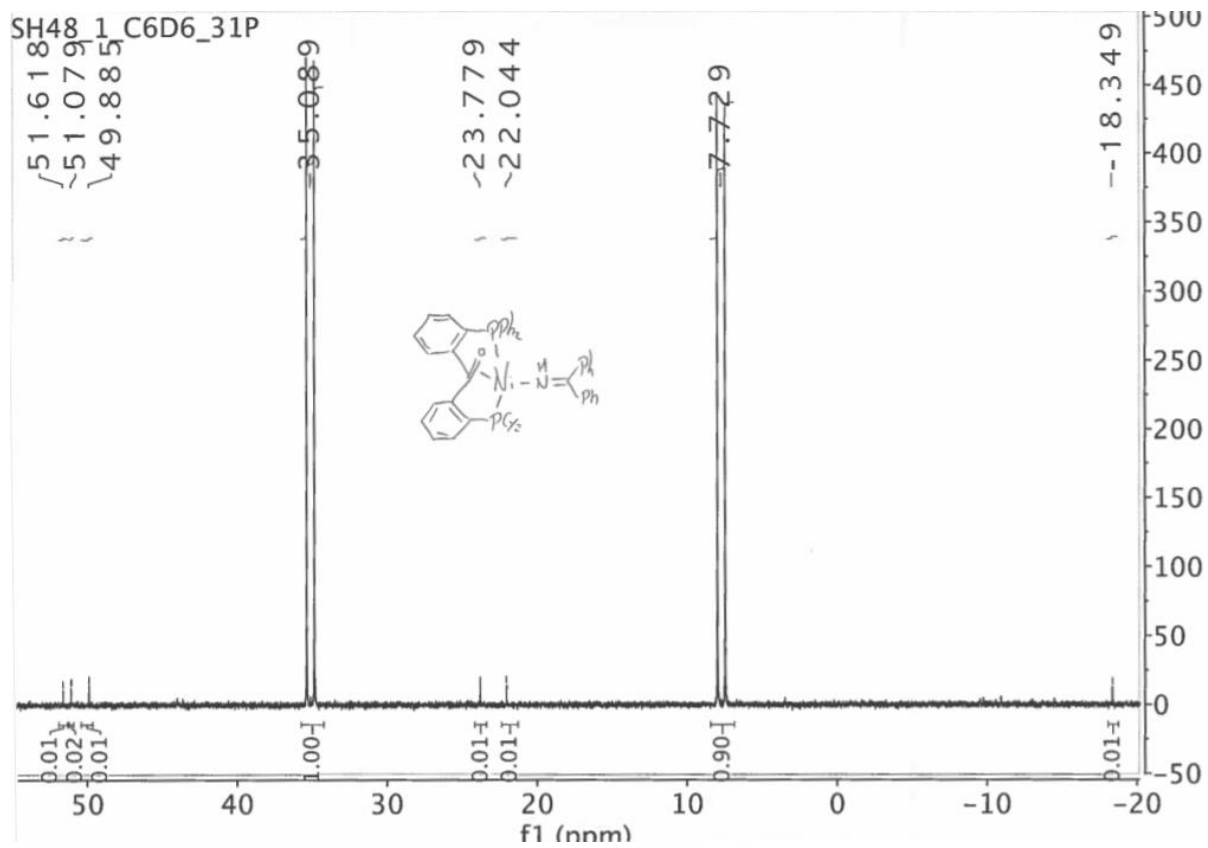
*Figure C 16: ^{31}P-NMR spectrum of **18** in C$_6$D$_6$*
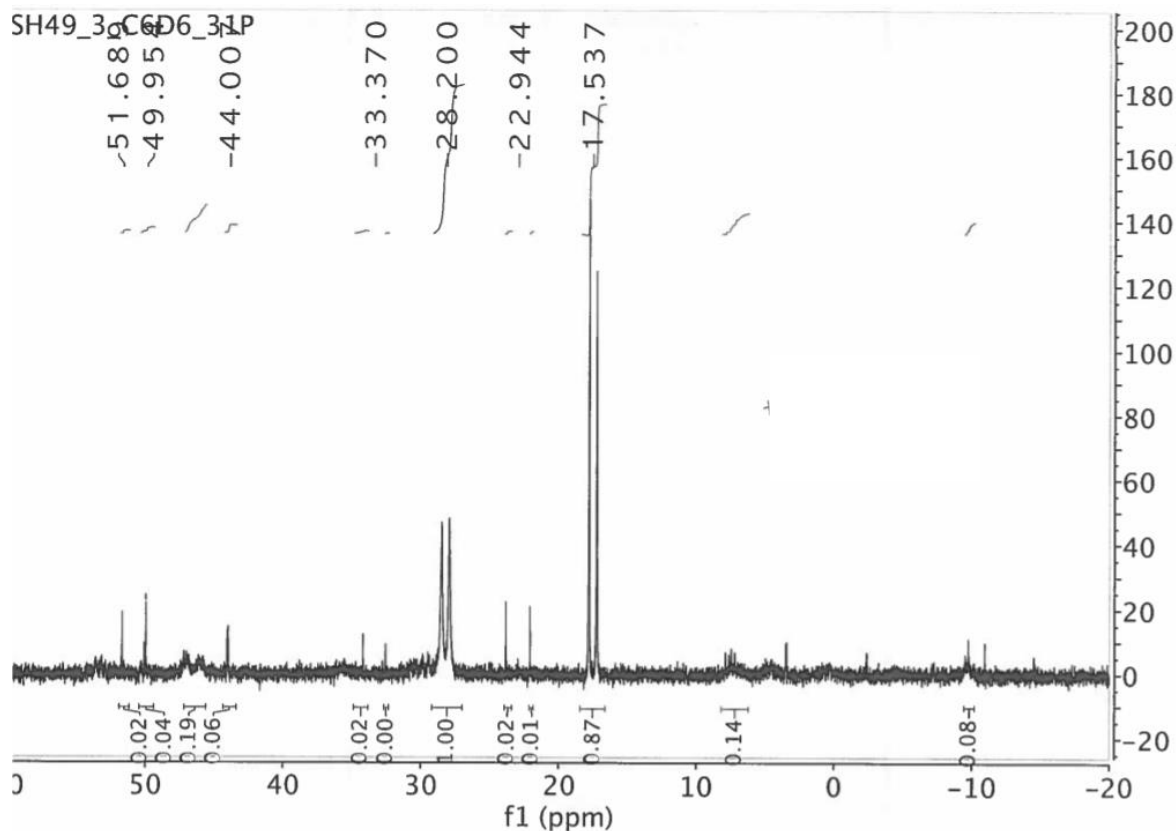
*Figure C 17: ^{31}P-NMR spectrum of the reaction between **L1**, Ni(COD)$_2$ and phenylacetylene*
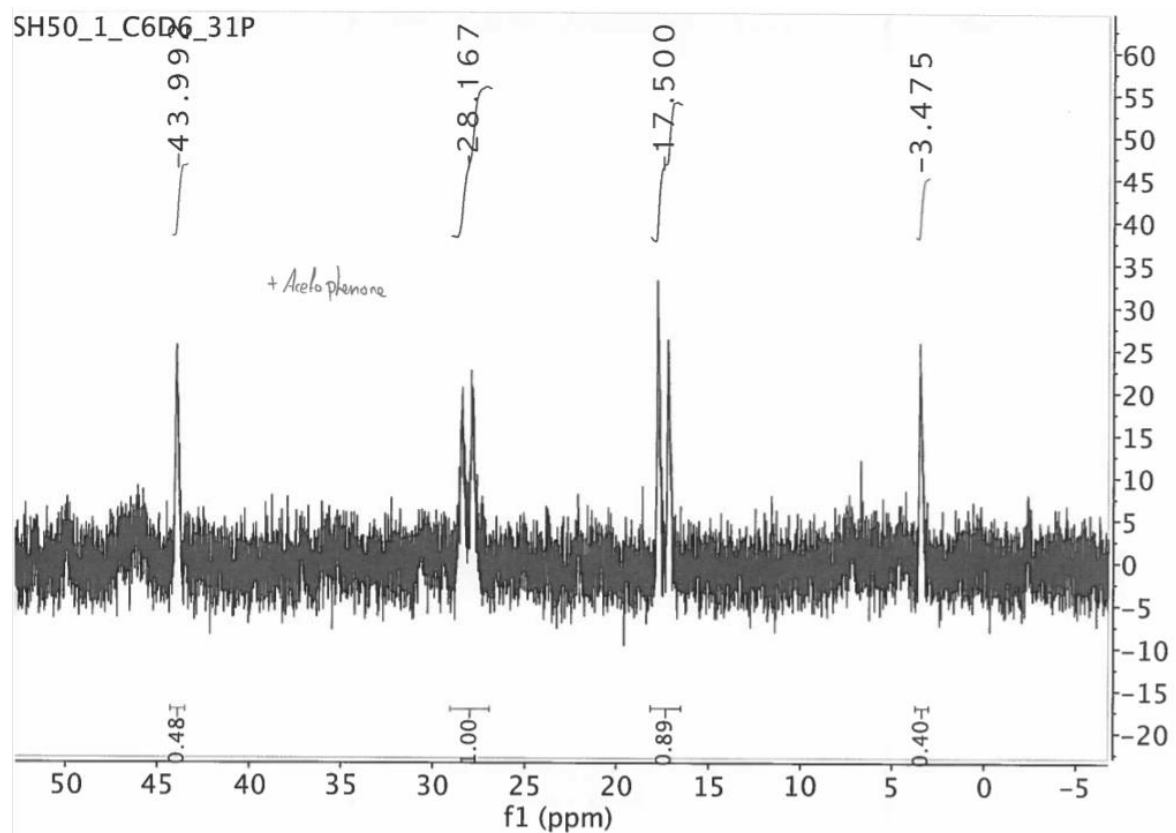
*Figure C 18: ^{31}P-NMR spectrum of the reaction between **L1** and Ni(COD)$_2$*
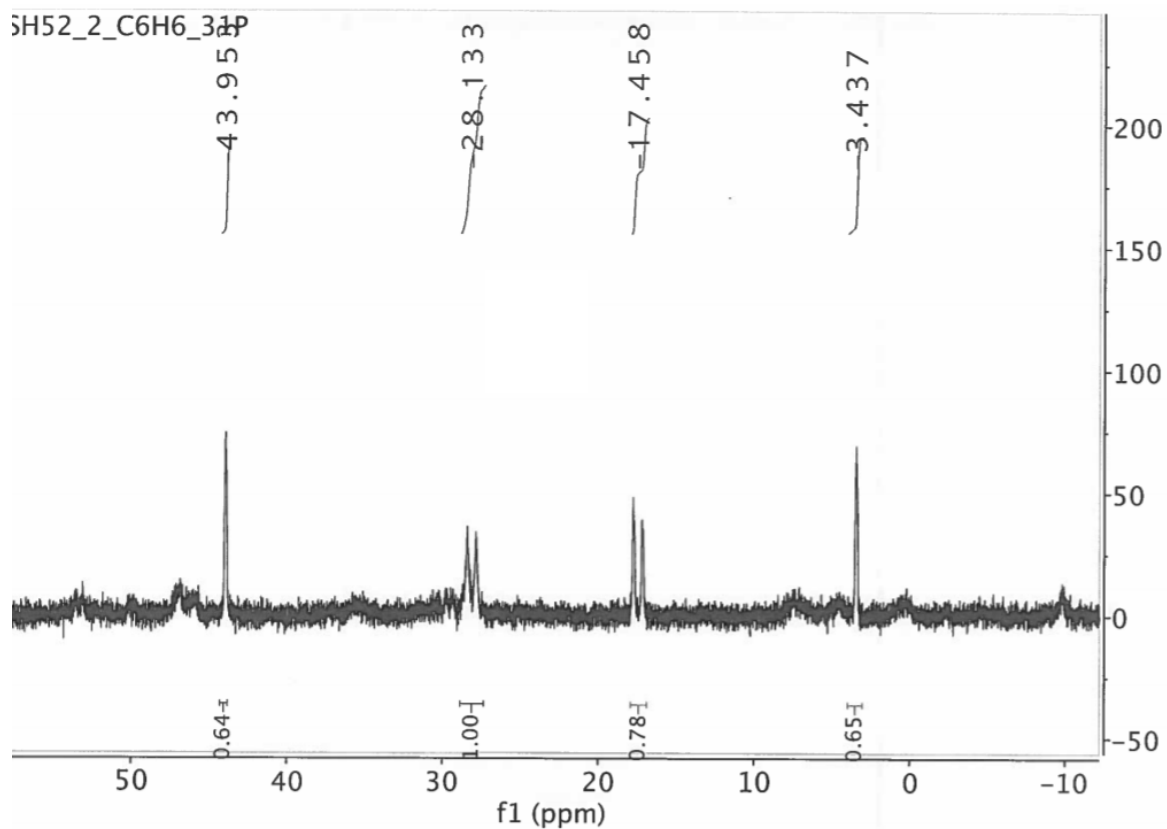
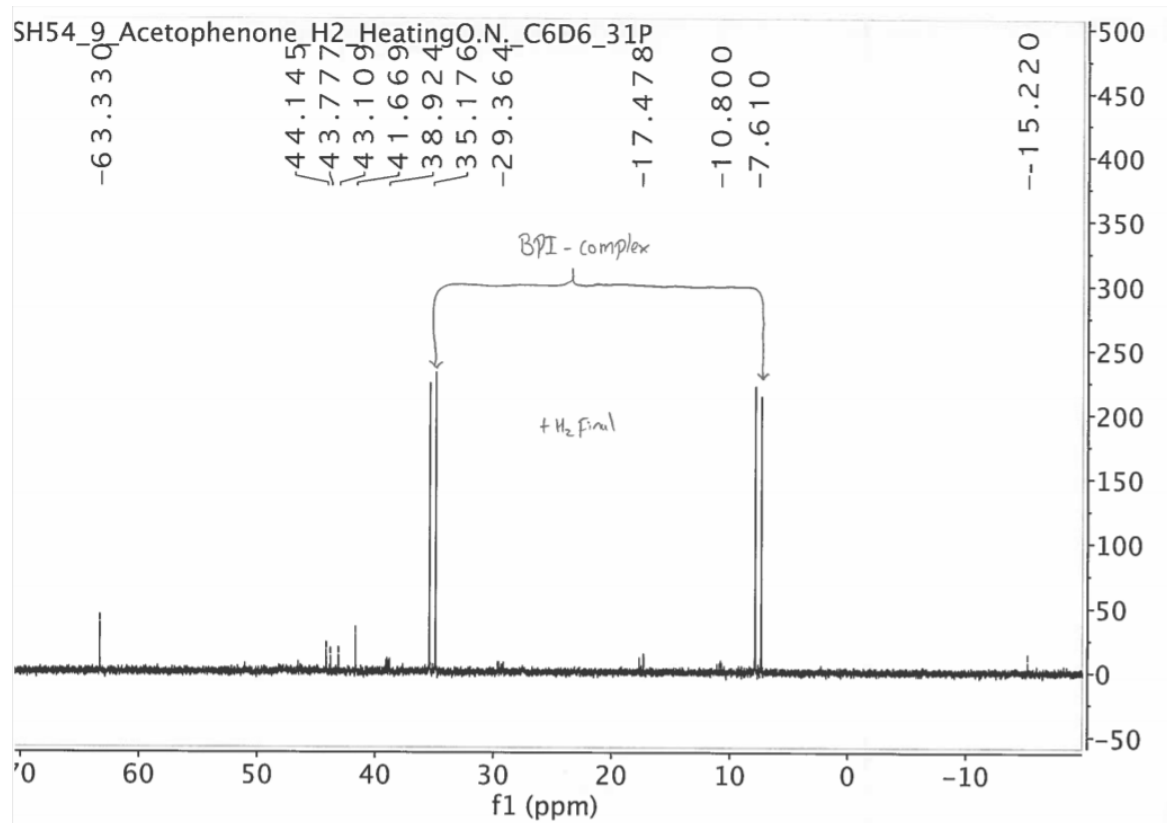*Figure C 19: ^{31}P-NMR spectrum of the reaction between **L1**, Ni(COD)$_2$ and acetophenone in C$_6$D$_6$*

*Figure C 20s: ^{31}P-NMR spectrum in C$_6$D$_6$ of the attempted hydrogenation of acetophenone with **18** and H$_2$*
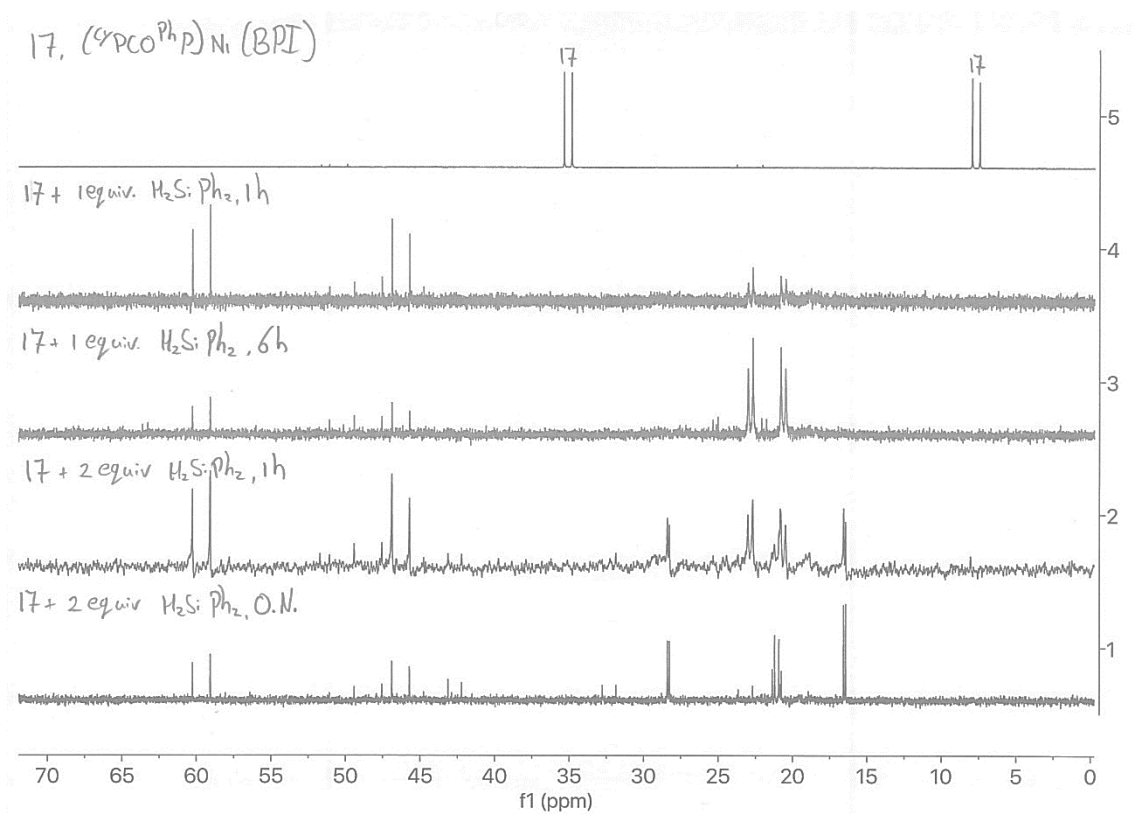
*Figure C 21: ^{31}P-NMR spectra of **18** with H_2SiPh_2. 5: No H_2SiPh_2. 4: 1 equiv. H_2SiPh_2, after 1 hour. 3: 1 equiv. H_2SiPh_2, after 6 hours. 2: 2 equiv. H_2SiPh_2, after 1 hour. 1: 2 equiv. H_2SiPh_2, after O.N. reaction.*
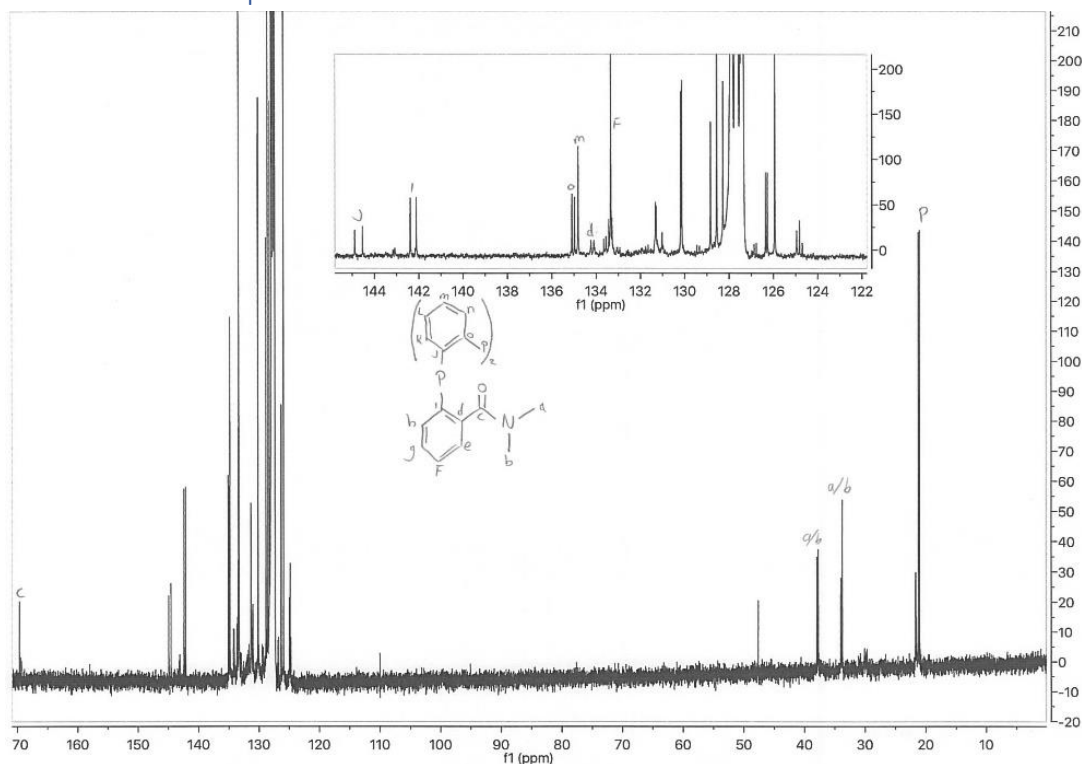
D. ^{13}C-NMR Spectra

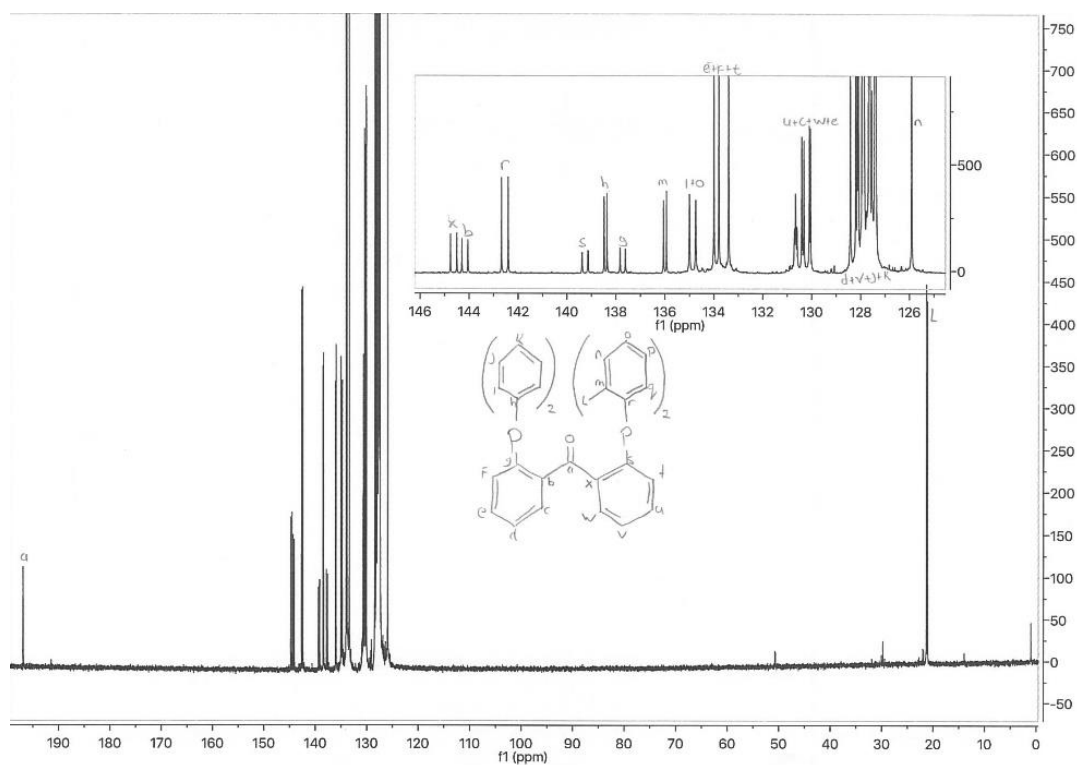*Figure D 1: ^{13}C-NMR spectrum in C_6D_6 of 2-(di(o-tolyl)phosphaneyl)-N,N-dimethylbenzamide (**7**).*

*Figure D 2: ^{13}C-NMR spectrum in C_6D_6 of 1, (2-(di-o-tolylphosphaneyl)phenyl)(2-(diphenylphosphaneyl)phenyl)methanone (**L1**).*
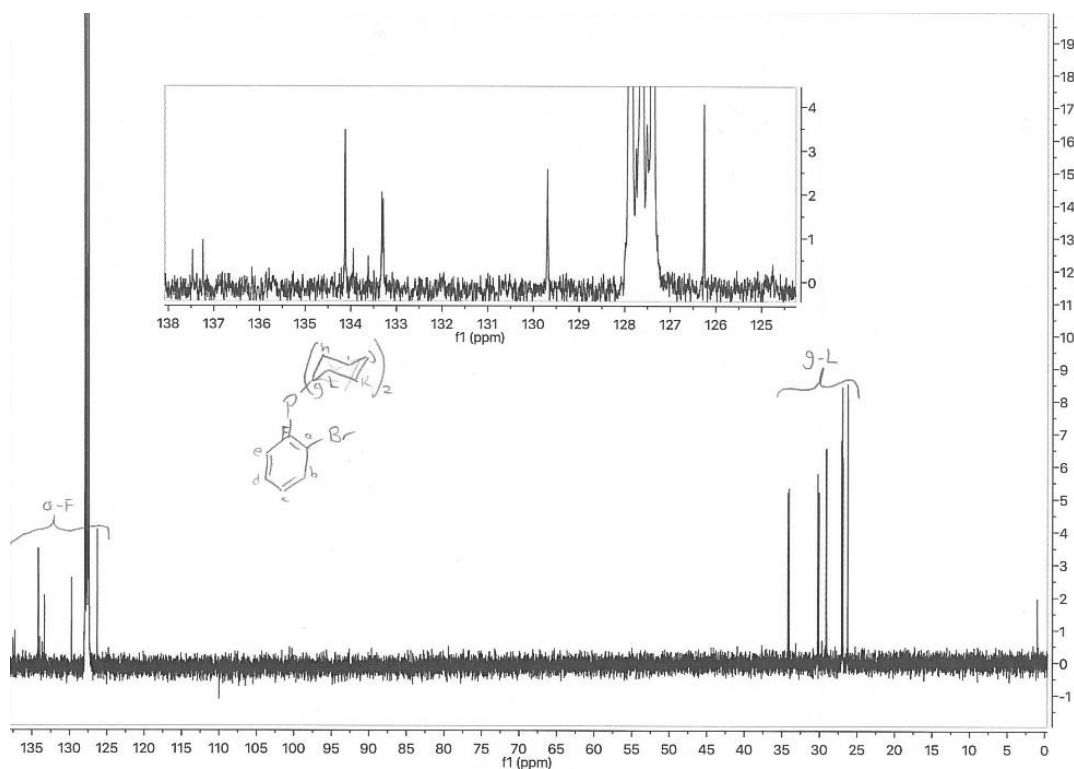
*Figure D 3: ^{13}C-NMR spectrum in C_6D_6 of (2-bromophenyl)dicyclohexylphosphane (**9**).*
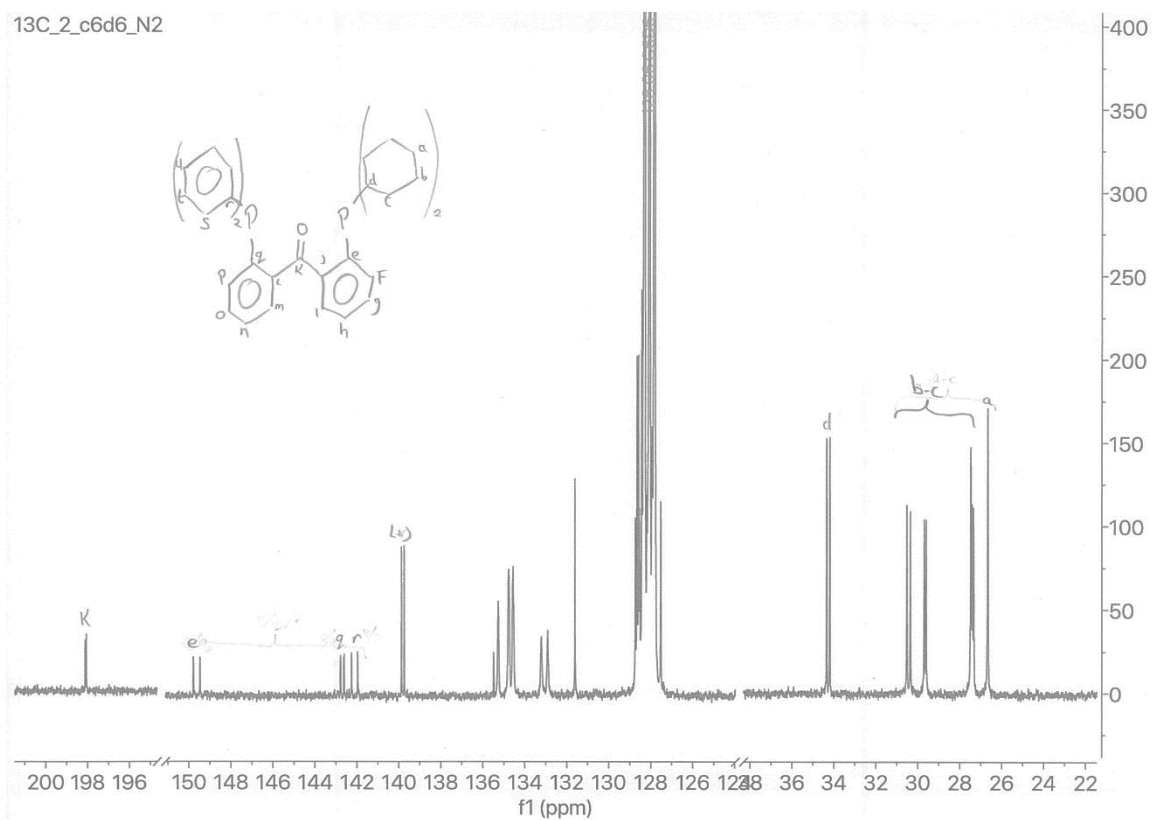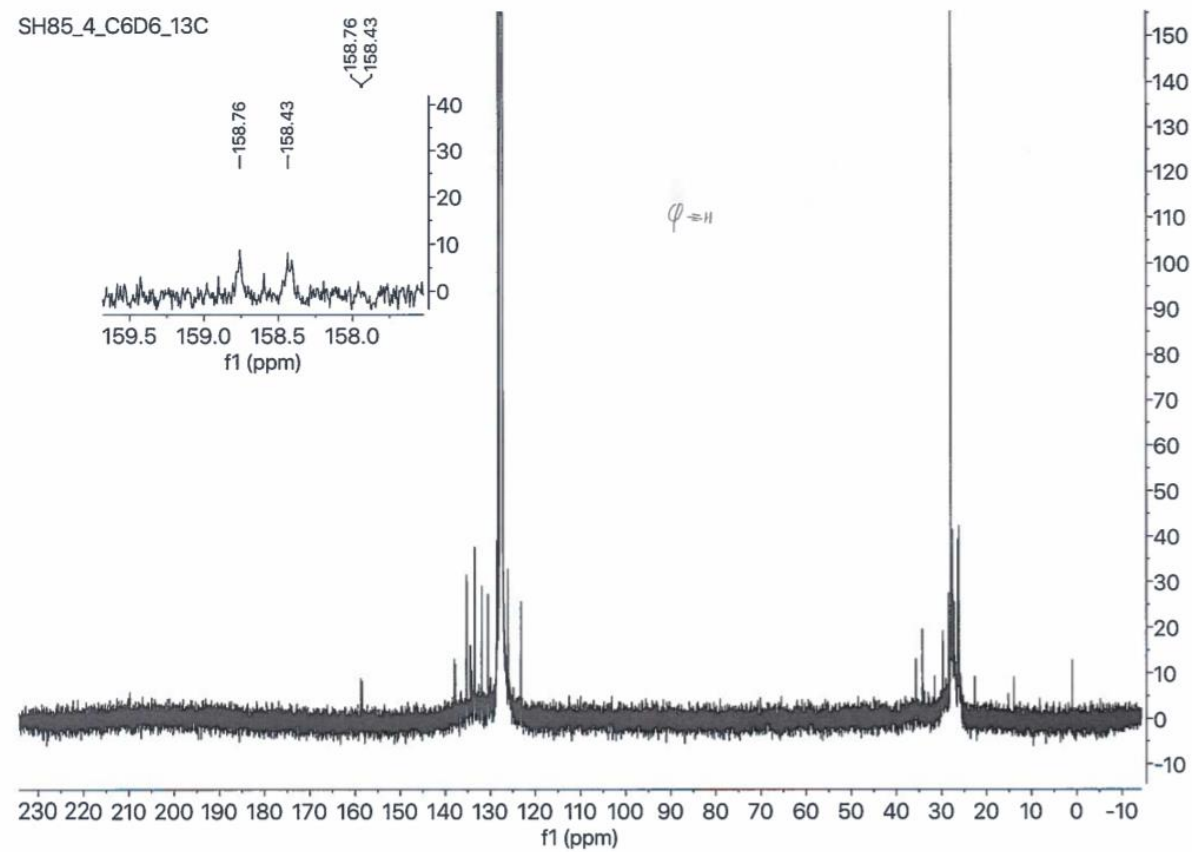

*Figure D 4: ^{13}C-NMR of (2-(dicyclohexylphosphaneyl)phenyl)(2-(diphenylphosphaneyl)phenyl)methanone (**L2**).*

*Figure D 5: ^{13}C-NMR of **18***

*Figure D 6: ^{13}C-NMR of the reaction between **L2**, Ni(COD)$_2$ and phenylacetylene, in C$_6$D$_6$.*
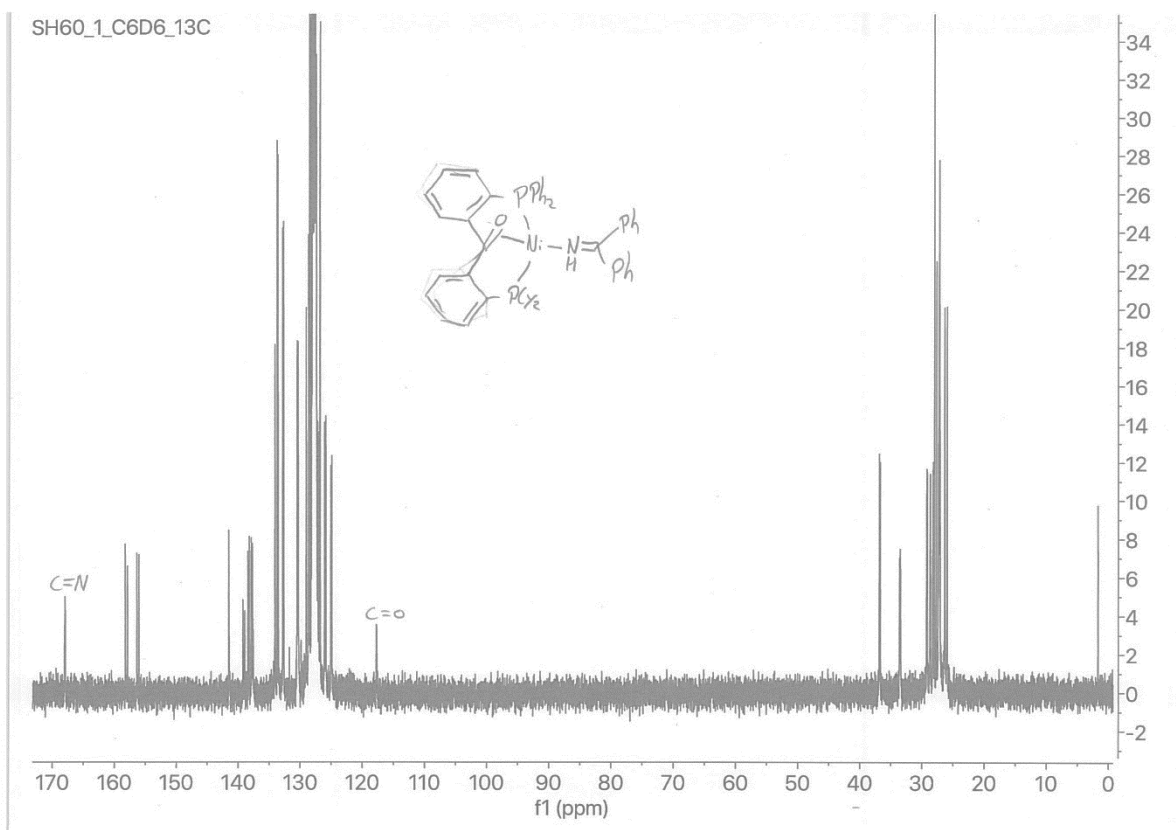
E. X-ray diffraction data of 18

	I0989a
Formula	$C_{50}H_{51}NNiOP_2 \cdot 0.5(C_7H_8)$
Fw	848063
Crystal Colour	Dark red
Crystal Size (mm^3)	0.17 x 0.21 x 0.40
T (K)	150
Crystal System	Monoclinic
Space Group	P21/c (No. 14)
a (Å)	9.1682(4)
b (Å)	22.4026(9)
c (Å)	21.164(2)
ß (º)	90.136(5)
V (Å^3)	4346.9(5)
Z	4
D_{calc} (g/cm^3)	1.297
Θ(min/max) (°)	1.8/27.6
μ (mm^{-1})	0.561
Abs. corr.	Multi-scan
Abs. corr. Range	0.868-0.909
Refl. Measured/unique	43272 / 9826
R1/wR2 (all refl.)	0.057/0.162
S	1.085
$\rho_{(min/max)}$ [eÅ^{-3}]	-0.68/0.48

-